AD-A074 776 METEOROLOGY INTERNATIONAL INC MONTEREY CALIF F/G 4/2
TECHNIQUES FOR PROCESSING VTPR SIDE-SCAN RADIANCES INCLUDING DI--ETC(U)
FEB 75 M M HOLL N66314-74-C-1281
UNCLASSIFIED MII-M-205 EPRF-TR-4-75-MII NL

1 OF 2
AD
A074776

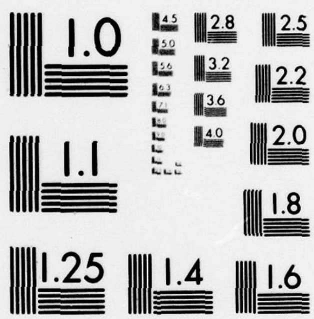

MICROCOPY RESOLUTION TEST CHART
NATIONAL BUREAU OF STANDARDS-1963-A

LEVEL II

EPRF Technical Report
No. 4-75 (MII)

Project M-205 TECHNICAL SUMMARY REPORT

TECHNIQUES FOR PROCESSING VTPR SIDE-SCAN RADIANCES INCLUDING DIAGNOSIS FOR THE CLEAR-COLUMN RADIANCE COMPONENTS

(Phase Two of the Development of Techniques for Operational Exploitation of Satellite-Observed Sounding Data for Resolution of Atmospheric Thermal-Structure Variabilities)

by
Manfred M. Holl
Meteorology International Incorporated
February 1975

Performed for:

The Commanding Officer
Environmental Prediction Research Facility
Naval Postgraduate School
Monterey, California 93940

Performed under Contract No. N66314-74-C-1281

METEOROLOGY INTERNATIONAL INCORPORATED

Monterey, California

Approved for Public Release;
Distribution Unlimited

18 EPRF Technical Report
No. 4-75 (MII)

19 TR-4-75-MII

---

14 MII- 9 Final

Project M-205 TECHNICAL SUMMARY REPORT.

1 Nov 74 - 28 Feb 75

6

TECHNIQUES FOR PROCESSING VTPR SIDE-SCAN RADIANCES INCLUDING DIAGNOSIS FOR THE CLEAR-COLUMN RADIANCE COMPONENTS.

(Phase Two of the Development of Techniques for Operational Exploitation of Satellite-Observed Sounding Data for Resolution of Atmospheric Thermal-Structure Variabilities)

10 by
Manfred M. Holl 12 126
Meteorology International Incorporated
11 February 1975

Performed for:

The Commanding Officer
Environmental Prediction Research Facility
Naval Postgraduate School
Monterey, California 93940

15

Performed under Contract No. N66314-74-C-1281

METEOROLOGY INTERNATIONAL INCORPORATED

Monterey, California

227 450

UNCLASSIFIED

SECURITY CLASSIFICATION OF THIS PAGE (When Data Entered)

REPORT DOCUMENTATION PAGE		READ INSTRUCTIONS BEFORE COMPLETING FORM
1. REPORT NUMBER Technical Summary Report	2. GOVT ACCESSION NO.	3. RECIPIENT'S CATALOG NUMBER
4. TITLE (and Subtitle) Techniques for Processing VTPR Side-Scan Radiances Including Diagnosis for the Clear-Column Radiance Components		5. TYPE OF REPORT & PERIOD COVERED Final 74NOV01 through 75FEB28
		6. PERFORMING ORG. REPORT NUMBER M-205
7. AUTHOR(s) Manfred M. Holl		8. CONTRACT OR GRANT NUMBER(s) N66314-74-C-1281
9. PERFORMING ORGANIZATION NAME AND ADDRESS Meteorology International Incorporated 205 Montecito Avenue Monterey, California 93940		10. PROGRAM ELEMENT, PROJECT, TASK AREA & WORK UNIT NUMBERS PE 35111N EPRF WU 114:6-1
11. CONTROLLING OFFICE NAME AND ADDRESS Environmental Prediction Research Facility Naval Postgraduate School Monterey, California 93940		12. REPORT DATE 75FEB28
		13. NUMBER OF PAGES 93 plus Appendix A
14. MONITORING AGENCY NAME & ADDRESS (if different from Controlling Office)		15. SECURITY CLASS. (of this report) UNCLASSIFIED
		15a. DECLASSIFICATION/DOWNGRADING SCHEDULE

16. DISTRIBUTION STATEMENT (of this Report)

DISTRIBUTION STATEMENT A

Approved for public release;
Distribution Unlimited

17. DISTRIBUTION STATEMENT (of the abstract entered in Block 20, if different from Report)

18. SUPPLEMENTARY NOTES

19. KEY WORDS (Continue on reverse side if necessary and identify by block number)

Satellite Sounders, Atmospheric Thermal-Structure, Structure Blending

20. ABSTRACT (Continue on reverse side if necessary and identify by block number)

Phase Two of the development of techniques for operational exploitation of satellite-observed sounding data for resolution of atmospheric thermal structure variabilities. Full side-to-side scans of measured multi-channel radiances are processed and examined for characteristics of cloud contamination. A general scheme is developed for diagnosis of the clear-column radiance components of a scan. The structure blending scheme developed under Phase One is also demonstrated as a general retrieval capability. Both schemes are applications of the Fields by Information Blending (FIB) methodology in which information elements, weighted for independent worth, are blended into the non-independent resultants implied by the focus of all input information.

DD FORM 1 JAN 73 1473 EDITION OF 1 NOV 65 IS OBSOLETE

UNCLASSIFIED

SECURITY CLASSIFICATION OF THIS PAGE (When Data Entered)

Table of Contents

THE DEVELOPMENT OF TECHNIQUES FOR OPERATIONAL EXPLOITATION OF SATELLITE-OBSERVED SOUNDING DATA FOR RESOLUTION OF ATMOSPHERIC THERMAL-STRUCTURE VARIABILITIES

Phase Two: Techniques for Processing VTPR Side-Scan Radiances Including Diagnosis for the Clear-Column Radiance Components

1. Summary of Developments

1.1 Developments of Phase One

The major developments performed under the earlier Phase One include:

(1) A generalization of the mass-structure model to any specified selection of standard pressure levels. The mass-structure model constitutes the information framework for upper-air analysis, including resolution of the atmospheric thermal structure.

The degrees of freedom of the mass-structure model are defined as follows: The atmospheric column is divided into N layers, or segments, with pressure as vertical coordinate. In each segment the virtual temperature is linear in p^{κ}, where $\kappa \equiv R/C_p$. This makes the chosen form of static stability constant in each layer, changing abruptly at the interfaces. The structure model incorporates the hydrostatic and gas-law approximations. With pressure as vertical coordinate, the relationship between heights, temperatures, and layer stabilities, is linear. This linearity is the virtue of the mass-structure model. The transformation matrices are produced by our generalized program.

The generalized program permits arbitrary selection of a set of N+2 pressure levels, referred to as the standard pressure levels, in monotonic order. The program locates the interfaces midway in pressure between the standard levels except for omitting interfaces between the

first two and the last two. This defines N layers, for the desired vertical-resolution powers.

A ten-level, eight-layer model, based on the traditional set of standard pressure levels, has been in operational use at the Fleet Numerical Weather Central (FNWC) for many years. The resolution powers require supplementation in the 1000-800 and 100-0 mb ranges.

(2) Radiances transformed into terms of the modelled thermal structure. The production of transformations which express each channel radiance anomaly in terms of a linear combination of the atmospheric thermal-structure anomalies including a sea-surface, or ground, temperature anomaly.

An arbitrary standard thermal structure is defined, including a sea surface or ground temperature. Given a transmission function, the standard radiance is calculated for that channel in terms of an atmospheric contribution and a ground contribution. This is done by integrating the radiative transfer equation for the defined standard atmosphere.

The thermal structure, being linear-in-p^κ in each layer, now has its degrees of freedom defined in terms of the temperature anomaly at each interface and at the base (1000 mb) and top. A ground temperature anomaly is also permitted. The Planck function is linearized about the assumed standard temperature structure, enabling transformation of the radiative-transfer equation: the radiance anomaly is defined as a linear combination of the temperature anomalies.

The mass-structure transforms, produced by program (1) above, enable the temperature anomalies to be expressed in terms of other sets defining the thermal-structure anomaly. This permits expressing the radiance anomaly in alternate forms: as a linear combination of height anomalies of the standard pressure levels, as a linear combination of

layer thicknesses, as a linear combination of layer stabilities and a thickness (e.g., 1000-300 mb), and in other forms.

For a specified transmission function and an assumed standard atmosphere, this program generates the standard radiance contributions from atmosphere and ground, and several sets of combination coefficients which express the radiance anomaly in terms of corresponding sets of thermal-structure parameter anomalies.

These transforms apply to clear-column radiances, as do the specified transmission functions on which they are based.

(3) *A generalized retrieval scheme for transforming clear-column radiance* estimates into enhanced resolution of the atmospheric thermal structure and the ground, or sea surface, temperature.

This retrieval is in the form of a structure blending scheme. The input information, expressed by weighted clear-column-radiance estimates and by independent weighted estimates of a set of atmospheric thermal-structure parameters, is blended to produce the optimum resultant implications, with associated resolutions afforded by the input information. The weights are defined as the inverse of the associated error variances.

Incorporated into this blending scheme is the absolute constraint that all static-stability implications be positive. This constraint represents additional input information.

The information blending methodology, in general, combines independent weighted estimates into the non-independent resultants implied by the focus of all the input information. It handles linear interrelationships and other extensions. The resolution that comes out reflects what went in. In the present application of the methodology we output not only the resultant implication for each thermal-structure parameter but also for each radiance.

The blending can be forced to perfectly accommodate all input radiance estimates* by setting the associated input weights very high compared to any conflicting information in the independent thermal-structure estimates. But realistic weighting is much to be preferred.

The blending scheme includes three cycles of retrieval in order to enable reevaluation of the input estimates and input weights in comparison with resultant indirect implications. Estimates judged to be in gross error are rejected, and the weights of maverick estimates are reduced. The constraint that the retrieved static stabilities be positive amplifies the disparity with contaminated estimates. The nature of the structure-blending scheme exploits the radiance information for adjustment of the related structure components in conformance with the firmness, and lack of firmness, in the input estimates. That is, the transformation of the input information is dictated by the specific set of input weights, and by the analysis framework and the interrelationships. Various examples of this interplay have been demonstrated.

The Phase One research effort is documented in the following Task Performance reports:

Task One: "The development of techniques for operational exploitation of satellite infrared channel radiances in the resolution of atmospheric thermal-structure variabilities--task one: perspective", Technical Report of Task One, Project M-181, Contract No. N62306-72-C-0125, September 1972, Meteorology International Incorporated, Monterey, California, 61 pp.

Contents: Nature of the Radiances and the Retrieval Problem, Context for the use of Radiance Information, Review of Retrieval Schemes with Comments.

---

*Provided that these estimates do not inherently violate the static-stability constraint.

Task Two: "The development of techniques for operational exploitation of satellite infrared channel radiances in the resolution of atmospheric thermal-structure variabilities--task two: new formulations", Technical Report of Task Two, Project M-181, Contract No. N62306-72-C-0125, March 1973, Meteorology International Incorporated, Monterey, California, 91 pp.

Contents: Mass-Structure Model, Parameterization of Thermal Structure in Terms of Layer Static Stabilities, Transformation of Radiances in Terms of Linear Combinations of Thermal-Structure Parameters, Retrieval by Structure Blending.

Task Three: "The development of techniques for operational exploitation of satellite observed sounding data for resolution of atmospheric thermal-structure variabilities--task three and final report", Technical Report of Task Three, Project M-181, Contract No. N62306-72-C-0125, June 1973, Meteorology International Incorporated, Monterey, California, 59 pp.

Contents: Generalization of the Mass-Structure Model, Corresponding Transformation of Radiances in Terms of Linear Combinations of Thermal-Structure Parameters, Generalization of Structure Blending Including Constrained Blending (Assuring a Statically-Stable Retrieval) and Reevaluations of Estimates and Weights.

1.2 Developments of Phase Two

The major developments performed under Phase Two, and detailed in the present Technical Summary Report, include:

(1) Generalization of the mass-structure model and the transforms for relating clear-column radiances to the atmospheric thermal structure. This program represents a merging of items (1) and (2) listed under Phase One, above, but with added generalizations and extensions.

A general capability has been developed which produces standard-radiance values, and the transforms which express radiance anomalies in terms of linear combinations of atmospheric thermal-structure-parameter anomalies. This capability is general in that it permits arbitrary specification of (a) a table of standard pressure levels which define the degrees of freedom of the thermal-structure model, (b) a standard temperature structure in terms of values for the degrees of freedom of the modelled thermal structure, and (c) the transmission function, for any channel and nadir angle, tabled in terms of a specified increment in p^{κ}.

This general capability was applied to the transmission functions of an operational Air Force VTPR sounder. We were provided with the transmission functions for a set of channels and a range of nadir angles. The general program, and the tables produced for an 18-level structure model and a specified standard thermal structure, are included in the deliverable items. The tables of transforms were used in several contexts including the normalization of radiances for any nadir angle. We also investigated the designed differential resolution powers of the sounder afforded by the specifications of the channels over the range of nadir angle.

(2) Examinations of real satellite radiances, and investigation of the characteristics of cloud contamination.

We were also provided with a sample of radiances measured by the Air Force VTPR sounder, taken in orbit on 26 March 1974. All complete side-to-side scans on this sample tape were transformed into normalized radiance anomalies for each channel and nadir angle. Each scan was plotted (by Varian plotter) in the form of a cross section, placing each normalized anomaly at the center of its energy source region. These cross sections were studied in our investigation of the character of cloud contamination.

(3) Development of a capability for diagnosing the clear-column radiance components (Program CLRX).

The study of radiance cross sections inspired the conceptions and the major achievement of Phase Two: a capability to diagnose each complete scan for the inherent resolution of the clear-column radiance component of each measured radiance. We refer to this programmed capability as CLRX. The program operates on the scan after it has been processed by the preceding development, item (2) above; however, it can be modified to operate directly on the measured radiances.

CLRX produces not only an estimate of the clear-column component of each radiance element of the scan but also an associated reliability for each such estimate.

During the latter part of the performance period we worked on producing a comprehensive version of CLRX for use in oceanic regions. In order to demonstrate and assess the potential powers of CLRX we did not input any independent thermal-structure information in the form of first-guess, or background, estimates of the clear-column radiances. We wished to demonstrate the powers of CLRX to diagnose the information inherent only in the measured radiances of the scan.

CLRX represents a significant breakthrough in the practical exploitation of satellite VTPR sounders. CLRX is not dependent on independent sea-surface-temperature (SST) values for categorical calibration of the clear-column radiances. Hence, its present applicability extends into all oceanic regions, even where there is little independent SST information. We have, in fact, conceived of the extension of CLRX for use over land regions. The formulations promise to be much more complex even for terrain of low and uniform elevation. Computer running time, however, would be comparable. Extension for application in regions of high and irregular elevations is also conceivable for diagnosis of the lesser penetrating channels.

Processing of the measured radiances by CLRX, for diagnosis of the clear-column components, is essentially independent of the accuracy of the specified transmission functions for the channels at nadir angles. We have not unduly involved ourselves with the accuracy of the transmission functions, with adjustments for attenuation by water vapor and aerosols, and with the quality control and calibration of channels. These matters have been outside the scope of our project. The techniques that we have developed are adaptable to specification of transmission functions relative to individual side-to-side scans. Complex refinements of the transmission functions can be entertained.

CLRX produces estimates of the clear-column radiance components across the entire scan, thus retaining whatever gradient information is inherent in the measured radiances of that scan.

CLRX is based on a model for interpreting cloud contamination. The largest differences that arise in the radiances between two spots in proximity, are generally due to differences in the amount of cloud at only one cloud-top level. Based on this interpretation, large

differences in radiances between nearby spots of a scan* produce estimates of the local correction axis (i.e., unit vector) for adjusting the measured radiances toward their clear-column components. CLRX does not require the cloud top to be at the same level over the entire scan; a gradual slope, or even stepwise changes, are tolerated in the exploitation.

It should be understood that CLRX can only exploit information that is inherent in the measured radiances. The yield of information is measured by the reliability estimate which is produced with each diagnosed clear-column radiance component. The yield is largely a function of the character of the cloudiness over the scan. The diagnosis is generally more reliable the greater are the contrasts of the clear proportions between spots. A solid cloud top over the entire scan defies all diagnosis of the affected channels. This variability in yield underlines how essential it is to produce the associated reliability measures.

(4) A retrieval demonstration.

We have now dealt with all technical impediments to the operational exploitation of the inherent information in radiances measured by scanning VTPR satellite sounders. The techniques we have developed address not only absolute temperature information but also information for resolution of relative properties such as horizontal gradients. Our techniques are not transforms based on idealized theories. They are

---

*The VTPR scans of NOAA spacecraft are more closely spaced along the orbital path, affording useful information redundancies. This redundancy warrants exploitation by analyzing differences between measured spots not just within one scan but also between adjoining scans.

designed for use in the real world of the operational context, and include the ability to cope with the concomitant problems of contributing normal error variances and gross, anormal errors in the data streams.

In order to demonstrate the essential completeness of the range of techniques developed under Phases One and Two we have submitted output from CLRX into the generalized structure-blending retrieval scheme developed under Phase One. This retrieval scheme accepts weighted clear-column radiances, and transforms this information into enhancement of the resolution of the thermal structure of the atmospheric column. This comprehensive capability also exploits the information that the real structure is statically stable.

This demonstration required modification of the structure-blending retrieval scheme from the 13-level, 11-layer atmospheric-structure model used in Phase One to the 18-level, 16-layer model used in Phase Two.

(5) The design of a generalized capability.

A test and evaluation phase is now essential for evaluating the inherent information, in VTPR scanning sounders, that can be exploited by the developed techniques under operational conditions. We have designed the generalized basic capability.

This capability involves interfacing with an analysis and prediction system, including upper-air thermal-structure parameters, and analyses of sea-surface-temperature fields. Provisions include the collection of high quality (i.e., of the highest associated weights) CLRX-diagnosed clear-column radiance estimates; values, weights, position and time data would be saved for calibration studies with any available

independent thermal-structure information. Supplemental components could be systematically incorporated. Competitive components and variations could be evaluated side by side. Realization of this capability will enhance prospects for systematic improvements and extensions, including use over land as well as sea.

2. Transforms and Measured Radiances

2.1 Production of the Transforms

A general capability has been developed which relates any radiance, for which the transmission function is specified, to parameterizations of the atmospheric thermal structure. This program represents a merging of items (1) and (2) listed under Section 1.1 above, but with added generalizations and extensions.

The program permits arbitrary specification of (a) the standard levels which define the atmospheric mass, and thermal structure, parameterization, (b) a standard temperature structure in terms of values for the degrees of freedom of the modelled thermal structure, and (c) the transmission function, for any channel and nadir angle, tabled in terms of a specified increment in p^{κ}.

The method of integrating the transmission function for the standard thermal structure, the linearization of the Planck function about the standard thermal structure, and the formation of the transforms are detailed in the Task Two Report of Phase One.

For development purposes we chose an 18-level, 16-layer mass-structure model. The specified standard pressure levels are listed in the first column of Table 1.

The arbitrary standard temperature structure that we have selected is also specified in Table 1. The integration of the radiative transfer equation is performed in terms of the layers in which temperature is modelled to be linear in p^{κ}. The top, layer interface, and bottom temperatures of the assumed standard thermal structure are listed in the last column of Table 1. This standard atmosphere is plotted on a Sigmagram in Fig. 1. The ground, or sea surface, temperature is specified to be the same as that for 1000 mb.

Table 1

Specification of the arbitrary standard atmosphere may be expressed in any of the following terms which are mutually consistent with the 18-level, 16-layer mass-structure model

By Heights		By Thickness and Layer Stabilities		By Temperature at Top Interface and Base	
Model-Standard Pressure Levels: (mb)	Specified Arbitrary Standard Heights: (meters)	Layer: (mb)	Stability: ($10^3 m^2 sec^{-2}$)	Level (mb)	Temperature (°K)
0	79,000	($Z_{300} - Z_{1000}$ =	9,063 meters)	0	249.8
4	37,100	0 - 5.5	20.49	5.5	224.9
7	33,400	5.5 - 8.5	16.40	8.5	228.2
10	31,024	8.5 - 15	20.04	15	225.3
20	26,451	15 - 25	21.08	25	220.3
30	23,831	25 - 40	19.61	40	217.6
50	20,574	40 - 60	19.62	60	215.0
70	18,455	60 - 85	19.11	85	213.1
100	16,226	85 - 125	16.79	125	214.1
150	13,681	125 - 175	14.11	175	218.3
200	11,843	175 - 225	13.57	225	222.3
250	10,391	225 - 275	12.14	275	226.6
300	9,180	275 - 350	7.27	350	236.5
400	7,191	350 - 450	6.29	450	248.4
500	5,571	450 - 600	7.28	600	262.0
700	2,998	600 - 775	8.72	775	273.9
850	1,445	775-1000	13.95	1000	281.7
1000	117				

T (ground) ≡ T (1000 mb)

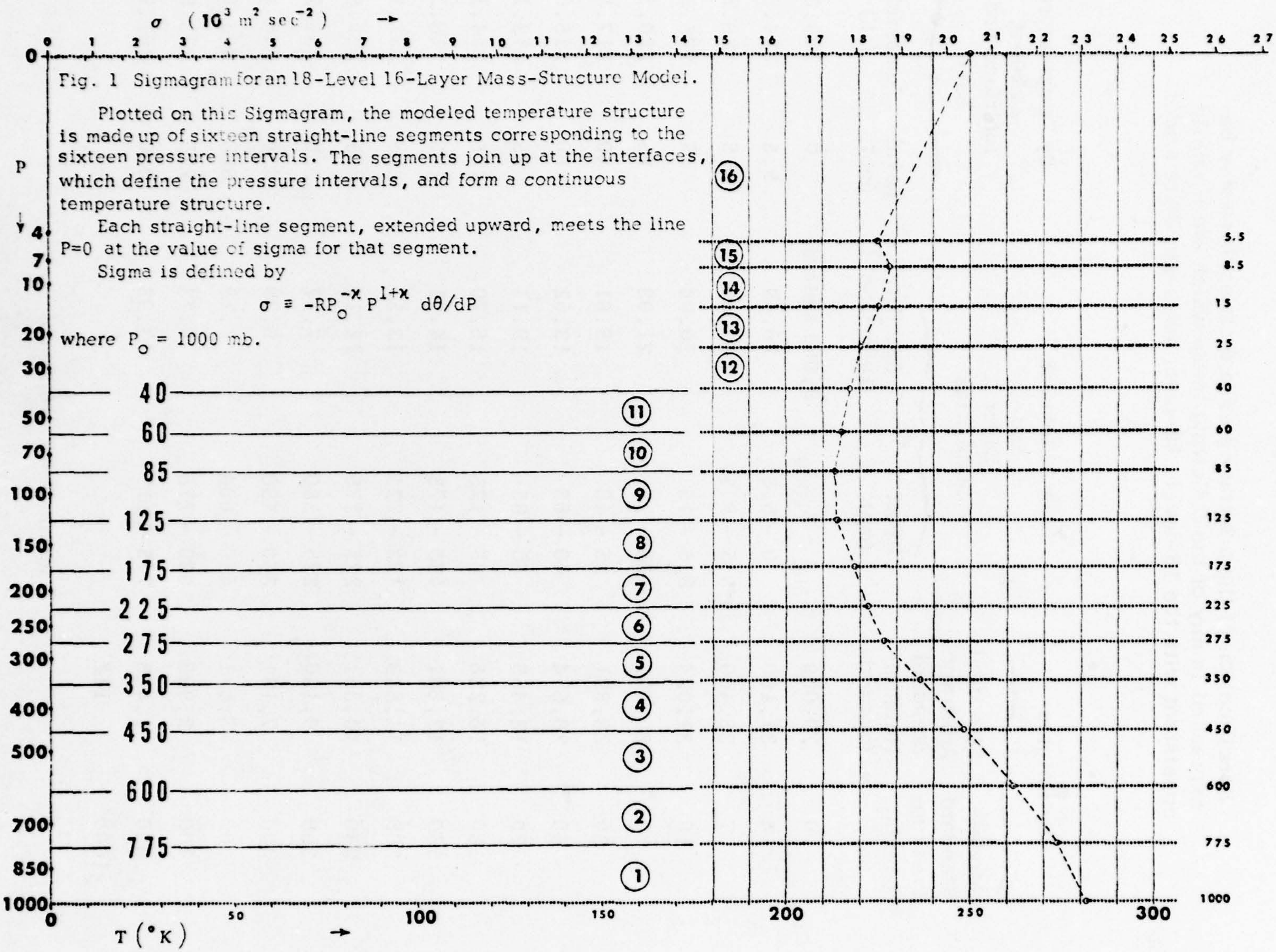

Fig. 1 Sigmagram for an 18-Level 16-Layer Mass-Structure Model.

Plotted on this Sigmagram, the modeled temperature structure is made up of sixteen straight-line segments corresponding to the sixteen pressure intervals. The segments join up at the interfaces, which define the pressure intervals, and form a continuous temperature structure.

Each straight-line segment, extended upward, meets the line P=0 at the value of sigma for that segment.

Sigma is defined by

$$\sigma \equiv -RP_o^{-\kappa} P^{1+\kappa} \, d\theta/dP$$

where P_o = 1000 mb.

The definitions and relationships may be identified as follows:

$E\ (\nu,\theta)$ denotes the radiance measured by channel ν at nadir angle θ.

$E_S(\nu,\theta)$ denotes the standard radiance composed of a ground, or sea-surface, contribution and an atmospheric contribution. The program produces standard values for both contributions.

The radiance anomaly is defined by

$$\epsilon(\nu,\theta) \equiv E(\nu,\theta) - E_S(\nu,\theta) \quad .$$

The radiance anomaly is related to the temperature anomalies, $\mathfrak{T}$, at the ground and at the top, layer interfaces, and bottom of the modelled thermal structure:

$$\epsilon(\nu,\theta) = C_G(\nu,\theta)\,\mathfrak{T}_G + \sum_n C_n(\nu,\theta)\,\mathfrak{T}_n \quad . \tag{1}$$

The program calculates the values of these coefficients, C_G for the ground, and the C_n's for the column levels. These column levels are identified in Table 2 under the heading C (I).

By virtue of the intentional linear properties of the mass-structure model the radiance anomaly may also be expressed in alternate terms of the thermal-structure anomaly:

A linear combination of the height anomalies of the standard pressure levels as identified in Table 2 under the heading CA(I). The corresponding combination coefficients always sum to zero because the thermal structure is not related to the absolute of the height structure.

Table 2

THE COLUMNS OF COEFFICIENTS, LISTED FOR EACH FREQUENCY AND ANGLE, ARE LINEAR COMBINATION COEFFICIENTS FOR EXPRESSING THE RADIANCE ANOMALY IN TERMS OF THE FOLLOWING SETS OF PARAMETER ANOMALIES:

I	C(I)	CA(I)	CB(I)	500-1000 MB CG(I)
1	T(0)	Z(0)	Z(0)-Z(4)	SIGMA16
2	T(5)	Z(4)	Z(4)-Z(7)	SIGMA15
3	T(8)	Z(7)	Z(7)-Z(10)	SIGMA14
4	T(15)	Z(10)	Z(10)-Z(20)	SIGMA13
5	T(25)	Z(20)	Z(20)-Z(30)	SIGMA12
6	T(40)	Z(30)	Z(30)-Z(50)	SIGMA11
7	T(60)	Z(50)	Z(50)-Z(70)	SIGMA10
8	T(85)	Z(70)	Z(70)-Z(100)	SIGMA 9
9	T(125)	Z(100)	Z(100)-Z(150)	SIGMA 8
10	T(175)	Z(150)	Z(150)-Z(200)	SIGMA 7
11	T(225)	Z(200)	Z(200)-Z(250)	SIGMA 6
12	T(275)	Z(250)	Z(250)-Z(300)	SIGMA 5
13	T(350)	Z(300)	Z(300)-Z(400)	SIGMA 4
14	T(450)	Z(400)	Z(400)-Z(500)	SIGMA 3
15	T(600)	Z(500)	Z(500)-Z(700)	SIGMA 2
16	T(775)	Z(700)	Z(700)-Z(850)	SIGMA 1
17	T(1000)	Z(850)	Z(850)-Z(1000)	W
18		Z(1000)		Z(1000)

A linear combination of the thickness anomalies of layers, defined by the succession of standard pressure levels, as identified in Table 2 under the heading CB(I).

A linear combination of the anomalies of a single thickness, H , and of the static stabilities of each of the 16 layers, as identified in Table 2 under the heading CC(I). We have chosen the thickness from 1000 to 300 mb; most of the variance of the atmospheric thermal structure is resolved by specification of this thickness.

We consider these to be the major expressions. Others can be designed within the linearities of the mass-structure model.

We were provided with the transmission functions for an operational Air Force VTPR sounder, for a set of channels at a set of nadir angles. Each transmission function was tabled in 69 equal increments in p^{κ}, from 1000 mb to 0.01 mb. We produced a complete set of standard radiances and anomaly combination coefficients for this sounder. A sampling is here included in Tables 3, A, B and C. The legend corresponds to Table 2.

Table 3 A

Transformation Table for Channel 668.4 angles 25° and 30°

FREQUENCY = 668,40 ANGLE = 25,00

ASSOCIATED PRESSURE: P= 11,96 P**KAPPA= 2,031933

STANDARD RADIANCE = 49,992937710 = 0,000000000 + 49,992937710

RADIANCE ANOMALY: GC= 0,000000000 X T(G)

I	C(I)	CA(I)	CB(I)	300-1000 MB CC(I)
1	,122530659	,001188542	,001188542	,001494068
2	,274365937	,011421784	,012610326	,000391261
3	,091101754	-,008396365	,004213960	,000608934
4	,112219104	,002955201	,007169161	,000655156
5	,111508215	,000807218	,007976380	,000694772
6	,096231677	-,000352803	,007623577	,000657161
7	,070346954	-,001199977	,006423600	,000588068
8	,049627105	-,001471789	,004951811	,000649513
9	,025381471	-,002599825	,002351986	,000539430
10	,006891675	-,001799339	,000552646	,000376215
11	,001112428	-,000441605	,000111041	,000282352
12	,000128734	-,000101162	,000009879	,000307824
13	0,000000000	-,000010645	-,000000765	,000246977
14	0,000000000	,000000922	,000000155	,000192570
15	0,000000000	-,000000168	-,000000013	,000096329
16	0,000000000	,000000017	,000000004	,000030902
17	0,000000000	-,000000004	-,000000001	,009102944
18		,000000001		,000000000

FREQUENCY = 668,40 ANGLE = 30,00

ASSOCIATED PRESSURE: P= 11,55 P**KAPPA= 2,011899

STANDARD RADIANCE = 50,140762727 = 0,000000000 + 50,140762727

RADIANCE ANOMALY: GC= 0,000000000 X T(G)

I	C(I)	CA(I)	CB(I)	300-1000 MB CC(I)
1	,126234032	,001225849	,001225849	,001539225
2	,277934210	,011433327	,012659176	,000396349
3	,091478368	-,008429966	,004229210	,000615378
4	,112689724	,002975152	,007204362	,000660901
5	,111295755	,000759945	,007954308	,000699041
6	,095378879	-,000407476	,007556832	,000659272
7	,069118783	-,001243223	,006313609	,000588278
8	,047906514	-,001528672	,004784937	,000647533
9	,023797600	-,002589390	,002195547	,000536102
10	,006117430	-,001728456	,000467091	,000373276
11	,000947531	-,000371371	,000095720	,000280040
12	,000099008	-,000090122	,000005598	,000305281
13	0,000000000	-,000006032	-,000000434	,000244937
14	0,000000000	,000000522	,000000088	,000190979
15	0,000000000	-,000000095	-,000000007	,000095534
16	0,000000000	,000000010	,000000002	,000030646
17	0,000000000	-,000000003	-,000000000	,009027743
18		,000000000		,000000000

Table 3 B

Transformation Table for Channel 677 angles 55° and 57.5°

FREQUENCY = 677,00   ANGLE = 55,00

ASSOCIATED PRESSURE: P= 22,69   P**KAPPA= 2,439987

STANDARD RADIANCE = 46,078737826 = 0,000000000 + 46,078737826

RADIANCE ANOMALY: GC= 0,000000000 X T(G)

I	C(I)	CA(I)	CB(I)	300-1000 MB CC(I)
1	,054038693	,000518668	,000518668	,000658917
2	,142336372	,006363416	,006882081	,000202979
3	,082283641	-,002644245	,004237836	,000379874
4	,120699380	,003326148	,007563984	,000492649
5	,140820787	,002472131	,010036115	,000609732
6	,138937842	,000979630	,011015745	,000649398
7	,111795766	-,000650588	,010365157	,000629956
8	,082335241	-,002062612	,008302545	,000732891
9	,040031277	-,004606014	,003696531	,000621408
10	,008626259	-,003165470	,000531961	,000433969
11	,001017929	-,000436153	,000094708	,000325517
12	,000156742	-,000075261	,000019647	,000354889
13	,000003066	-,000020639	-,000000993	,000284742
14	0,000000000	,000001194	,000000201	,000222015
15	0,000000000	-,000000218	-,000000017	,000111059
16	0,000000000	,000000022	,000000005	,000035627
17	0,000000000	-,000000006	-,000000001	,010494845
18		,000000001		,000000000

FREQUENCY = 677,00   ANGLE = 57,50

ASSOCIATED PRESSURE: P= 21,70   P**KAPPA= 2,409060

STANDARD RADIANCE = 46,265691395 = 0,000000000 + 46,265691395

RADIANCE ANOMALY: GC= 0,000000000 X T(G)

I	C(I)	CA(I)	CB(I)	300-1000 MB CC(I)
1	,056800186	,000545745	,000545745	,000692589
2	,147597779	,006550803	,007096548	,000210482
3	,084451583	-,002734817	,004361731	,000392320
4	,123156720	,003363943	,007725674	,000506311
5	,142251483	,002429075	,010154749	,000622849
6	,138629315	,000842882	,010997631	,000658970
7	,109726187	-,000820112	,010177519	,000634948
8	,078462247	-,002245471	,007932047	,000732941
9	,036091009	-,004637818	,003294229	,000617044
10	,007102529	-,002911696	,000382533	,000429686
11	,000756239	-,000309839	,000072694	,000322133
12	,000127179	-,000055952	,000016741	,000351178
13	,000003066	-,000017509	-,000000767	,000281764
14	0,000000000	,000000923	,000000155	,000219693
15	0,000000000	-,000000168	-,000000013	,000109897
16	0,000000000	,000000017	,000000004	,000035254
17	0,000000000	-,000000004	-,000000001	,010385087
18		,000000001		,000000000

Table 3 C

Transformation Table for Channel 746.5 angles 0° and 10°

FREQUENCY = 746,50   ANGLE = 0,00

ASSOCIATED PRESSURE: P= 700,44   P**KAPPA= 6,500743

STANDARD RADIANCE = 89,219897408 = 45,277022937 + 43,942874471

RADIANCE ANOMALY: GC= ,626594317 X T(G)

I	C(I)	CA(I)	CB(I)	300-1000 MB CC(I)
1	,001848667	,000017840	,000017840	,000022542
2	,004523313	,000194549	,000212388	,000006450
3	,002490520	-,000089051	,000123338	,000011845
4	,003827063	,000113534	,000236672	,000015466
5	,005249576	,000114895	,000351567	,000020412
6	,006834653	,000176347	,000527914	,000024652
7	,008232029	,000211915	,000739828	,000028520
8	,011723397	,000281151	,001020979	,000043353
9	,016459664	,000515452	,001536431	,000052508
10	,019005922	,000707007	,002243438	,000052111
11	,020837654	,000936471	,003179910	,000053163
12	,032492660	,001187951	,004367860	,000062636
13	,058678837	,003492737	,007860597	-,000003149
14	,103728607	,004295510	,012156107	-,000054637
15	,153671655	,006944593	,019100700	-,000048590
16	,190206422	,009419283	,028519983	-,000009330
17	,083367789	-,006774252	,021745730	,019873231
18		-,021745730		,000000000

FREQUENCY = 746,50   ANGLE = 10,00

ASSOCIATED PRESSURE: P= 698,19   P**KAPPA= 6,494772

STANDARD RADIANCE = 89,046456921 = 44,907734327 + 44,138722604

RADIANCE ANOMALY: GC= ,621483686 X T(G)

I	C(I)	CA(I)	CB(I)	300-1000 MB CC(I)
1	,001850287	,000017828	,000017828	,000022561
2	,004612321	,000201269	,000219097	,000006577
3	,002490520	-,000099265	,000119832	,000011988
4	,003887009	,000120715	,000240548	,000015676
5	,005340843	,000117303	,000357851	,000020720
6	,006940646	,000178840	,000536691	,000025028
7	,008306311	,000208970	,000745061	,000028896
8	,011832381	,000284218	,001029079	,000043866
9	,016639976	,000523728	,001553606	,000053113
10	,019197358	,000713729	,002267335	,000052688
11	,020979170	,000931778	,003199113	,000053691
12	,032734340	,001202791	,004401905	,000063325
13	,059095734	,003515105	,007917010	-,000002621
14	,104337174	,004319783	,012236793	-,000054148
15	,154302546	,006942040	,019178033	-,000048235
16	,190744654	,009433719	,028612652	-,000009094
17	,083429948	-,006861197	,021751355	,019959612
18		-,021751355		,000000000

2.2 Normalization of the Radiance Anomalies

The purpose of the present section is to develop a feeling for the resolution powers of this Air Force sounder. The combination coefficients C(I), which apply to the temperature anomalies, are all positive--suggesting the concept of a smoothing operation. A radiance measure is, in fact, a smoother; it has such a broad-in-depth energy-source function.

Application of the concept of a smoother requires normalization of the combination coefficients. Unless already normalized,

$$\sum C_n \neq 1 \quad .$$

Normalization, i.e., scaling the radiance anomaly as a smoothed temperature anomaly, is accomplished by dividing the radiance measure by $\sum C_n$. This requirement is obvious when applying Eq. (1) to a temperature profile of constant anomaly, $\mathfrak{T}_n \equiv \mathfrak{T}$. We obtain

$$\epsilon / \sum C_n = \mathfrak{T} \quad .$$

If we are to consider a normalized radiance as a value in a smoothed temperature profile then we must also be able to associate the value with some level in the profile. In the preceding we have explained normalization on the basis of a constant temperature-anomaly profile. We now use, as basis for the definition of an associated pressure level, a temperature anomaly profile which is linear in p^κ, including the surface value. Such a profile is not altered by a smoothing operator which is symmetric in p^κ, when applied

at any level, p. On this basis we define the associated pressure level as that level where

$$\frac{\sum C_n \mathfrak{T}_n}{\sum C_n} = \mathfrak{T} \tag{2}$$

for $\mathfrak{T}$ linear in p^{κ}:

$$\mathfrak{T} = \beta(\alpha + p^{\kappa}) \quad . \tag{3}$$

The selection of interfaces, p_n, in the modelling, is immaterial for this determination. Any segment of Eq. (3) is linear in p^{κ} and the segments join up at the interfaces to form a complete linear profile.

Substitution of Eq. (3) into Eq. (2) yields the associated pressure level

$$p = \left[\frac{\sum C_n p_n^{\kappa}}{\sum C_n}\right]^{1/\kappa} \quad . \tag{4}$$

Note that Eq. (4) is independent of the α and β of Eq. (3). The implication is not that all radiances are equivalent to <u>symmetric</u> smoothing operators. An asymmetric smoother applied at any level in a linear profile produces an increase or decrease at that level. Our definition of the associated pressure level accordingly involves an upward or downward displacement of the level of application of an equivalent smoothing operator. This shift is pronounced for radiances having large surface contributions.

Calculation of this associated pressure level, for each channel and nadir angle, has been added to the general program which produces the combination coefficients. These values are found on the second line of Tables 3 A, B and C, expressed both in mb and in units of p^{κ}. The normalizing factor is obtained by summing column C(I) and adding the coefficient for the ground anomaly contribution found on the fourth line of these Tables.

Table 4 summarizes the standard radiance, the normalizing factor, and the associated pressure level in mb and in units of p^{κ}, for each channel and nadir angle of the Air Force VTPR sounder.

Table 4

Summary of Channels for Specified Zenith Angles

FREQ	ANG	STAND,RAD,	NORM,FACTOR	P	P**KAI
834,0	0,00	99,006959011	1,518409621	1008,00	7,196
668,4	0,00	49,680547940	,958161138	12,88	2,075
668,4	10,00	49,728760202	,958667467	12,74	2,068
668,4	20,00	49,876862263	,960225510	12,29	2,047
668,4	25,00	49,992937710	,961445712	11,96	2,031
668,4	30,00	50,140762727	,962997833	11,59	2,011
668,4	35,00	50,323424117	,964914149	11,07	1,987
668,4	40,00	50,547146630	,967258021	10,51	1,958
668,4	42,50	50,676764895	,968614482	10,21	1,942
668,4	45,00	50,818986784	,970100625	9,88	1,924
668,4	47,50	50,975709137	,971737685	9,54	1,904
668,4	50,00	51,148482919	,973539544	9,10	1,883
668,4	52,50	51,339265769	,975526379	8,79	1,861
668,4	55,00	51,549289174	,977710215	8,39	1,836
668,4	57,50	51,783010239	,980136719	7,97	1,809
668,4	60,00	52,042367708	,982822889	7,53	1,780
677,0	0,00	44,716063462	,907959938	33,04	2,716
677,0	10,00	44,747762727	,908296355	32,70	2,708
677,0	20,00	44,845211028	,909382937	31,69	2,684
677,0	25,00	44,923743896	,910252216	30,92	2,665
677,0	30,00	45,024900312	,911373233	29,99	2,642
677,0	35,00	45,152788811	,912799842	28,89	2,614
677,0	40,00	45,314179252	,914593758	27,62	2,580
677,0	42,50	45,408551241	,915643077	26,92	2,561
677,0	45,00	45,514393969	,916818560	26,16	2,541
677,0	47,50	45,632620643	,918131687	25,36	2,518
677,0	50,00	45,764086372	,919598616	24,52	2,494
677,0	52,50	45,913056969	,921289576	23,63	2,468
677,0	55,00	46,078737826	,923082998	22,69	2,439
677,0	57,50	46,205691395	,925195522	21,70	2,409
677,0	60,00	46,476212717	,927487079	20,65	2,375
695,0	0,00	45,219780059	,916579442	107,00	3,801
695,0	10,00	45,151993301	,915893975	105,97	3,789
695,0	20,00	44,951367066	,913862557	102,63	3,755
695,0	25,00	44,804543392	,912573138	100,12	3,728
695,0	30,00	44,630064112	,910683639	97,03	3,695
695,0	35,00	44,431743037	,908551951	93,39	3,655
695,0	40,00	44,211971525	,906344253	89,16	3,607
695,0	42,50	44,096370920	,905163789	86,82	3,580
695,0	45,00	43,978759749	,903963731	84,34	3,550
695,0	47,50	43,859997591	,902751354	81,71	3,518
695,0	50,00	43,741952200	,901546033	78,91	3,483
695,0	52,50	43,625624951	,900341941	75,97	3,446
695,0	55,00	43,510074733	,899189228	72,86	3,405
695,0	57,50	43,403458569	,898102813	69,59	3,360
695,0	60,00	43,307004403	,897133289	66,15	3,312
707,5	0,00	55,841029630	1,025595756	252,12	4,849
707,5	10,00	55,648633996	1,023763936	249,84	4,836
707,5	20,00	55,067979528	1,018243474	241,97	4,798
707,5	25,00	54,626020687	1,014038081	236,73	4,768
707,5	30,00	54,066305633	1,008863323	230,29	4,730
707,5	35,00	53,440210763	1,002695341	222,59	4,684
707,5	40,00	52,659442309	,995407505	213,46	4,629
707,5	42,50	52,273025290	,991374855	208,40	4,597
707,5	45,00	51,829719217	,987054189	202,96	4,563
707,5	47,50	51,358479614	,982451651	197,16	4,529
707,5	50,00	50,859218621	,977560178	190,96	4,484
707,5	52,50	50,331169919	,972380240	184,34	4,439
707,5	55,00	49,775521519	,966866383	177,29	4,390
707,5	57,50	49,192124991	,961067933	169,80	4,336
707,5	60,00	48,580391298	,954954924	161,82	4,277
722,0	0,00	70,520772473	1,163485716	418,67	5,580
722,0	10,00	70,301985581	1,161591945	407,79	5,569
722,0	20,00	69,634556555	1,155611645	398,98	5,535
722,0	25,00	69,119651552	1,151029074	392,20	5,509
722,0	30,00	68,474239679	1,145237578	383,70	5,473
722,0	35,00	67,687941643	1,138258721	373,37	5,431
722,0	40,00	66,745231062	1,129822306	361,05	5,379
722,0	42,50	66,209716603	1,125019425	354,06	5,349
722,0	45,00	65,628444914	1,119890701	347,43	5,316
722,0	47,50	64,997114081	1,114158756	339,27	5,280
722,0	50,00	64,311937423	1,107959444	329,40	5,240
722,0	52,50	63,570839714	1,101242938	319,80	5,196
722,0	55,00	62,767590401	1,093985201	309,43	5,147
722,0	57,50	61,895952084	1,086039171	298,24	5,093
722,0	60,00	60,950364983	1,077411705	286,14	5,033
746,5	0,00	89,219897408	1,349772745	708,44	6,500
746,5	10,00	89,046456921	1,348204903	698,19	6,494
746,5	20,00	88,511503835	1,343370328	691,12	6,479
746,5	25,00	88,094811634	1,339600961	688,64	6,461
746,5	30,00	87,568280291	1,334833454	678,67	6,442
746,5	35,00	86,917366737	1,328936029	670,04	6,418
746,5	40,00	86,123005165	1,321780368	659,50	6,389
746,5	42,50	85,663692968	1,317559577	653,42	6,372
746,5	45,00	85,161860158	1,313081126	643,71	6,354
746,5	47,50	84,608799335	1,307971392	630,35	6,333
746,5	50,00	84,001978169	1,302449479	633,23	6,310
746,5	52,50	83,331013899	1,296390918	622,29	6,284
746,5	55,00	82,592083076	1,289630118	613,43	6,256
746,5	57,50	81,775007098	1,282182149	603,47	6,223
746,5	60,00	80,868346470	1,273801982	588,31	6,187

2.3 Radiance Anomaly Expectations

Based on the transformation tables, we calculated the normalized radiance anomalies to be expected for a sampling of specified temperature-anomaly profiles. The purpose of these samples is to evaluate our contention that the normalized radiance anomalies, each at associated pressure levels, can, to a degree, be regarded as equivalent smoothed temperature-anomaly-profile values.

The profile is specified in terms of the temperature anomaly of the ground and at each of the interfaces identified in column one, C(I), of Table 2. The expected normalized radiance anomaly was calculated by linearly combining the specified temperature anomalies with the coefficient sets corresponding to each channel and nadir angle, and then dividing the summation by the sum of these coefficients in order to normalize to temperature scale. For each specified profile a plot was prepared which shows the specified temperature-anomaly profile by connected linear-in-p^{κ} segments in accordance with the mass-structure model; the calculated normalized radiance anomaly, for each channel and each nadir angle, is shown by a dot plotted at associated pressure level.

Samples are given as Figs. 2, 3, 4, 5, and 6. The vertical scale is linear in p^{κ}, rescaled in mb on the right. The horizontal scale is linear in temperature anomaly; the calibration is irrelevant. The profile connects horizontally, at 1000 mb, to the ground temperature anomaly if it differs from the air temperature anomaly (See, e.g., Fig. 3).

Figure 2 is a demonstration showing the general character of the sounder. Each of the six strings of dots corresponds to one of the six channels as identified in Table 4.

Figure 3 demonstrates the ground contribution.

Figure 4, depicting a cold anomaly ranging from 450 mb to 85 mb, demonstrates that the normalized radiance anomalies cannot be strictly interpreted as smoothed temperature-anomaly-profile values. Note the discontinuities between channels. These discontinuities do not relate to channel calibrations, but rather to the differential character of channel source functions. Figure 5 shows that the shift between channels can also be of the other sign. This disparity in channel-to-channel smoothness is associated with enhanced vertical discrimination powers of the sounder. By the same token, the angle-to-angle smoothness for any <u>one</u> channel demonstrates that little is added as to <u>vertical</u> discrimination powers by views over a range of zenith angles.

Figure 6 demonstrates the concept of the normalized radiance anomaly and associated pressure level. This anomaly profile is linear in p^{κ}. All dots fall on the profile by definition.

The surface contribution can be removed from each channel radiance by sacrificing one channel for that purpose. For example, the window channel may be used for that purpose. However, in our calculated profile examples this is accomplished by merely setting the coefficient for the ground contribution to zero. The normalizing factor, and associated pressure for each radiance, change according to definition. Figures 7, 8 and 9 are a repeat of profiles shown in Figs. 2, 4 and 5 respectively, without ground contribution in the calculated radiances.

These examples, with and without ground contribution, demonstrate the following: the angle-to-angle normalized-radiance-anomaly continuity for any one channel is pronounced and can be interpreted as a smoothing of the temperature-anomaly profile at associated pressure levels. Whereas a coarse continuity in normalized radiance anomaly exists from one channel to the next, strict continuity is not to be imposed in processing true radiances, or in relative calibrations.

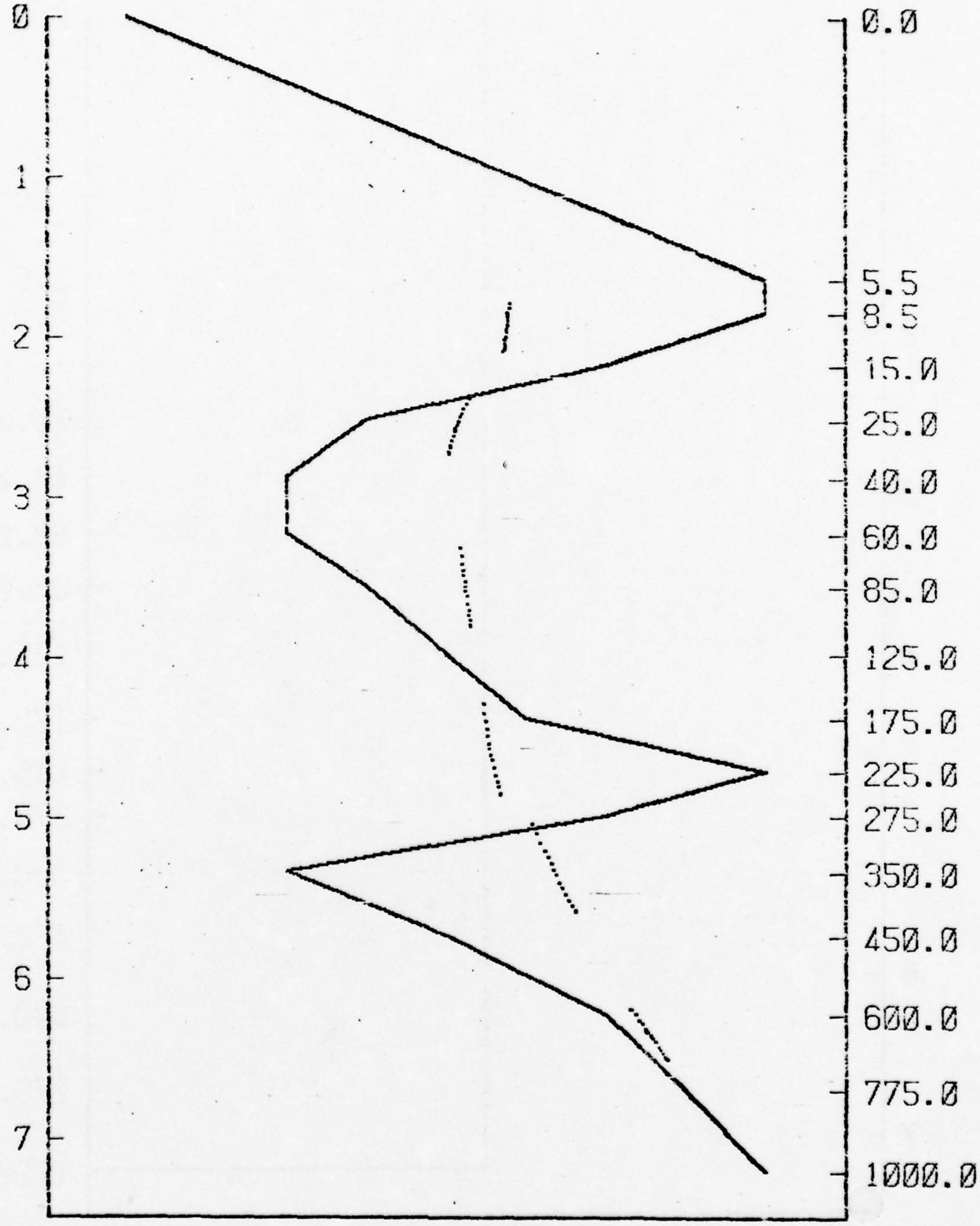

Fig. 2 A specified temperature anomaly profile and plotted values of calculated normalized radiance anomalies.

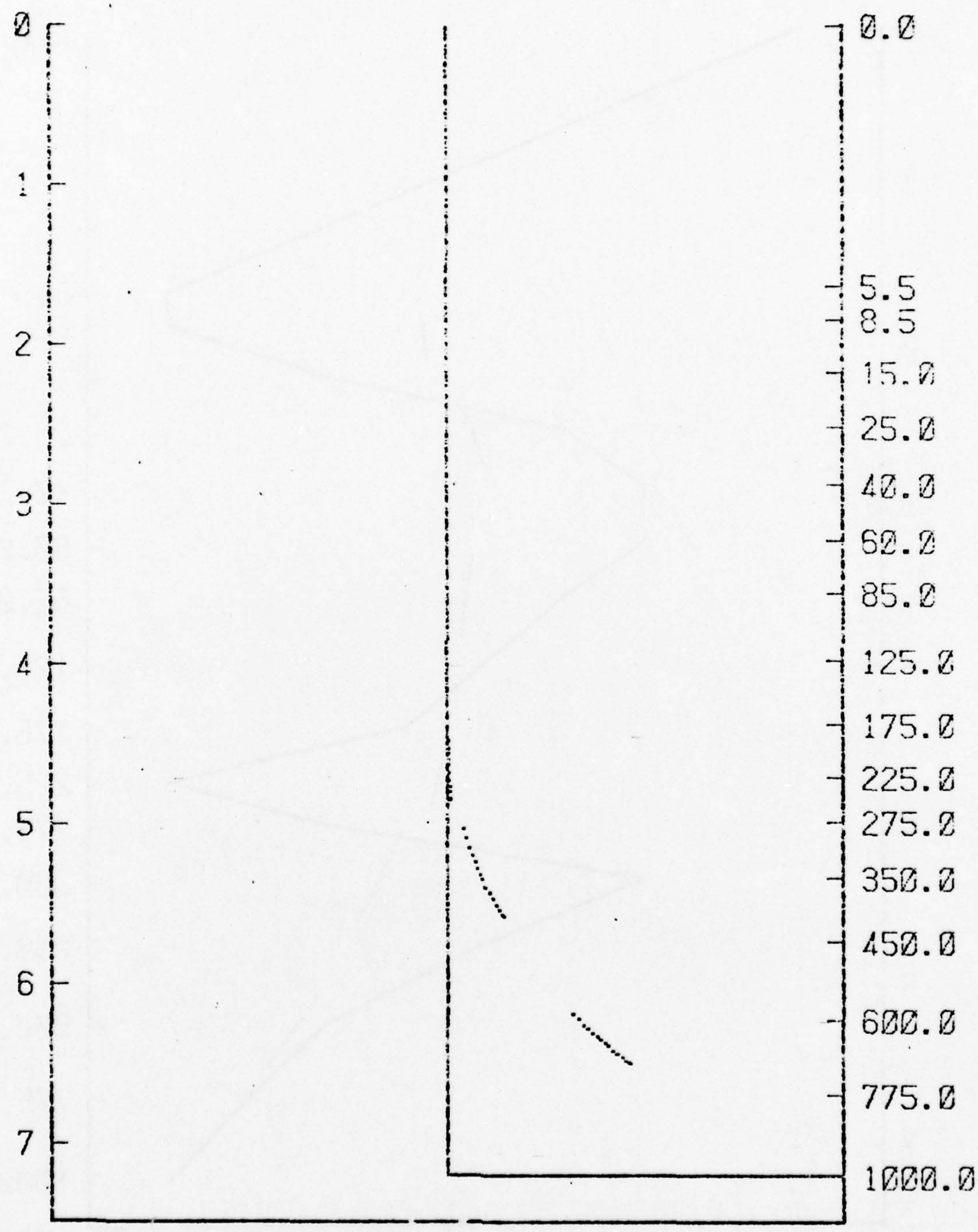

Fig. 3 A specified temperature anomaly profile and plotted values of calculated normalized radiance anomalies.

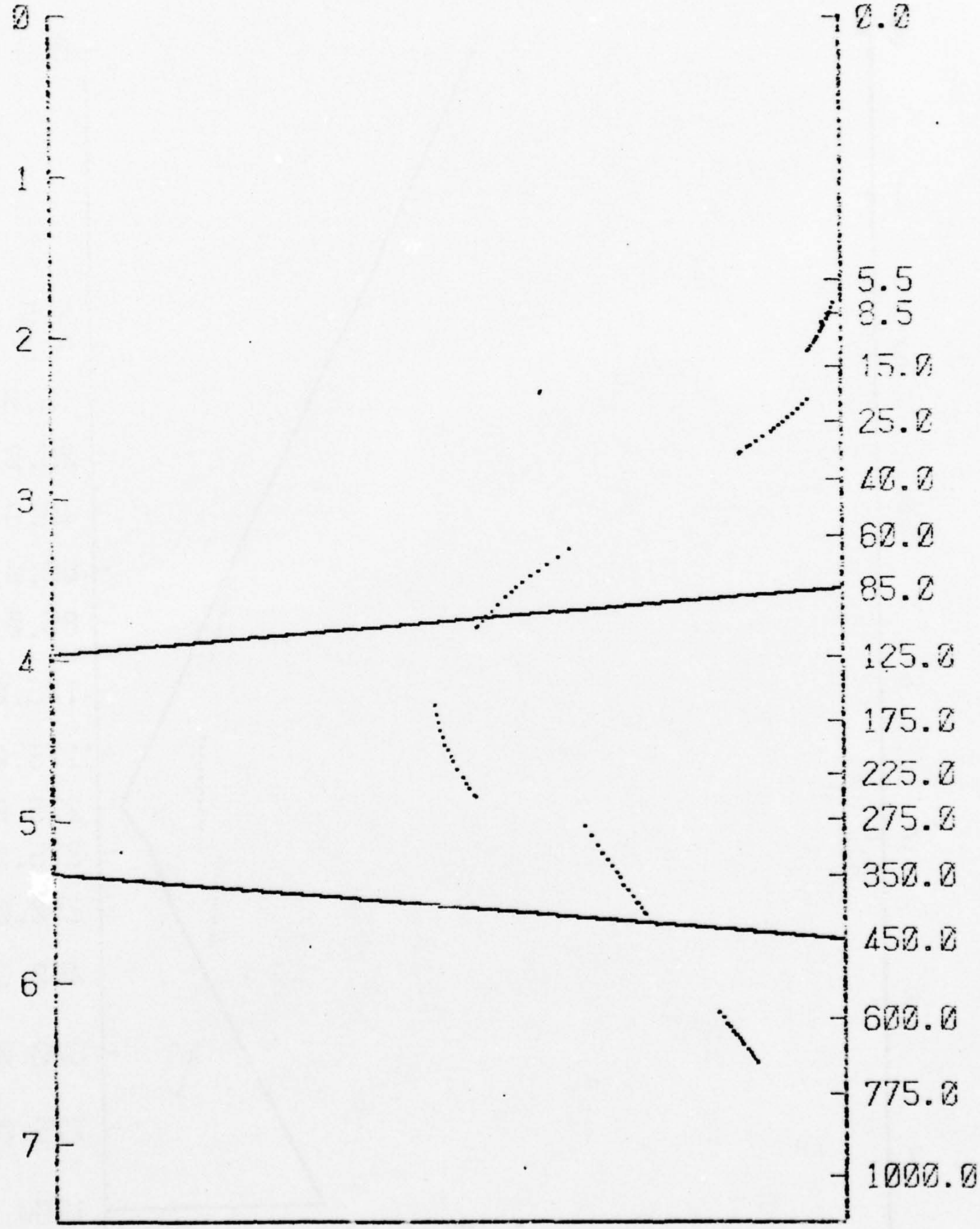

Fig. 4 A specified temperature anomaly profile and plotted values of calculated normalized radiance anomalies.

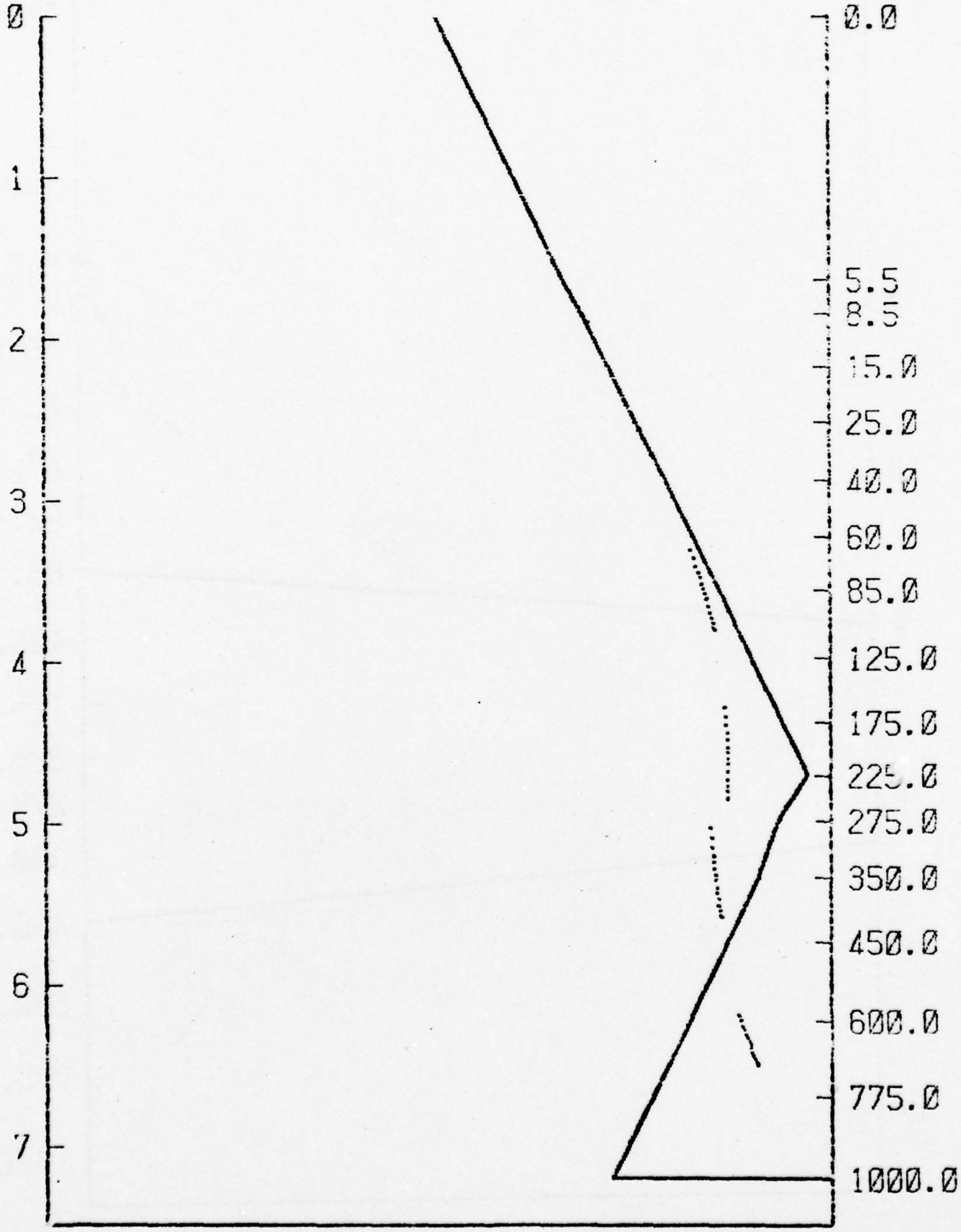

Fig. 5 A specified temperature anomaly profile and plotted values of calculated normalized radiance anomalies.

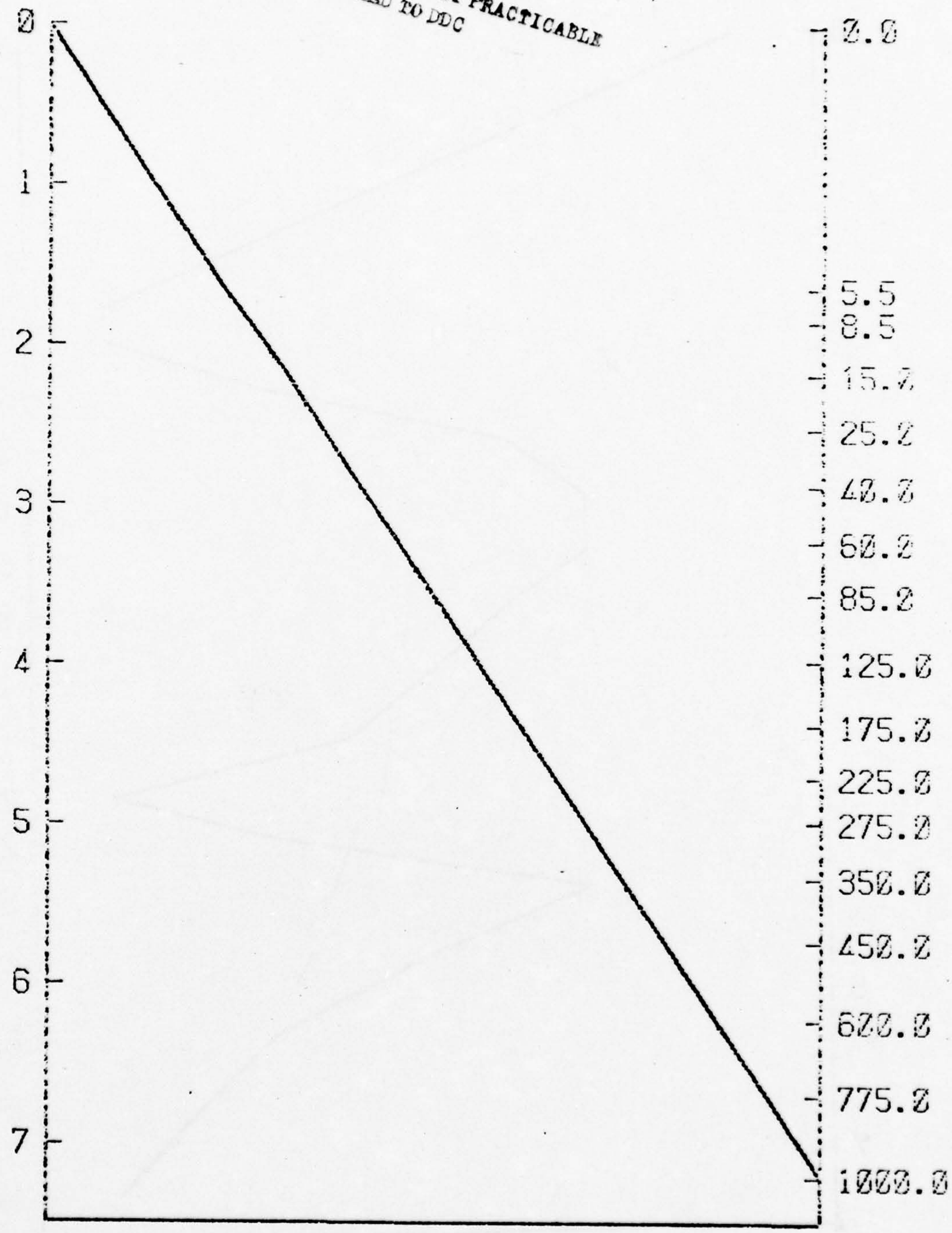

Fig. 6 A specified temperature anomaly profile and plotted values of calculated normalized radiance anomalies.

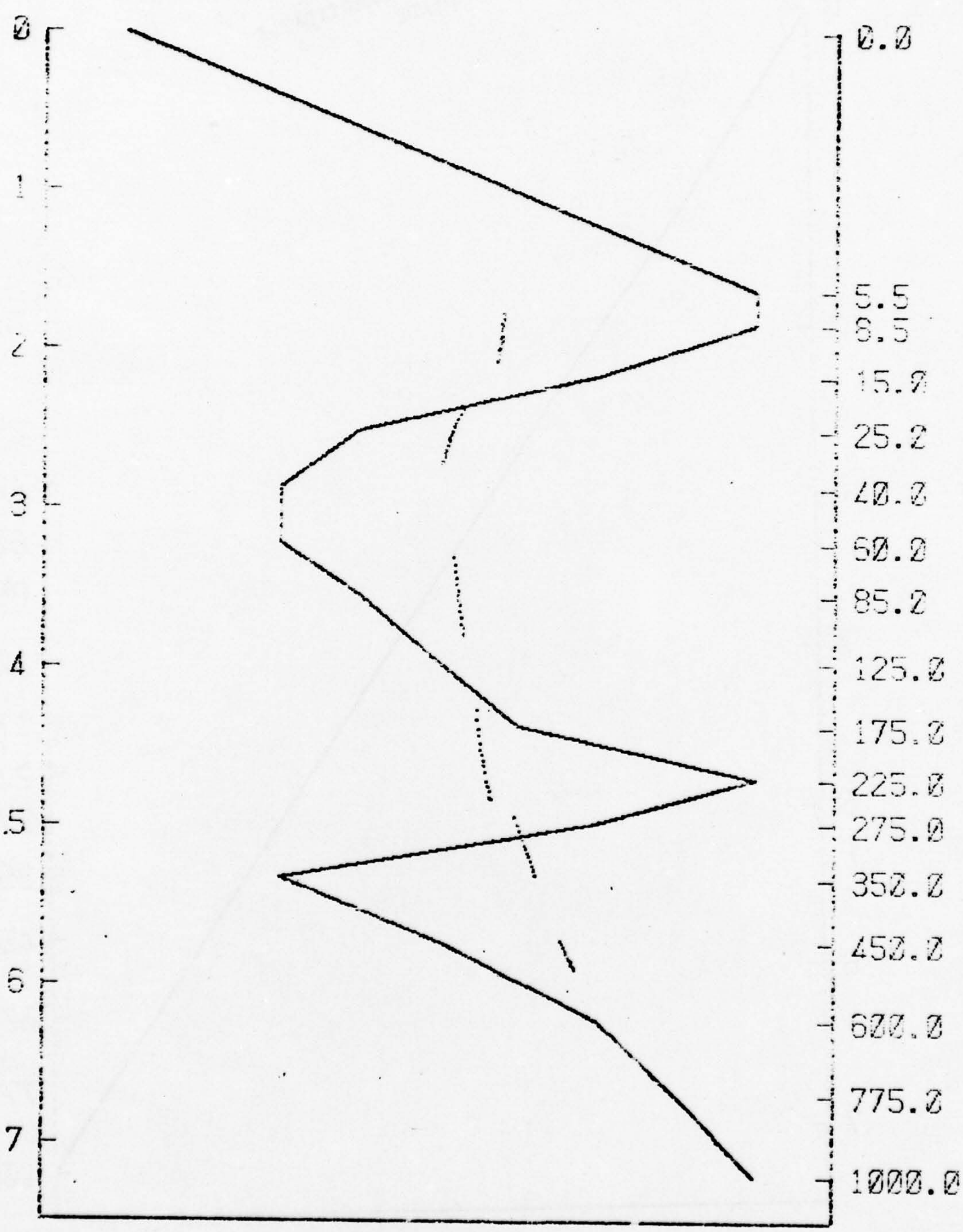

Fig. 7 A specified temperature anomaly profile and plotted values of calculated normalized radiance anomalies without ground contribution.

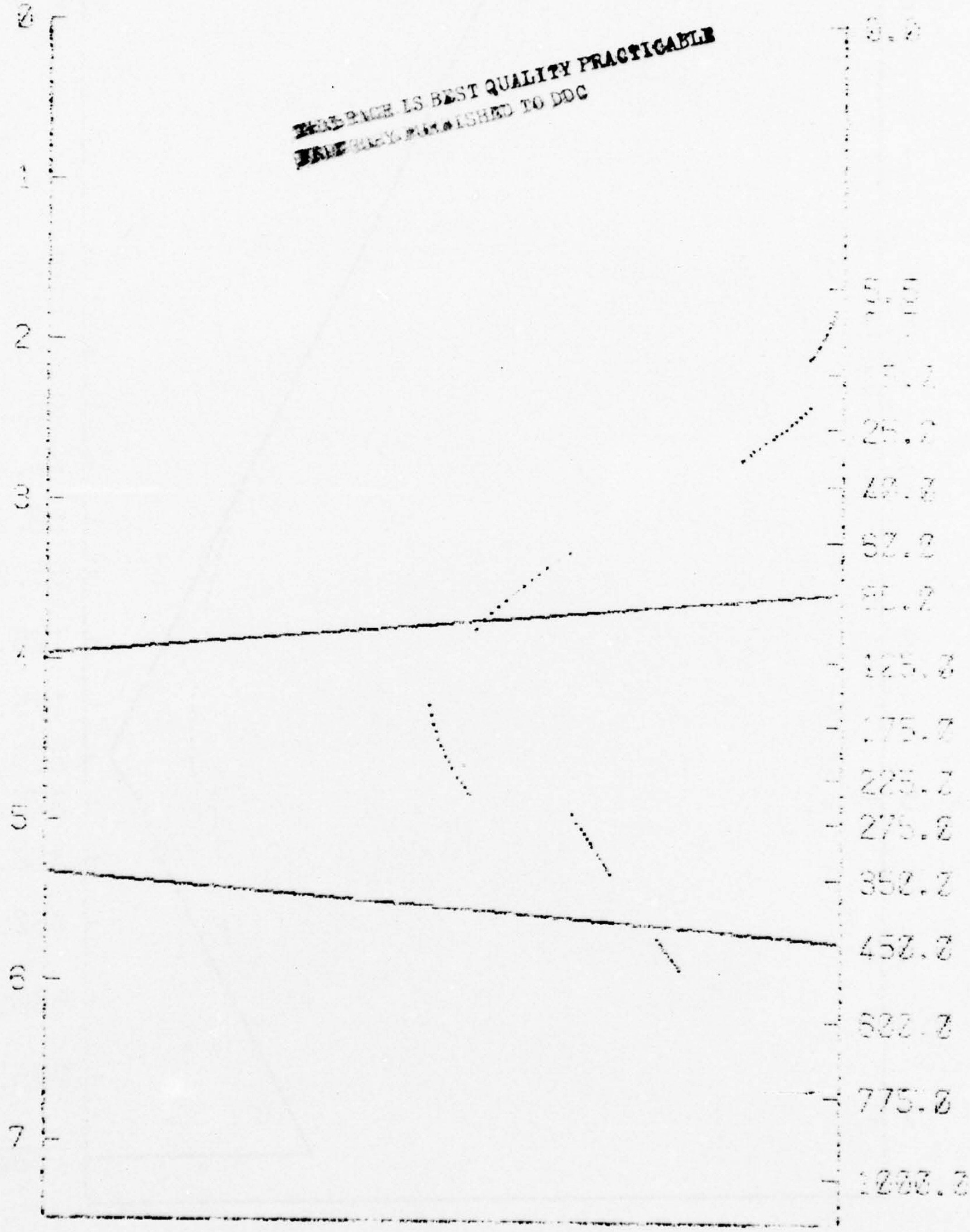

Fig. 8 A specified temperature anomaly profile and plotted values of calculated normalized radiance anomalies without ground contribution.

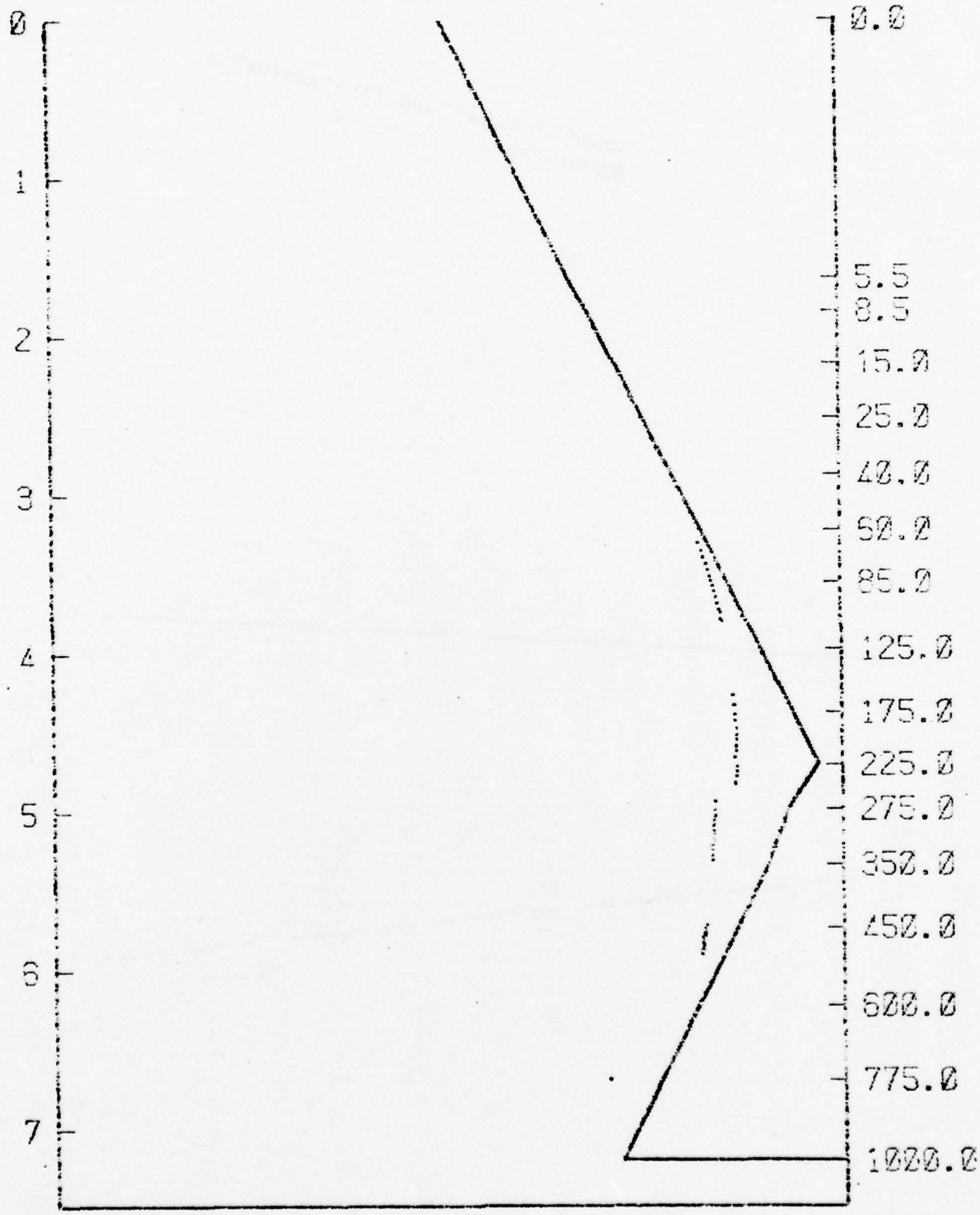

Fig. 9 A specified temperature anomaly profile and plotted values of calculated normalized radiance anomalies without ground contribution.

2.4 Processing of Real Satellite Data

We were provided with a sample of raw radiances measured by the Air Force VTPR sounder in orbits of March 26, 1974. These data include full side-to-side scans with the position of each spot given in latitude and longitude, and with nadir angle, and time data.

The specified nadir angles are not limited to the discrete values for which we have generated tables. For nadir angles which fall between our tables, linear interpolation is used for tabled quantities.

We have processed each complete side-to-side scan into a cross section. Standard radiances are removed to form radiance anomalies which are then normalized for plotting at associated pressure levels. The decimal point marks the cross-section position of each normalized radiance anomaly. The vertical coordinate of the cross section is linear in p^{κ}. Sample cross sections begin with Fig. 10.

The horizontal coordinate of the cross section is calibrated in units of standard grid length measured along the scan base line. For each spot viewed, the grid locations are given below the base line, with I above J. These grid coordinates are for the standard 63x63 grid array for the northern-hemisphere polar-stereographic projection.*

The purpose of these cross sections is a graphical rendering to facilitate subjective examination of the character of the radiances and the nature of cloud contamination. In a cloud-free section, over open ocean, the normalized-radiance-anomaly values for any one channel, strung across the section, can generally be expected to be relatively smooth (See, e.g., Fig. 10). Any lack of smoothness generally implies cloud discontinuities, or abrupt changes in surface temperature. In both cases, cloud or ground induced, the discontinuities become less pronounced for channels with higher (i.e., smaller pressure) associated levels,

*As shown in Fig. 13, page 59.

reflecting a decrease in the contribution of lower levels to these channels. These characteristics are demonstrated in Fig. 12.

About eighty of these cross sections were produced. On the whole, the radiance values appear credible. The discontinuities from channel to channel generally appear to be small and acceptable. In some cases--such as in Figs. 10 and 11--the discontinuities between lower channels appear to be rather pronounced. However, we are not as yet in a position to comment on relative and/or absolute calibration of channels.

We have studied these cross sections and other graphical formats in order to evaluate cloud-top models and in order to develop our approach for diagnosing the radiances for their clear-column components.

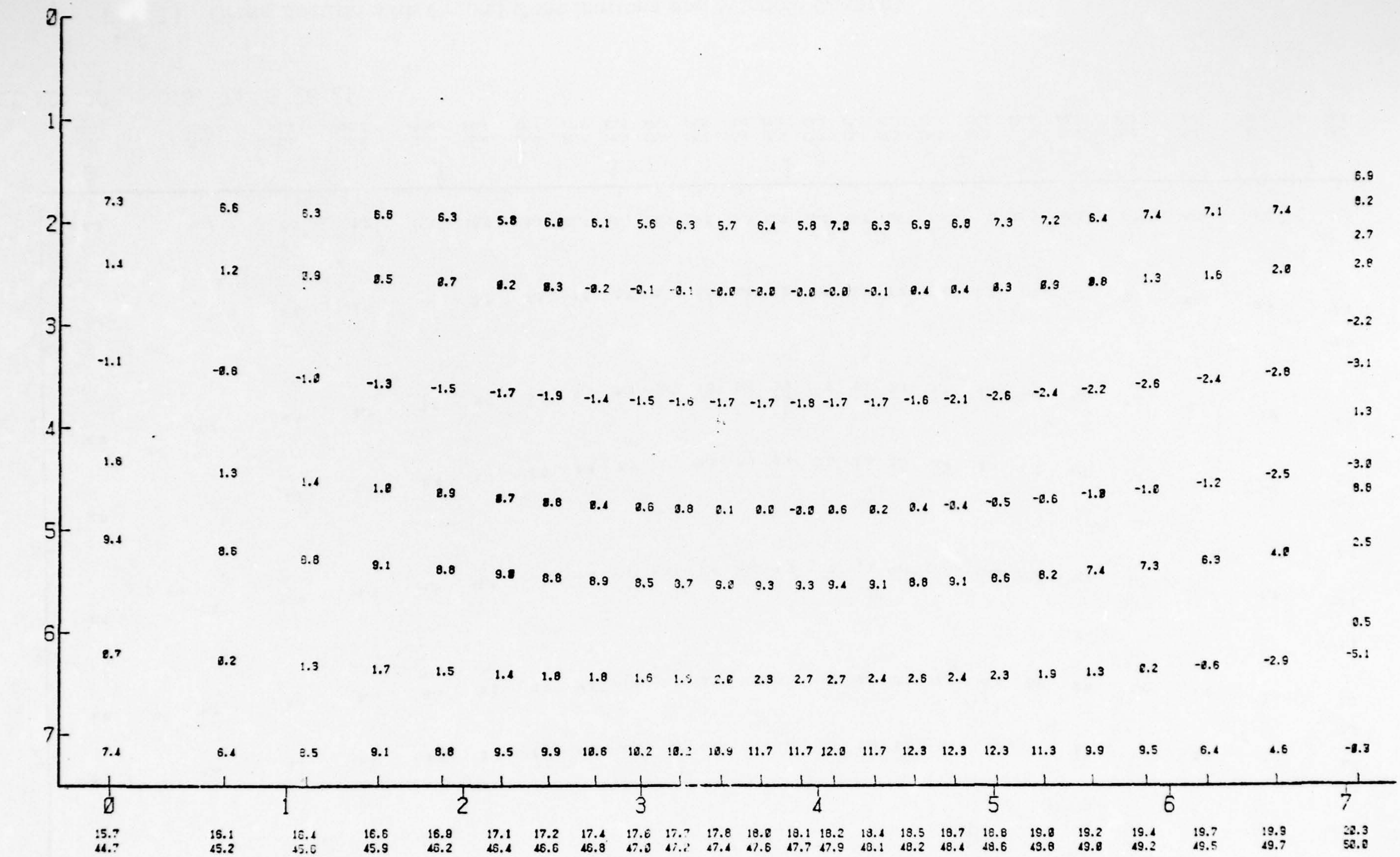

REC NO. 19 DTG. 74 3 26 21

Fig. 10 Cross Section with Ground Contributions and Window Channel

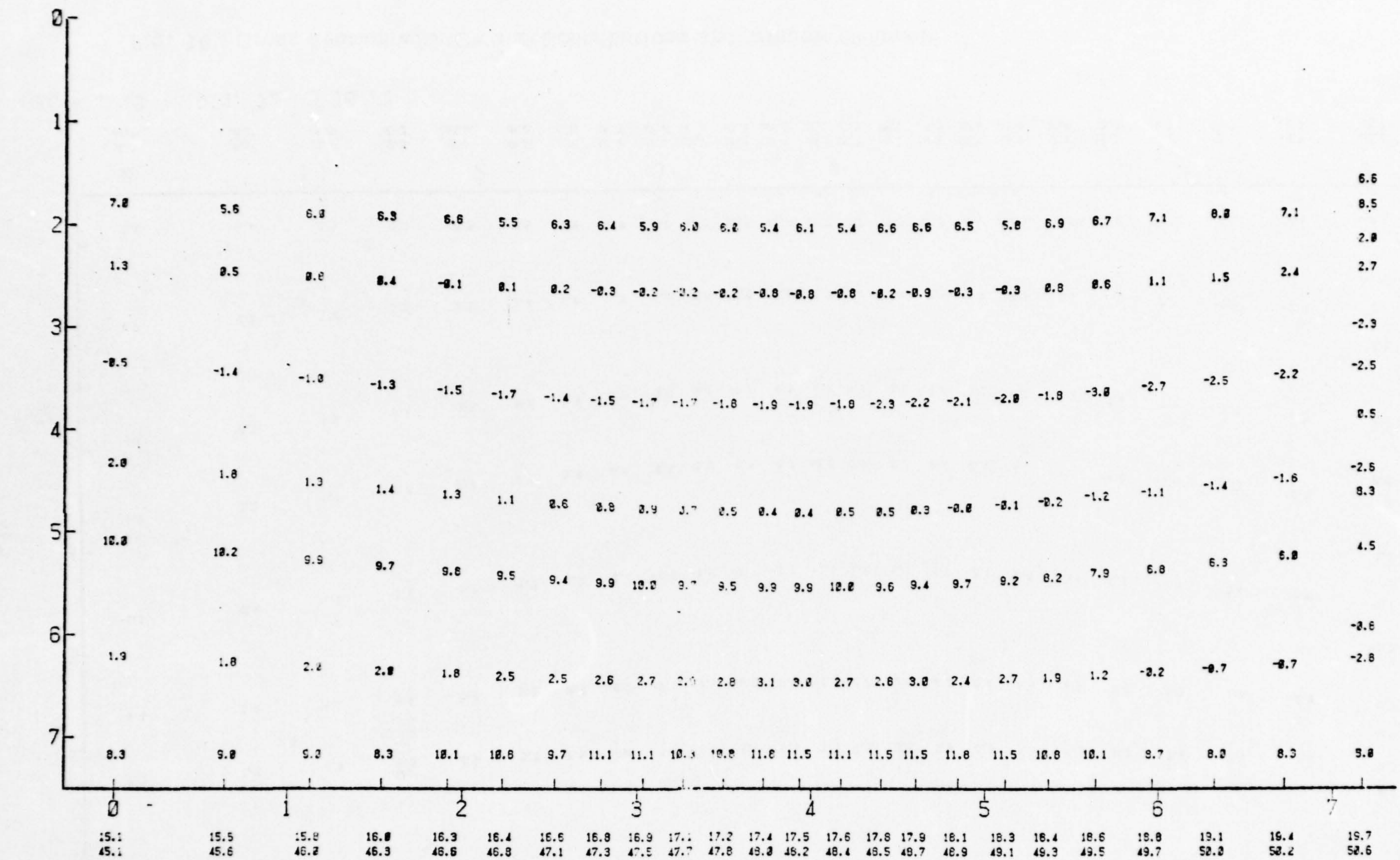

REC NO. 20 DTG. 74 3 26 21

Fig. 11 Cross Section with Ground Contributions and Window Channel

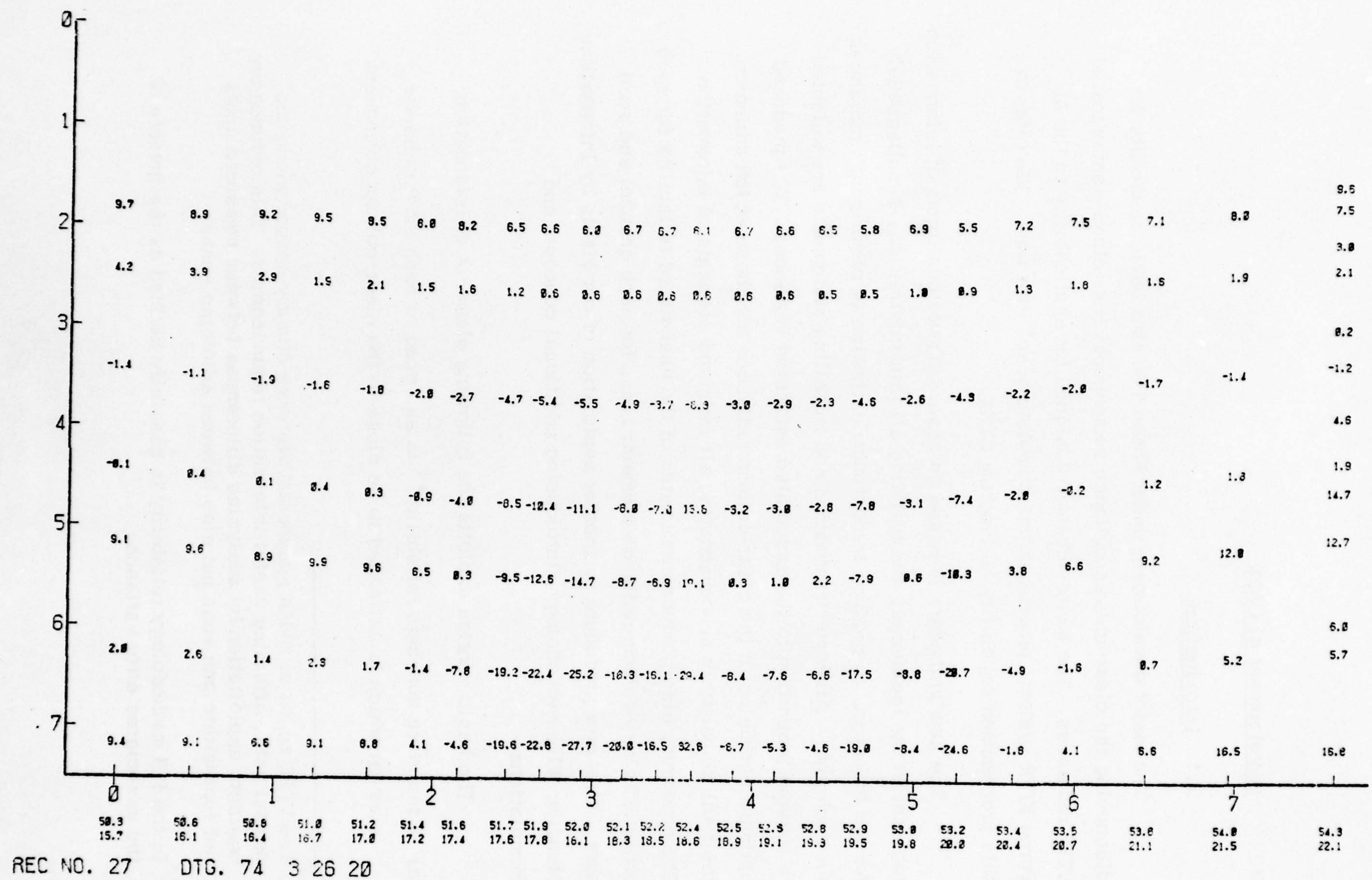

Fig. 12 Cross Section with Ground Contributions and Window Channel

3. Development of CLRX

3.1 Introduction

The major development under Phase Two is a basic capability for diagnosing the clear-column radiance components from cloud-contaminated VTPR radiances. The basic scheme, designed for applicability to the Air Force VTPR system, processes one complete scan* at a time. We refer to this programmed capability as Program CLRX.

The new procedure is based on assessing various forms of information inherent in the radiances, and blending all this information, simultaneously for the full scan, to produce the optimum estimates of clear-colum radiances for each spot. All input information and modelling statements are weighted in inverse proportion to the associated estimated variances. The produced optimum estimates of the clear-column radiances are those which minimize the total disparity in accommodating all weighted elements of information. The procedure also produces estimates of the associated reliability for each produced clear-column radiance element; i.e., for each channel and scan spot. This new procedure is another application of our Fields by Information Blending (FIB) methodology, introducing additional concepts and formulations.

The basic version exploits the following elements of information:

(a) A tentative non-zero reliability** is assigned to each VTPR radiance element which is estimated to be close to the clear-column component

*The VTPR scans of NOAA spacecraft are more closely spaced along the orbital path, affording useful information redundancies. This redundancy warrants exploitation by analyzing differences between measured spots not just within one scan but also between adjoining scans.

**In the FIB methodology reliability is generally defined as the inverse of the associated error variance.

for that element. This assessment is based on the variance character for spots and channels in the ambience of the element.

(b) An information statement which states that the clear-column component for each channel does not vary abruptly from spot to spot across the scan. This smoothness condition can generally be imposed on all channels in oceanic regions. The basic version is designed for application in oceanic regions.

(c) A model for interpreting cloud contamination. The interpretation model is based on the following consideration: For any pair of spots, in proximity to each other, the largest difference between them--of significance to the radiation--is generally the amount of cloud of a single cloud-top level. Even a cursory inspection of satellite videographs confirms this impression. Based on this interpretation, large differences in radiance between nearby spots produce estimates of the correction axis (i.e., unit vectors) for adjusting the measured radiances toward their clear-column components.

(d) Independent Sea-Surface Temperature (SST) information. This new capability does not involve any categorical use of independent SST information. However, any available estimates of SST, and/or SST gradient along a scan, can be exploited to enhance the resolution of the clear radiance components. Other independent information, especially radiance estimates derived from preliminary upper-air analyses and extrapolation, can be exploited by this capability.

The application of the FIB methodology includes the following component operations:

- The input of VTPR radiances, and the derivation and weighting of all elements of information, is called the assembly operation. Assembly includes input of independent sources of information such as transformed sea-surface temperature estimates and difference estimates along the scan base.

- Assembly is followed by the blending operation which may be performed by iterative solution or by explicit matrix inversion schemes. The blending operation produces the resultant of all assembled information: the clear-column radiance elements and their associated reliabilities.

- The reevaluation and error-checking operation follows the blending. All tentatively assigned weights are subjected to reevaluation in comparison to the corresponding implications of all information.

- Recycling: The blending is repeated using reevaluated information statements. This is followed by a second reevaluation and a final blending.

The resultant clear-column estimates will generally be of uneven accuracy as indicated by the distribution of associated reliability estimates. There will be great variations in associated reliabilities within scans, varying from channel to channel and spot to spot, and there will be large variations from scan to scan. The associated distribution of reliability estimates, produced for each scan, will depend on the quality of the input information and on the character of the scan: the distribution of cloudiness and the degree of spot-to-spot compliance with the imposed interpretation model.

The associated reliabilities can be used for categorical acceptance or rejection of the individual diagnosed clear-column radiance components.

Properly tuned, the associated reliabilities can be more fully exploited as weights for the radiance estimates in comprehensive methods for thermal-structure resolution. The reliabilities can also be used to select spots having highest resolution, for retrievals of individual thermal profiles.

A major benefit of a scanning sensor is its resolution of gradient along scans. The new procedure addresses this information component of the VTPR system in producing the full scan for each channel.

3.2 The Two-State Interpretation Model

An interpretation model forms the basis for diagnosing the VTPR radiances for their clear-column components. The simplest such model is the two-state model.

The two-state model allows any spot to be a mixture of clear portions and of cloudy portions for which all cloud top is at the same level. Furthermore, the effectiveness of the model depends on having pairs of spots, in proximity, for which the cloud top is at the same level but which differ in cloud proportion. These and other conditions are involved in the effectiveness.

Based on this model an arbitrary VTPR radiance may be expressed as a combination of a cloud-top component and a clear-column component:

$$\mathfrak{J}^{P}_{\nu,n} = x_n \mathfrak{J}^{c}_{,n} + \left(1 - x_n\right) \mathfrak{J}^{*}_{\nu,n} , \qquad (5)$$

where $\mathfrak{I}$ denotes the radiance expressed as a normalized radiance anomaly,

subscript ν denotes an arbitrary channel,

subscript n denotes an arbitrary spot,

x denotes the proportion of cloudy area,

superscript P denotes a VTPR radiance,

superscript c denotes the cloud-top radiance component, and

superscript * denotes the clear-column radiance component.

Expressed in terms of cloud proportion, Eq. (5) takes the form

$$x_n = \frac{\mathfrak{I}^*_{\nu,n} - \mathfrak{I}^P_{\nu,n}}{\mathfrak{I}^*_{\nu,n} - \mathfrak{I}^c_{\nu,n}} \quad . \tag{6}$$

The cloud proportion applies to every channel of the n-th spot.

It is convenient to introduce a vector notation: Any parameter which takes on a value for each channel of a spot may be expressed as a vector for that spot--one element per channel. For example, $\underset{\sim}{\mathfrak{I}}^P_n$ denotes the set of VTPR radiances for the n-th spot:

$$\underset{\sim}{\mathfrak{I}}^P_n \equiv \left(\mathfrak{I}^P_{1,n}, \mathfrak{I}^P_{2,n}, \ldots \mathfrak{I}^P_{\nu,n}, \ldots \mathfrak{I}^P_{7,n} \right) \quad . \tag{7}$$

Accordingly we define the vectors $\underset{\sim}{\varphi}_n$ and $\underset{\sim}{\theta}_n$:

$$\varphi_{\nu,n} \equiv \mathfrak{I}^*_{\nu,n} - \mathfrak{I}^P_{\nu,n} \tag{8}$$

$$\theta_{\nu,n} \equiv \mathfrak{I}^*_{\nu,n} - \mathfrak{I}^c_{\nu,n} \quad . \tag{9}$$

It is apparent from Eq. (6) that these vectors are parallel:

$$\underset{\sim}{\varphi}_n = x_n \underset{\sim}{\theta}_n \quad . \tag{10}$$

According to Eq. (5) the VTPR radiance difference between two spots, n and n+1, is expressed by

$$\mathfrak{I}^P_{\nu,n+1} - \mathfrak{I}^P_{\nu,n} = x_{n+1}\, \mathfrak{I}^C_{\nu,n+1} + \left(1 - x_{n+1}\right) \mathfrak{I}^*_{\nu,n+1}$$

$$- x_n\, \mathfrak{I}^C_{\nu,n} - \left(1 - x_n\right) \mathfrak{I}^*_{\nu,n} \quad . \tag{11}$$

This equation may be rewritten in the form:

$$\mathfrak{I}^P_{\nu,n+1} - \mathfrak{I}^P_{\nu,n} = \left(x_n - x_{n+1}\right) \left(\mathfrak{I}^*_{\nu,n} - \mathfrak{I}^C_{\nu,n}\right)$$

$$+ x_{n+1} \left(\mathfrak{I}^C_{\nu,n+1} - \mathfrak{I}^C_{\nu,n}\right)$$

$$+ \left(1 - x_{n+1}\right) \left(\mathfrak{I}^*_{\nu,n+1} - \mathfrak{I}^*_{\nu,n}\right) \quad . \tag{12}$$

Of the three terms on the right-hand side of Eq. 12 the first term will dominate if

(1) there is a significant difference in cloud amount from one spot to the other,

(2) there is a significant difference between the clear and the cloud-top radiance components, and

(3) there is relatively little change in each of the two radiance components from one spot to the other. This implies that the cloud tops are at the same level in both spots.

The probability that these conditions are satisfied is enhanced if the two spots are in proximity. Except that in regions of extensive overcast the first condition is not satisfied. For those channels for which a significant portion of the clear-column component is contributed by the underlying surface, the probability is enhanced over ocean areas.

The larger the VTPR radiance difference between spots the more likely it is that the right-hand side is dominated by the first term.

Based on these conditions, Eq. (12) reduces to

$$\mathfrak{I}^{P}_{\nu,n+1} - \mathfrak{I}^{P}_{\nu,n} = \left(x_n - x_{n+1}\right)\theta_{\nu,n} \quad . \tag{13}$$

Introduce another vector, $\underset{\sim}{\psi}_n$, with elements

$$\psi_{\nu,n} \equiv \mathfrak{I}^{P}_{\nu,n+1} - \mathfrak{I}^{P}_{\nu,n} \quad . \tag{14}$$

Equation (13) states that

$$\underset{\sim}{\psi}_n = \left(x_n - x_{n+1}\right)\underset{\sim}{\theta}_n \quad . \tag{15}$$

The vector $\underset{\sim}{\psi}_n$ is parallel to the vector $\underset{\sim}{\theta}_n$, in the same or in opposite direction.

Equations (10) and (15) combine to yield

$$\underset{\sim}{\varphi}_n = \frac{x_n}{x_n - x_{n-1}}\underset{\sim}{\psi}_n \quad . \tag{16}$$

The vector $\underset{\sim}{\varphi}_n$ is the adjustment to be added to the VTPR radiance vector for the n-th spot, to form the clear-column radiance vector:

$$\underset{\sim}{\mathfrak{I}}^{*}_{n} = \underset{\sim}{\mathfrak{I}}^{P}_{n} + \underset{\sim}{\varphi}_{n} \quad . \tag{17}$$

The vector $\underset{\sim}{\psi}_n$ is an ambient spot-to-spot difference between the measured VTPR radiances. Under suitable conditions the vector $\underset{\sim}{\psi}_n$ gives an approximation of the <u>vector axis</u> for the adjustment vector $\underset{\sim}{\varphi}_n$. The scalar proportionality factor of Eq. (16) is not directly resolved by the VTPR radiances.

In the ambience of the n-th spot several estimates of the adjustment vector axis may be formed using the spots from a single scan:

From single differences:

$$\underset{\sim}{\mathfrak{I}}^{P}_{n+m} - \underset{\sim}{\mathfrak{I}}^{P}_{n+m-1} \qquad \text{for } m = -1, 0, 1, 2$$

From double differences:

$$\underset{\sim}{\mathfrak{I}}^{P}_{n+m} - \underset{\sim}{\mathfrak{I}}^{P}_{n+m-2} \qquad \text{for } m = 0, 1, 2$$

From triple differences:

$$\underset{\sim}{\mathfrak{I}}^{P}_{n+m} - \underset{\sim}{\mathfrak{I}}^{P}_{n+m-3} \qquad \text{for } m = 1, 2$$

The differences need not necessarily involve the n-th spot. Spots of adjoining scans, if in suitable proximity, may be used to form additional estimates of the adjustment vector axis.

In order to combine several estimates of the adjustment vector axis to form a single estimate for the n-th spot it is convenient to normalize each estimate to unit length and to set its sign so that it has a positive component along the positive orientation of the vector space. We define the positive orientation of the vector space by a vector which has +1 in each element:

$$\underset{\sim}{I} \equiv (1, 1, \ldots 1) \quad .$$

The normalized, sign-adjusted vector is denoted by $\underset{\sim}{N}_n$:

$$\underset{\sim}{N}_n \equiv \frac{\underset{\sim}{I} \cdot \underset{\sim}{\psi}_n}{|\underset{\sim}{I} \cdot \underset{\sim}{\psi}_n|} \; \frac{\underset{\sim}{\psi}_n}{|\underset{\sim}{\psi}_n|} \quad . \tag{18}$$

A preliminary resultant can be formed, from several individual estimates of the adjustment vector axis, by weighted combination. The magnitude of the difference vector has some value as a weight because it is indicative of the desired interpretation conditions. We have chosen to weight by magnitude squared. This formulation is given by

$$\underset{\sim}{N}_n = \frac{\sum \psi_n^2 \underset{\sim}{N}_n}{\sum \psi_n^2} \quad . \tag{19}$$

The left-hand side is the resultant of the several estimates combined on the right-hand side by weighting according to magnitude squared. Many refinements can be introduced to form the resultant by processes of selecting and weighting individual estimates. These processes are also included in the reevaluation operation.

The unit vector $\underset{\sim}{N}_n$ is an estimate of the <u>axis</u> of correction from measured cloud-contaminated to clear-column radiances at spot n. The components are denoted by $N_{\nu,n}$. The <u>amount</u> of displacement along this correction axis; i.e., the length of the correction vector, for spot n, is not directly revealed. We denote this length, which may turn out to be positive or negative, by L_n.

The interpretation model yields the following information statements at each spot, n:

$$\varphi_{\nu,n} = L_n N_{\nu,n} , \quad \text{for all } \nu . \tag{20}$$

The exploitation of these information statements is discussed in the following section.

3.3 <u>Formulation of the Error Functional</u>

Program CLRX is a new application of our Fields by Information Blending (FIB) methodology.* This information blending methodology, in general concept, combines independent weighted estimates into the non-independent resultants implied by the focus of all input information. It handles linear interrelationships and other extensions. The present application involves a new extension.

---

*Holl, Manfred M. and Bruce R. Mendenhall, 1971; "Fields by Information Blending, Sea-Level Pressure Version", Final Report, Project M-167, Contract No. N66314-70-C-5226 (Fleet Numerical Weather Central), Meteorology International Incorporated, Monterey, California, 66 pp. plus Appendix.

The blending of all independent elements of information is accomplished by minimization of a total error functional. This error functional is the total weighted sum of the squares of all resultant disparities with the information estimates. Each weight is the inverse of the error variance, or sum of contributing error variances, associated with the particular information estimate.

The present version of CLRX is based on the following formulation of the error functional:

$$E \equiv \sum_{\nu,n} \Bigg\{ A_{\nu,n} \left(\varphi^*_{\nu,n} - \varphi_{\nu,n} \right)^2 + B_{\nu,n} \left(\varphi^*_{\nu,n+1} - \varphi^*_{\nu,n} - \mu_{\nu,n} \right)^2 + C_n W_{\nu,n} \left(\varphi^*_{\nu,n} - L_n N_{\nu,n} \right)^2 \Bigg\} . \tag{21}$$

A FIB convention in notation is to denote the resultants of the blending by superscript asterisks. The above formulation of the error functional is expressed in terms of the resultant correction elements, $\varphi^*_{\nu,n}$, to be added to the measured normalized radiances, $\mathfrak{I}^P_{\nu,n}$, to form the resultant clear-column normalized radiance anomalies:

$$\mathfrak{I}^*_{\nu,n} \equiv \mathfrak{I}^P_{\nu,n} + \varphi^*_{\nu,n} . \tag{22}$$

The above error functional includes provision for the following elements of information:

(a) Direct estimates of correction elements:

$\varphi_{\nu,n}$ represents an assembled estimate for channel ν and spot n, and

$A_{\nu,n}$ represents the assembled weight for that estimate.

In the present formulation of CLRX non-zero weights occur only in conjunction with zero estimates of the correction element. These occurrences are assignments based on quantitative measures of the smoothness in the radiances in the ambience of the element. The assigned weight is inversely proportional, within bounds, to radiance variabilities in the ambience. Low variability would, generally, be the case in a clear atmosphere. For channels with a significant ground contribution the clear-column-smoothness expectation is generally limited to oceanic regions. Low variability can also be the case over a uniform solid cloud top. Any assigned weight is tentative and all weights are subject to two cycles of reevaluation.

(b) First-difference estimates:

$\mu_{\nu,n}$ represents an assembled estimate of the first difference:

$$\varphi^*_{\nu,n+1} - \varphi^*_{\nu,n} \quad .$$

$B_{\nu,n}$ represents the assembled weight for that estimate.

In the present formulation of CLRX we impose the expectation of low variability on the clear-column radiances:

$$\mathfrak{I}^*_{\nu,n} \approx \mathfrak{I}^*_{\nu,n+1} \quad , \qquad \text{for any } \nu \text{ and } n \quad . \tag{23}$$

This assumed condition is also implicit in how we have formulated (c) below. The imposition of this expectation on channels with a significant ground contribution limits the applicability of the present CLRX formulation to oceanic regions. The imposition of Eq. (23) on the correction elements related by Eq. (22) takes the form of the estimates,

$$\mu_{\nu,n} = \mathfrak{I}^{P}_{\nu,n} - \mathfrak{I}^{P}_{\nu,n+1} \quad . \tag{24}$$

The assigned weight is proportioned to estimations of the variability in Eq. (23). In the present formulation a uniform weight is assigned.

A refinement is introduced in the second and third cycles of blending. A reduced average value of the clear-column radiance gradient which emerges from the first cycle is introduced into the second-cycle assembly, and that from the second into the third. This correction takes the form of a factor added to the Eq. (24) estimate:

$$\mu_{\nu,n} = \mathfrak{I}^{P}_{\nu,n} - \mathfrak{I}^{P}_{\nu,n+1} + f\,K_{\nu} \quad . \tag{25}$$

The assigned weight is increased in proportion to the expected associated reduction in variance. Refinements such as this one are easily formulated and are as easily improvable.

(c) Correction vector estimates:

$N_{\nu,n}$ represents an assembled estimate of the component for channel ν of the unit-vector correction axis for spot n .

$C_n W_{\nu,n}$ represents the weight appropriate to the product $L_n N_{\nu,n}$.

The basis and derivation of correction axes has been discussed in Section 3.2 where the information element is expressed by Eq. (20). Additional details of the present formulation of CLRX are given in the Appendix.

The resolution of the L_n value, for each spot n, is expressed in the following section.

3.4 3.4 The Blending System of Equations

The blending equations are based on the minimization of the total error functional, E, expressed by Eq. (21). They are obtained by setting

$$\frac{\partial E}{\partial \varphi^*_{\nu,n}} = 0 \tag{26}$$

for each ν and n. This procedure produces the general equation

$$\begin{aligned} & A_{\nu,n}\left(\varphi^*_{\nu,n} - \varphi_{\nu,n}\right) - B_{\nu,n}\left(\varphi^*_{\nu,n+1} - \varphi^*_{\nu,n} - \mu_{\nu,n}\right) \\ & + B_{\nu,n-1}\left(\varphi^*_{\nu,n} - \varphi^*_{\nu,n-1} - \mu_{\nu,n-1}\right) \\ & + C_n W_{\nu,n}\left(\varphi^*_{\nu,n} - L_n N_{\nu,n}\right) = 0 \quad . \end{aligned} \tag{27}$$

Since the L_n values are completely unspecified we are free to use them to also minimize the error functional. By setting

$$\frac{\partial E}{\partial L_n} = 0 \tag{28}$$

for each n, we obtain the general equation

$$\sum_{\nu} N_{\nu,n} W_{\nu,n}\left(\varphi^*_{\nu,n} - L_n N_{\nu,n}\right) = 0 \quad . \tag{29}$$

Equation (29) defines each L_n in terms of the resultants for that column:

$$L_n = H_n \sum_{\nu} N_{\nu,n} W_{\nu,n} \varphi^*_{\nu,n} \tag{30}$$

where

$$H_n \equiv \left\{ \sum_{\nu} W_{\nu,n} N^2_{\nu,n} \right\}^{-1} \quad . \tag{31}$$

The blending system of equations, represented by Eq. (27), may also be expressed with L_n eliminated, as represented by Eq. (30). The result is

$$\begin{aligned} & A_{\nu,n}\left(\varphi^*_{\nu,n} - \varphi_{\nu,n}\right) \\ & + B_{\nu,n}\left(\varphi^*_{\nu,n} - \varphi^*_{\nu,n+1} + \mu_{\nu,n}\right) \\ & + B_{\nu,n-1}\left(\varphi^*_{\nu,n} - \varphi^*_{\nu,n-1} - \mu_{\nu,n-1}\right) \\ & + C_n W_{\nu,n}\left(\varphi^*_{\nu,n} - N_{\nu,n} H_n \sum_{\omega} N_{\omega,n} W_{\omega,n} \varphi^*_{\omega,n}\right) = 0 \end{aligned} \tag{32}$$

in which ω has been introduced as a dummy variable for ν.

The most economical solution of the blending system appears to be an iterative method of successive approximation: successive over-relaxation (SOR) by columns (i.e., spots), with the inner solution for each column by explicit inversion. The scheme we have devised uses Eqs. (27) and (30) rather than (32). The convergence rate can be judged on successive values of L_n at each n.

The system of blending equations, as represented by Eq. (32), may be expressed in matrix notation:

$$\underset{\approx}{M}\,\underset{\sim}{\varphi}^{*} = \underset{\sim}{F} \tag{33}$$

where $\underset{\sim}{\varphi}^{*}$ is the desired resultant expressed as a vector containing the ν, n elements in some orering, $\underset{\approx}{M}$ is the square coefficient matrix, and $\underset{\sim}{F}$ is the forcing vector. In general, the FIB methodology produces coefficient matrices which are symmetric and positive definite.

The FIB methodology also provides for the resultant resolution weights, which measure the focus of all information on each solution element. The resultant weights are represented by

$$A^{*}_{\nu,n} \text{ to be associated with } \varphi^{*}_{\nu,n} .$$

According to the FIB methodology* the diagonal elements of the inverse matrix

$$\underset{\approx}{M}^{-1}$$

contain the individual elements

$$\left(A^{*}_{\nu,n}\right)^{-1} .$$

---

*Ibid. page 49.

The inversion of large matrices is not always practical in a routine operation stressing economy. In such applications FIB uses a perturbation, or leverage, approach to establish estimates of the elements of $\underset{\sim}{A}^*$. In the present situation the number of elements are reasonable and the form of the matrix $\underset{\approx}{M}$ is simple. Explicit calculation of the diagonal elements of the inverse matrix is warranted.

Additional details including reevaluation formulations are given in the Appendix.

3.5 A Note about the Resultant Reliabilities

The input to CLRX is in the form of a full scan of normalized radiance anomaly values. The weights assigned to the inherent information elements are determined by specified factors and diagnostic schemes internal to the program. These are subject to adjustments and modifications--a tuning process. The objective is to have $A^*_{\nu,n}$ be a realistic weight for the resultant correction element, $\varphi^*_{\nu,n}$, and equivalently, by Eq. (22), for the resultant clear-column normalized radiance anomaly, $\mathfrak{I}^*_{\nu,n}$.

We must emphasize that $A^*_{\nu,n}$ represents the reliability of the resultant normalized radiance anomaly. The variance associated with that normalized radiance anomaly is given by

$$\left(A^*_{\nu,n}\right)^{-1} \quad .$$

The clear-column radiance anomaly, $\epsilon^*_{\nu,n}$, is related to the normalized clear-column radiance anomaly, $\mathfrak{I}^*_{\nu,n}$, by a normalizing factor:

$$\epsilon^*_{\nu,n} = f_{\nu,n}\,\mathfrak{I}^*_{\nu,n} \tag{34}$$

where $f_{\nu,n}$ denotes the normalizing factor for channel ν for the nadir angle of spot n . The corresponding reliability of $\epsilon^*_{\nu,n}$ is

$$A^*_{\nu,n} \; f^{-2}_{\nu,n} \quad . \tag{35}$$

And if the radiance anomaly is to be interpreted as an estimate of a linear combination of thermal-structure parameters such as expressed by Eq. (1)--based on physical relationships and modelling approximations--then the weight must be reduced by the addition of the contributing variances inherent in these approximations:

$$\text{Associated Weight} = \frac{1}{f^2_{\nu,n}\left(A^*_{\nu,n}\right)^{-1} + \sigma^2} \tag{36}$$

where σ^2 represents the sum of the appropriate estimates of contributing variances.

3.6 Results of CLRX

The R&D version of CLRX includes options for diagnostic printout which permits following of each stage of the calculations through the three cycles. This output is too voluminous for inclusion here.

The input to CLRX is in the form of a full scan of normalized radiance anomalies, $\mathfrak{J}^P_{\nu,n}$, such as depicted in Figs. 10-12. The present version of CLRX does not include provisions for exploitation of additional independent radiance estimates.

The standard output includes the resultant fields of the clear-column normalized radiance anomalies, $\mathfrak{I}^*_{\nu,n}$, and the associated reliabilities, $A^*_{\nu,n}$. The input and output fields can be had in the form of Varian Plots (Figs. 14-16) and/or in the form of printouts (Tables 5-14). In order to simplify the boundary treatments, two spots on each end of the scan are omitted from the blending.

Figure 13 shows the location of the series of scans which are here reproduced as examples. The variability in yield amongst these samples is obvious. The results must speak for themselves. We have not entered into any evaluation studies embracing correlations, tunings, calibrations, quality analyses, etc. Evaluation should be performed under real, or simulated, operational conditions in which all available relevant information is exploited.

The present version of CLRX has not been optimized for running time. Such optimizations will be dependent on refinements and extensions of the formulations. The approximate running time, in terms of CP time of a CDC-6500 computer, for the processing of one scan through three blending cycles and an A^* calculation is now 33 seconds. The expensive portion is the A^* calculation which uses about 26 seconds; we believe this calculation will be amenable to considerable reduction.

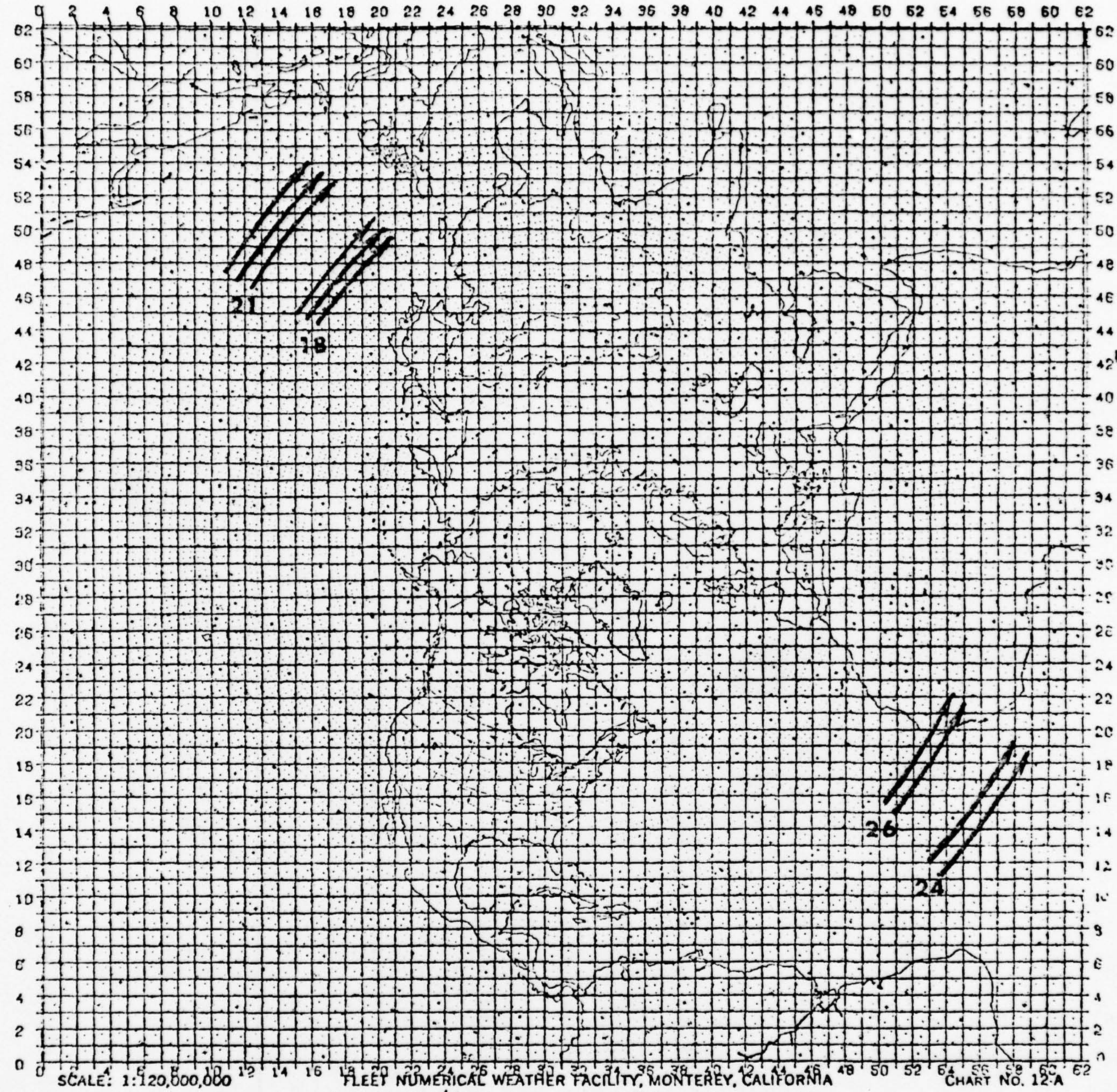

63x63 Northern Hemisphere Polar Stereographic Grid

Fig. 13 Locations of the Consecutive Complete Scans Numbered 18 through 27 (March 26, 1974)

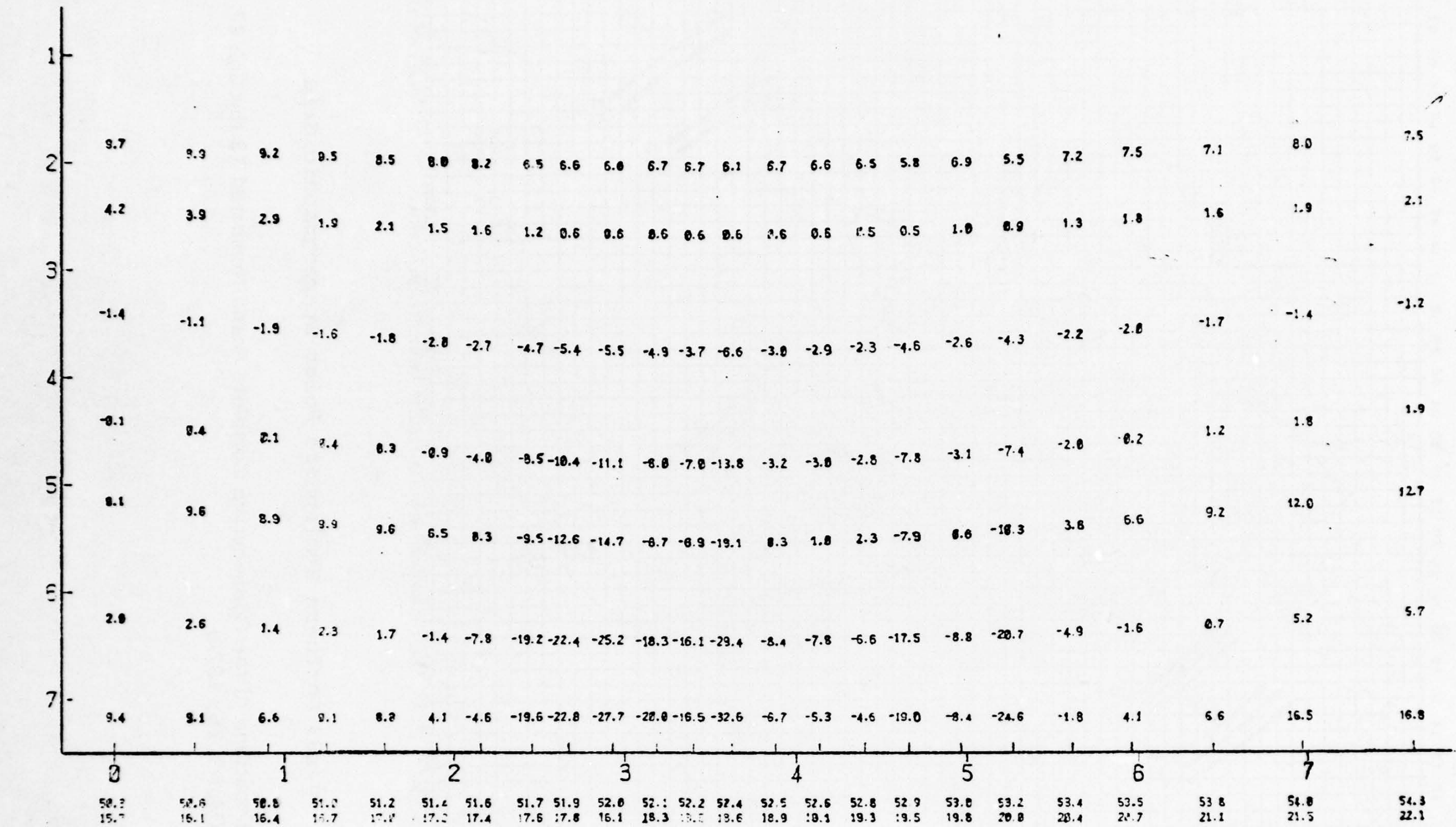

REC NO. 27

Fig. 14 The Normalized Radiance Anomalies, $\mathfrak{I}^P$, in Cross-Sectional Format

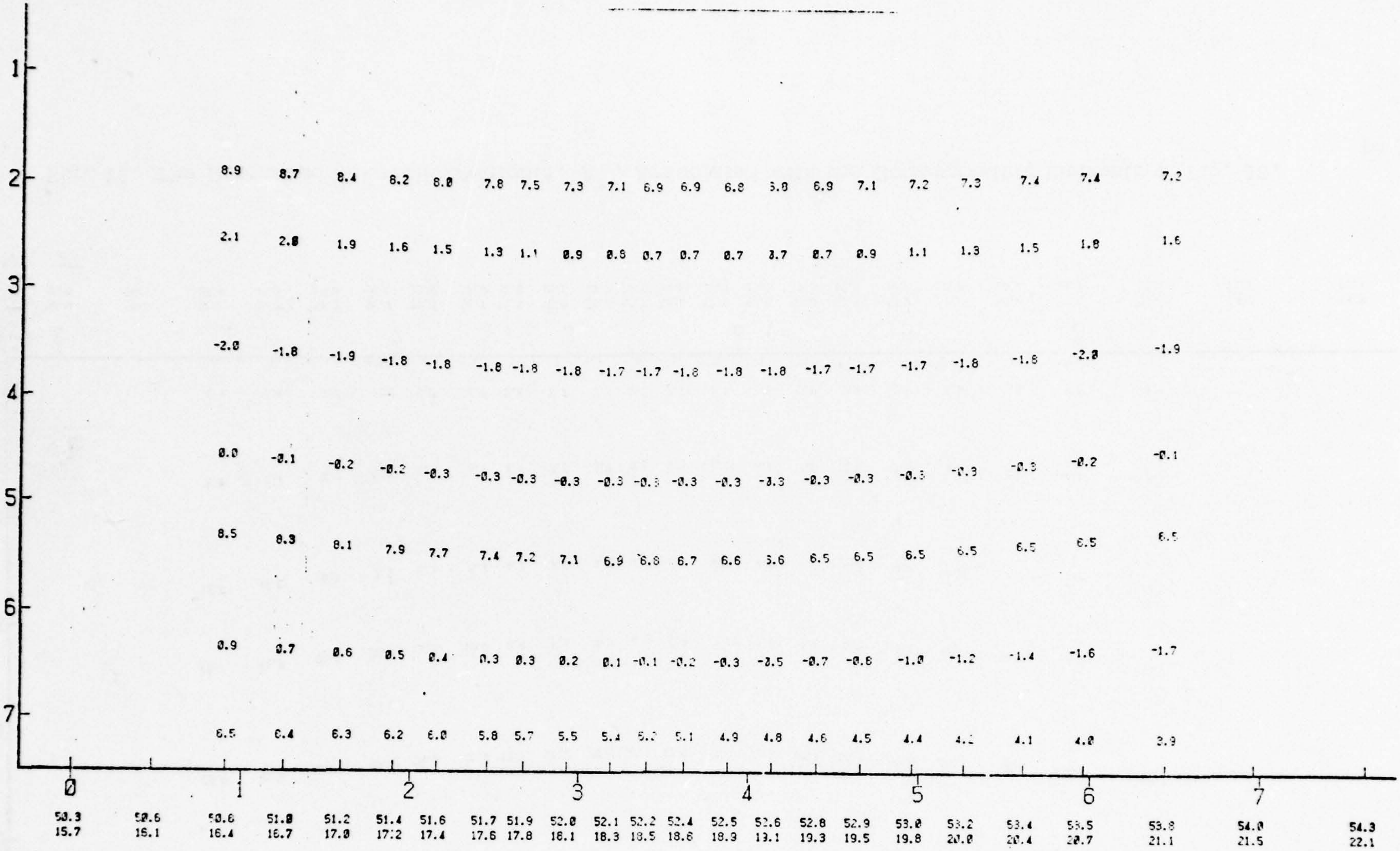

REC NO. 27

Fig. 15 The Diagnosed Clear-Column Radiance Anomalies, $\mathfrak{I}^*$, corresponding to Fig. 14. Two spots at the beginning and two at the end are omitted in the blending.

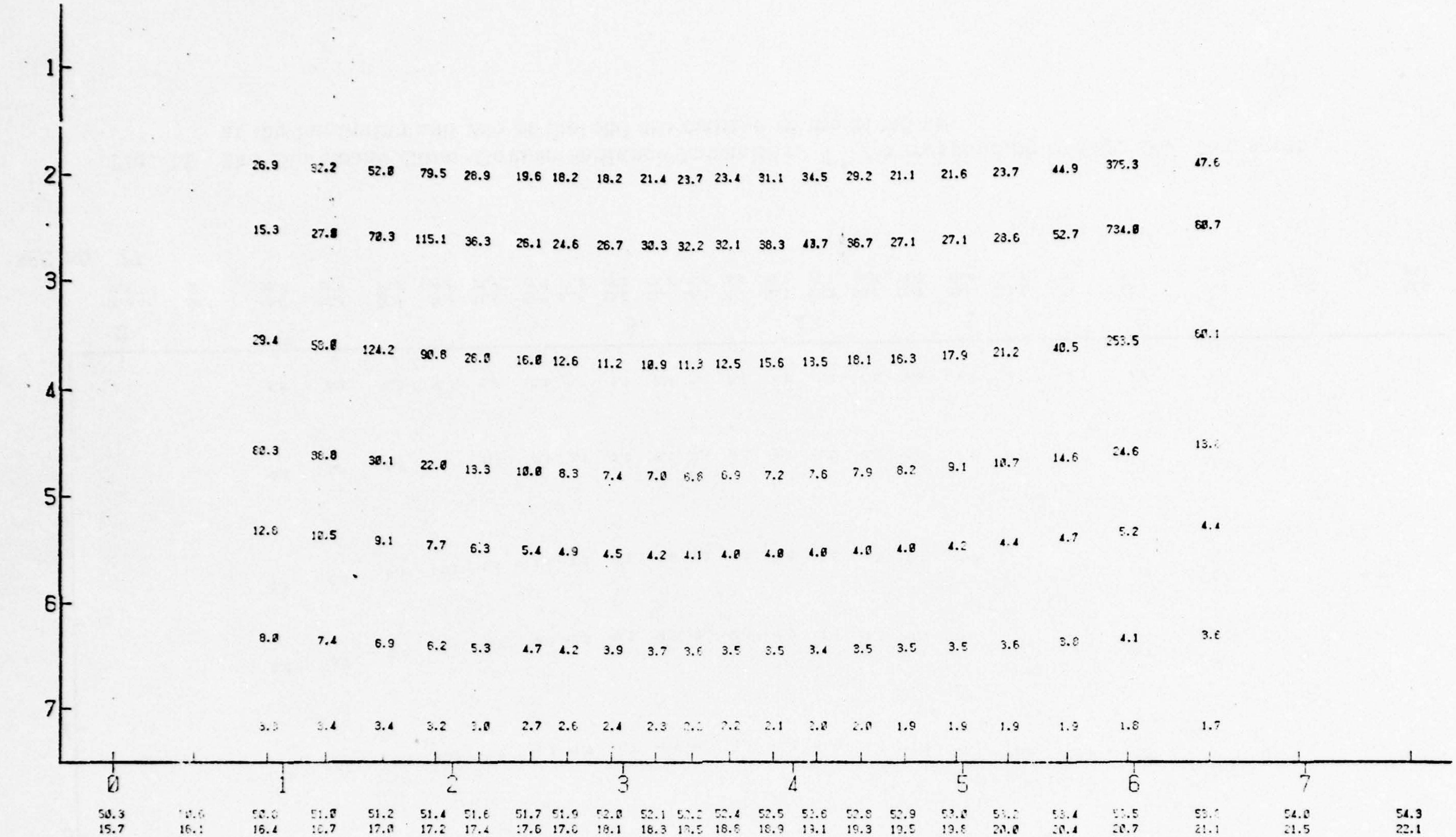

REC NO. 27

Fig. 16 The Diagnosed Reliability Weights, A*, Associated with the Corresponding Elements of Fig. 15.

Table 5

REC RD NO, 18

THE VTPR NORMALIZED RADIANCE ANOMALIES (CLRX INPUT)

SPOT NO.	CHANNEL NO. 1	2	3	4	5	6	WINDOW
1	5.75	1,55	-,84	.73	7,11	-2,56	-5,21
2	6,25	1,29	-1,11	,63	8,89	1,40	7,50
3	6,02	1,04	-2,04	,10	9,07	,83	6,45
4	5,70	.61	-1,63	-,28	8.42	,46	7,11
5	5,33	.79	-1,87	,08	8,06	.23	6,78
6	6,15	,93	-1,42	-,05	8,30	,58	8,16
7	6,31	,49	-2,26	-,57	8,14	,56	8,56
8	5,81	-,08	-2,41	-1,00	5,76	-2,44	2,89
9	5,28	,64	-2,52	-,72	4.47	-4,21	-,60
10	5,35	,03	-2,62	-1,57	.92	-8,92	-11,53
11	5,40	,73	-2,69	-1,16	1,68	-7,55	-9,09
12	5,43	,08	-2,72	-,76	5,38	-2,64	2,28
13	5,44	,09	-2,74	-,80	7,22	-,37	6,78
14	5,42	,07	-2,05	-,71	7,75	,43	8,16
15	6,64	,06	-2,67	-1,11	7,41	-,25	7,11
16	5,32	.67	-2,58	-,85	6,75	-,81	3,62
17	6,49	,62	-3,13	-1,18	7,98	,49	10,27
18	6,38	,54	-2,34	-1,30	7,45	,02	9,61
19	6,85	,44	-2,83	-,82	6.50	-1,20	3,29
20	6,67	,86	-2,63	-1,34	6,19	-1,15	3,95
21	7,07	1,36	-2,97	-1,66	6.99	-,23	8,56
22	6,80	1,71	-2,73	-1,98	6.53	-1,09	6,78
23	7,69	2,76	-3,13	-2,16	5,74	-1,49	6,78
24	7,87	2,95	-2,87	-2,18	4,68	-2,43	6,78

Table 5 (Continued)

RECORD NO. 18

THE DIAGNOSED CLEAR-COLUMN COMPONENTS (CLRX OUTPUT)

SPOT NO.	CHANNEL NO. 1	2	3	4	5	6	WINDOW
1	0,00	0,00	0,00	0,00	0,00	0,00	0,00
2	0,00	0,00	0,00	0,00	0,00	0,00	0,00
3	5,79	,82	-1,82	-,09	8,67	,57	7,00
4	5,81	,72	-1,75	-,17	8,46	,49	7,12
5	5,88	,76	-1,78	-,16	8,23	,39	7,23
6	6,04	,75	-1,74	-,27	8,03	,27	7,35
7	6,17	,48	-2,25	-,56	7,85	,17	7,45
8	5,97	,31	-2,33	-,69	7,77	,12	7,44
9	5,72	,32	-2,43	-,73	7,69	,07	7,43
10	5,57	,24	-2,54	-,81	7,63	,03	7,40
11	5,50	,20	-2,62	-,83	7,56	-,01	7,38
12	5,46	,09	-2,67	-,78	7,49	-,05	7,35
13	5,46	,07	-2,70	-,79	7,45	-,09	7,31
14	5,72	,11	-2,43	-,82	7,44	-,11	7,28
15	6,22	,12	-2,61	-1,06	7,40	-,21	7,21
16	6,25	,39	-2,65	-1,04	7,31	-,26	7,22
17	6,35	,53	-2,72	-1,10	7,25	-,30	7,21
18	6,46	,57	-2,57	-1,19	7,11	-,41	7,21
19	6,65	,68	-2,69	-1,25	6,96	-,52	7,20
20	6,75	,93	-2,73	-1,44	6,83	-,62	7,19
21	6,90	1,15	-2,86	-1,62	6,78	-,66	7,19
22	6,85	1,31	-2,77	-1,85	6,71	-,79	7,19
23	0,00	0,00	0,00	0,00	0,00	0,00	0,00
24	0,00	0,00	0,00	0,00	0,00	0,00	0,00

THE ASSOCIATED RELIABILITIES (CLRX OUTPUT)

1	0.00	0.00	0.00	0.00	0.00	0.00	0.00
2	0.00	0.00	0.00	0.00	0.00	0.00	0.00
3	44.89	60.31	24.95	41.81	28.55	29.10	15.02
4	47.03	72.04	40.34	54.82	36.99	41.08	19.42
5	38.46	66.66	48.49	53.24	41.49	45.60	17.38
6	58.87	110.65	86.35	63.43	42.21	36.54	15.42
7	138.46	115.07	145.69	84.60	32.98	25.68	12.30
8	53.60	44.22	55.53	38.74	18.91	16.25	9.54
9	37.78	30.86	43.82	28.47	14.74	13.09	8.12
10	35.81	26.72	35.46	24.59	13.59	12.15	7.38
11	41.50	29.54	37.82	29.47	14.61	12.79	7.02
12	70.80	55.39	60.10	44.78	19.08	15.60	6.99
13	374.91	564.06	306.85	170.86	35.67	23.95	7.22
14	59.33	121.41	78.40	104.95	39.53	27.69	6.83
15	53.20	126.33	81.91	147.20	60.12	39.95	6.28
16	31.63	50.76	44.02	51.59	30.21	25.01	5.80
17	34.50	74.07	44.48	52.11	27.04	22.53	5.50
18	49.65	116.18	55.69	55.03	28.49	23.06	5.33
19	53.33	47.88	48.61	39.38	25.99	21.49	5.20
20	54.88	39.09	59.15	41.69	27.07	22.46	5.17
21	79.79	35.99	141.82	52.73	31.20	23.65	5.22
22	51.65	24.32	184.20	56.16	23.97	19.91	5.25
23	0.00	0.00	0.00	0.00	0.00	0.00	0.00
24	0.00	0.00	0.00	0.00	0.00	0.00	0.00

Table 6

RECORD NO. 19

THE VTPR NORMALIZED RADIANCE ANOMALIES (CLRX INPUT)

SPOT NO.	CHANNEL NO. 1	2	3	4	5	6	WINDOW
1	7.29	1.44	-1.07	1.56	9.41	.70	7.44
2	6.56	1.18	-.78	1.35	8.62	.24	6.38
3	6.33	.93	-1.05	1.42	8.80	1.28	8.49
4	6.63	.50	-1.30	1.03	9.13	1.67	9.15
5	6.26	.68	-1.54	.88	8.76	1.51	8.82
6	5.83	.16	-1.74	.74	9.00	1.40	9.54
7	6.00	.27	-1.93	.81	8.83	1.75	9.87
8	6.12	-.19	-1.42	.38	8.87	1.81	10.60
9	5.59	-.13	-1.54	.55	8.53	1.59	10.20
10	6.29	-.08	-1.64	.78	8.68	1.77	10.20
11	5.72	-.05	-1.71	.11	9.00	2.02	10.93
12	6.37	-.03	-1.74	.02	9.33	2.33	11.65
13	5.75	-.02	-1.76	-.02	9.29	2.67	11.65
14	6.98	-.04	-1.73	.55	9.38	2.73	11.98
15	6.33	-.05	-1.69	.16	9.05	2.42	11.65
16	6.88	.45	-1.59	.42	8.82	2.61	12.31
17	6.80	.40	-2.15	-.40	9.10	2.42	12.31
18	7.31	.32	-2.56	-.51	8.58	2.33	12.31
19	7.17	.88	-2.39	-.63	8.15	1.94	11.26
20	6.36	.75	-2.19	-1.04	7.42	1.26	9.87
21	7.38	1.25	-2.64	-.96	7.25	.22	9.54
22	7.11	1.60	-2.39	-1.17	6.27	-.63	6.38
23	7.38	1.99	-2.80	-2.47	4.04	-2.94	4.61
24	8.17	2.85	-3.09	-3.01	2.49	-5.06	-.66

Table 6 (Continued)

RECORD NO. 19

THE DIAGNOSED CLEAR-COLUMN COMPONENTS (CLRX OUTPUT)

SPOT NO.	CHANNEL NO. 1	2	3	4	5	6	WINDOW
1	0,00	0,00	0,00	0,00	0,00	0,00	0,00
2	0,00	0,00	0,00	0,00	0,00	0,00	0,00
3	6,32	,76	-1,22	1,27	8,92	1,55	9,03
4	6,41	,57	-1,33	1,07	9,01	1,58	9,15
5	6,24	,48	-1,52	,91	8,91	1,55	9,31
6	6,04	,27	-1,70	,78	8,94	1,53	9,60
7	6,02	,16	-1,80	,73	8,87	1,70	9,91
8	6,03	-,02	-1,64	,57	8,83	1,73	10,19
9	6,03	-,07	-1,61	,51	8,82	1,78	10,40
10	6,12	-,06	-1,67	,48	8,90	1,92	10,65
11	5,99	-,04	-1,71	,19	9,03	2,07	10,99
12	6,08	-,03	-1,73	,12	9,19	2,27	11,33
13	6,14	-,02	-1,76	,13	9,28	2,50	11,59
14	6,34	-,02	-1,76	,20	9,22	2,55	11,74
15	6,51	,07	-1,73	,13	9,05	2,49	11,85
16	6,69	,26	-1,81	,00	8,90	2,49	12,03
17	6,87	,36	-2,13	-,29	8,82	2,38	12,12
18	7,12	,40	-2,41	-,48	8,58	2,31	12,15
19	7,12	,63	-2,39	-,53	8,46	2,26	12,10
20	7,00	,61	-2,31	-,70	8,33	2,23	12,17
21	7,06	,77	-2,41	-,72	8,31	2,22	12,26
22	7,04	,87	-2,35	-,74	8,30	2,25	12,38
23	0,00	0,00	0,00	0,00	0,00	0,00	0,00
24	0,00	0,00	0,00	0,00	0,00	0,00	0,00

THE ASSOCIATED RELIABILITIES (CLRX OUTPUT)

1	0,00	0,00	0,00	0,00	0,00	0,00	0,00
2	0,00	0,00	0,00	0,00	0,00	0,00	0,00
3	66,86	104,83	79,78	78,33	54,40	30,16	13,91
4	57,84	87,29	69,69	85,62	74,09	45,87	21,37
5	43,45	49,52	56,24	60,15	58,04	56,06	25,28
6	52,02	47,89	88,51	66,07	79,91	62,77	27,48
7	60,76	51,54	85,50	71,85	72,27	63,71	28,57
8	39,39	51,04	51,70	46,61	48,66	51,46	27,91
9	33,63	62,51	56,30	46,46	44,77	52,04	31,87
10	41,88	287,36	128,62	63,53	60,47	58,27	31,88
11	43,86	802,85	478,62	71,42	68,63	60,06	32,53
12	31,46	759,84	520,83	51,15	63,18	49,92	33,22
13	27,39	795,87	600,56	58,47	67,62	47,87	40,91
14	26,65	64,02	218,09	56,33	48,45	48,44	39,44
15	31,59	57,65	93,41	48,55	51,05	58,68	38,49
16	46,01	57,73	58,73	38,81	50,91	62,40	37,07
17	53,36	56,43	55,85	45,44	43,79	57,73	33,28
18	61,24	100,58	84,61	87,48	49,15	56,43	25,36
19	47,06	77,43	112,97	101,50	38,15	32,52	16,88
20	32,94	55,18	72,71	53,20	24,33	18,61	11,05
21	31,16	50,38	58,55	33,86	15,77	12,12	8,11
22	27,09	31,53	38,32	18,69	10,31	8,55	6,24
23	0,00	0,00	0,00	0,00	0,00	0,00	0,00
24	0,00	0,00	0,00	0,00	0,00	0,00	0,00

Table 7

RECORD NO. 20

THE VTPR NORMALIZED RADIANCE ANOMALIES (CLRX INPUT)

SPOT NO.	CHANNEL NO. 1	2	3	4	5	6	WINDOW
1	6.99	1.33	-.51	1.98	9.96	1.87	8.29
2	5.63	.53	-1.45	1.76	10.25	1.76	9.02
3	6.02	.82	-1.05	1.31	9.87	2.05	9.02
4	6.32	.39	-1.30	1.43	9.75	2.05	8.29
5	6.57	-.09	-1.54	1.28	9.82	1.82	10.07
6	5.52	.05	-1.74	1.14	9.52	2.53	10.80
7	6.31	.16	-1.38	.61	9.44	2.50	9.74
8	6.44	-.30	-1.53	.77	9.91	2.56	11.13
9	5.90	-.24	-1.65	.95	10.00	2.70	11.13
10	5.98	-.19	-1.75	.68	9.71	2.69	10.80
11	6.03	-.16	-1.82	.50	9.51	2.76	10.80
12	5.43	-.80	-1.85	.41	9.94	3.07	11.85
13	6.07	-.79	-1.87	.37	9.89	3.04	11.45
14	5.42	-.81	-1.84	.46	9.98	2.73	11.13
15	6.64	-.16	-2.35	.55	9.57	2.79	11.45
16	6.57	-.87	-2.25	.32	9.42	2.98	11.45
17	6.49	-.26	-2.15	-.00	9.71	2.42	11.85
18	5.75	-.34	-2.01	-.11	9.18	2.70	11.45
19	6.85	.77	-1.84	-.23	8.24	1.94	10.80
20	6.67	.64	-2.96	-1.24	7.94	1.18	10.07
21	7.07	1.14	-2.75	-1.06	6.81	-.23	8.69
22	8.04	1.49	-2.51	-1.38	6.34	-.72	7.96
23	7.08	2.43	-2.25	-1.56	6.00	-.66	8.29
24	8.49	2.74	-2.54	-2.61	4.48	-2.76	5.86

Table 7 (Continued)

RECORD NO, 20

THE DIAGNOSED CLEAR-COLUMN COMPONENTS (CLRX OUTPUT)

SPOT NO,	CHANNEL NO, 1	2	3	4	5	6	WINDOW
1	0,00	0,00	0,00	0,00	0,00	0,00	0,00
2	0,00	0,00	0,00	0,00	0,00	0,00	0,00
3	6,04	,68	-1,13	1,38	9,89	2,04	9,28
4	6,15	,45	-1,30	1,37	9,86	2,01	9,48
5	6,46	,10	-1,52	1,28	9,80	2,01	9,89
6	6,14	,10	-1,67	1,11	9,67	2,31	10,28
7	6,20	-,04	-1,51	,85	9,68	2,47	10,43
8	6,20	-,15	-1,52	,78	9,76	2,56	10,65
9	6,05	-,15	-1,63	,80	9,81	2,68	10,82
10	5,99	-,23	-1,73	,68	9,75	2,79	10,90
11	5,95	-,32	-1,81	,55	9,69	2,83	11,04
12	5,91	-,43	-1,82	,49	9,75	2,89	11,20
13	6,00	-,53	-1,88	,42	9,79	2,90	11,28
14	6,10	-,51	-2,04	,47	9,76	2,82	11,30
15	6,26	-,49	-2,17	,44	9,64	2,80	11,37
16	6,43	-,55	-2,23	,26	9,50	2,77	11,45
17	6,44	-,40	-2,17	,02	9,46	2,60	11,48
18	6,12	-,13	-2,12	-,22	9,05	2,48	11,32
19	6,48	,43	-1,99	-,30	8,76	2,31	11,20
20	6,40	,31	-2,55	-,72	8,58	2,07	11,09
21	6,49	,36	-2,90	-,90	8,47	1,95	11,05
22	6,54	,36	-2,88	-1,01	8,42	1,91	11,08
23	0,00	0,00	0,00	0,00	0,00	0,00	0,00
24	0,00	0,00	0,00	0,00	0,00	0,00	0,00

THE ASSOCIATED RELIABILITIES (CLRX OUTPUT)

1	0,00	0,00	0,00	0,00	0,00	0,00	0,00
2	0,00	0,00	0,00	0,00	0,00	0,00	0,00
3	38,45	44,95	49,83	46,32	45,68	51,50	18,00
4	55,79	54,78	62,12	55,11	57,48	58,80	21,26
5	167,07	82,38	186,11	65,59	84,73	63,56	23,83
6	48,07	92,21	156,92	50,51	55,75	50,87	21,68
7	39,84	82,50	96,36	52,62	55,35	53,92	20,88
8	42,44	104,44	88,98	74,89	62,36	58,26	24,01
9	44,94	104,87	69,02	70,14	56,35	53,12	30,44
10	45,16	64,51	87,99	54,76	51,58	52,09	35,12
11	48,31	51,45	170,44	61,87	59,60	60,29	32,09
12	34,72	43,27	337,33	94,07	57,08	57,73	30,29
13	28,96	38,45	74,94	128,75	51,39	52,15	33,82
14	28,31	44,21	75,68	108,06	59,22	53,53	41,00
15	31,17	43,51	77,15	66,47	59,01	54,33	46,40
16	44,81	40,70	77,57	59,39	58,70	49,64	46,06
17	173,25	46,94	134,76	55,21	79,28	48,39	42,19
18	88,85	86,12	158,07	79,85	55,04	43,51	38,62
19	79,54	102,78	77,34	55,17	40,33	32,05	27,43
20	58,38	79,06	51,52	44,82	29,19	22,08	17,89
21	24,25	27,44	57,85	36,03	16,67	13,74	11,64
22	14,05	15,85	30,52	21,38	10,98	9,48	8,28
23	0,00	0,00	0,00	0,00	0,00	0,00	0,00
24	0,00	0,00	0,00	0,00	0,00	0,00	0,00

Table 8

RECORD NO. 21

THE VTPR NORMALIZED RADIANCE ANOMALIES (CLRX INPUT)

SPOT NO.	CHANNEL NO. 1	2	3	4	5	6	WINDOW
1	7.19	1.22	-2.62	.11	8.40	-.15	4.21
2	6.45	.42	-2.33	.01	8.71	.63	5.26
3	6.33	.06	-2.60	-.51	7.37	-1.15	2.83
4	6.01	-.37	-3.40	-2.48	2.40	-6.50	-3.50
5	5.63	-.20	-4.29	-3.70	1.56	-7.06	-2.11
6	5.83	-.61	-3.83	-2.72	3.76	-4.07	1.77
7	6.62	-.50	-2.80	-.07	7.97	.12	6.71
8	5.50	-1.07	-2.30	.09	8.45	.62	7.77
9	5.59	-1.01	-3.07	-1.31	6.20	-1.91	4.21
10	5.65	-.96	-3.17	-1.07	7.30	-.50	4.61
11	6.97	-.93	-3.24	-.67	8.05	.46	7.04
12	6.99	-.91	-2.61	.81	9.85	3.07	10.86
13	6.33	-1.45	-2.63	.17	10.75	3.41	11.92
14	6.93	-.92	-2.60	.26	10.41	3.10	11.92
15	6.95	-.93	-2.56	.35	9.99	3.53	11.92
16	6.88	-.32	-2.47	.61	11.23	4.83	14.02
17	6.80	-.37	-3.03	.38	11.52	4.65	13.69
18	7.32	-.45	-2.89	.28	11.00	4.19	13.69
19	7.69	.00	-2.72	.16	11.11	4.55	14.02
20	7.51	.54	-2.53	-.25	10.30	3.43	13.36
21	7.23	1.03	-2.97	-.67	9.72	2.86	12.31
22	8.25	.84	-2.73	-.99	8.73	1.93	11.28
23	7.93	1.78	-3.03	-1.68	5.98	-1.51	4.61
24	8.03	1.99	-3.43	-2.21	4.46	-3.23	2.50

Table 8 (Continued)

RECORD NO. 21

THE DIAGNOSED CLEAR-COLUMN COMPONENTS (CLRX OUTPUT)

SPOT NO.	CHANNEL NO. 1	2	3	4	5	6	WINDOW
1	0.00	0.00	0.00	0.00	0.00	0.00	0.00
2	0.00	0.00	0.00	0.00	0.00	0.00	0.00
3	6.41	.10	-2.10	1.00	9.79	1.96	8.75
4	6.32	-.12	-2.12	.99	9.82	2.06	9.08
5	6.26	-.32	-2.17	.97	9.84	2.18	9.33
6	6.26	-.54	-2.20	.95	9.88	2.28	9.60
7	6.32	-.69	-2.20	.96	9.91	2.39	9.87
8	6.22	-.90	-2.10	.91	9.94	2.50	10.14
9	6.32	-.93	-2.36	.86	9.99	2.67	10.44
10	6.51	-.94	-2.58	.79	10.05	2.86	10.74
11	6.73	-.96	-2.68	.74	10.10	3.03	11.04
12	6.85	-.96	-2.59	.74	10.15	3.20	11.32
13	6.55	-1.31	-2.67	.36	10.44	3.28	11.68
14	6.87	-.98	-2.59	.34	10.46	3.40	12.05
15	6.93	-.80	-2.58	.40	10.44	3.74	12.42
16	6.94	-.65	-2.58	.45	10.64	3.97	12.82
17	7.01	-.57	-2.80	.34	10.86	4.12	13.19
18	7.30	-.30	-2.81	.22	10.90	4.14	13.55
19	7.53	.10	-2.71	.06	10.90	4.22	13.80
20	7.50	.32	-2.61	-.04	10.82	4.15	14.01
21	7.50	.54	-2.77	-.27	10.81	4.23	14.28
22	7.73	.51	-2.69	-.41	10.84	4.32	14.58
23	0.00	0.00	0.00	0.00	0.00	0.00	0.00
24	0.00	0.00	0.00	0.00	0.00	0.00	0.00

THE ASSOCIATED RELIABILITIES (CLRX OUTPUT)

1	0.00	0.00	0.00	0.00	0.00	0.00	0.00
2	0.00	0.00	0.00	0.00	0.00	0.00	0.00
3	44.15	45.03	20.99	7.64	4.32	3.87	3.11
4	32.67	34.72	17.46	8.30	4.83	4.33	3.44
5	26.92	33.77	17.54	9.41	5.52	4.93	3.85
6	26.72	37.43	22.21	11.55	6.52	5.78	4.40
7	30.19	51.29	43.41	16.08	8.08	7.04	5.14
8	27.47	50.26	51.32	20.23	9.69	8.41	5.98
9	23.19	41.60	30.63	17.60	10.56	9.26	6.65
10	23.21	48.40	32.56	19.13	12.61	11.00	7.76
11	31.07	54.62	49.35	25.91	17.39	14.76	9.68
12	92.69	255.32	337.82	67.26	34.25	25.93	13.61
13	140.47	166.69	345.14	66.02	44.76	36.71	19.71
14	97.16	70.98	671.92	69.44	51.68	37.83	26.21
15	179.76	120.13	116.54	137.53	41.91	34.76	23.52
16	88.33	115.23	66.82	83.24	34.56	30.93	22.86
17	63.80	143.23	71.06	94.64	39.19	37.68	29.31
18	63.73	63.62	99.29	110.44	51.81	43.42	41.28
19	75.50	61.57	92.19	101.14	47.88	35.92	31.45
20	61.27	51.19	100.65	75.14	32.39	24.72	20.16
21	41.17	51.94	83.69	42.03	18.88	14.78	11.88
22	25.90	38.59	52.30	24.62	11.83	9.91	8.24
23	0.00	0.00	0.00	0.00	0.00	0.00	0.00
24	0.00	0.00	0.00	0.00	0.00	0.00	0.00

Table 9

RECORD NO, 22

THE VTPR NORMALIZED RADIANCE ANOMALIES (CLRX INPUT)

SPOT NO,	CHANNEL NO. 1	2	3	4	5	6	WINDOW
1	7,18	,79	-1,84	1,89	12,09	4,14	10,78
2	6,56	,53	-2,11	1,76	11.33	2,86	9,28
3	6,94	,27	-1,71	1,83	11.50	3,05	8,23
4	6,63	,50	-1,96	1,44	11,35	3,11	10,78
5	7,50	,02	-1,64	1,29	10.45	2,50	8,62
6	6,45	-,39	-2,40	1,15	11,10	3,13	10,34
7	7,24	-,28	-2,03	1,11	10.49	2,73	8,95
8	6,75	-,85	-2,19	1,27	10.96	3,16	11,39
9	5,59	-1,34	-2,30	1,44	10,61	2,56	9,68
10	6,29	-,74	-2,95	-,39	8,94	1,26	8,62
11	5,72	-1,26	-3,02	-2,72	2.11	-6,44	-1,52
12	5,74	-1,24	-2,51	,42	9.59	1,81	10,01
13	6,38	-,68	-1,87	,86	11.43	3,63	12,44
14	6,98	-,70	-1,84	,94	11,01	4,06	12,44
15	6,33	-,71	-2,46	,55	9.74	2,27	10,78
16	6,88	-,76	-2,36	,81	10.97	3,57	12,44
17	6,80	-,15	-2,81	,48	10.74	4,13	12,77
18	6,69	-,23	-2,67	,37	10.74	3,30	12,44
19	7.17	,22	-2,50	,36	10.76	3,28	12,44
20	7,61	,76	-2,97	-,15	9,51	2,23	11,06
21	6.77	,60	-3,96	-4,88	-2.74	-12,70	-11,33
22	6,49	,95	-3,73	-5,73	-8.26	-19,87	-24,96
23	6,77	2,00	-2,92	-2,69	,68	-8,62	-8,17
24	8,70	2.21	-3,21	-2,12	3,08	-5,64	-2,57

Table 9 (Continued)

RECORD NO. 22

THE DIAGNOSED CLEAR-COLUMN COMPONENTS (CLRX OUTPUT)

SPOT NO.	CHANNEL NO. 1	2	3	4	5	6	WINDOW
1	0,00	0,00	0,00	0,00	0.00	0,00	0,00
2	0,00	0,00	0,00	0,00	0.00	0,00	0,00
3	6,64	,37	-1,88	1,61	11,41	3,09	10,22
4	6,65	,31	-1,94	1,46	11,29	3,07	10,34
5	6,57	,03	-2,07	1,32	11,18	3,06	10,45
6	6,45	-,30	-2,27	1,19	11,10	3,10	10,58
7	6,36	-,56	-2,24	1,18	10,99	3,07	10,68
8	6,18	-,89	-2,25	1,28	10,95	3,06	10,81
9	5,79	-1,25	-2,29	1,45	11,02	3,09	10,88
10	6,02	-,98	-2,55	1,16	10,99	3,15	11,11
11	5,97	-1,05	-2,46	1,03	10,95	3,18	11,32
12	5,99	-1,07	-2,30	,89	10,90	3,20	11,52
13	6,32	-,74	-1,97	,73	10,87	3,22	11,68
14	6,61	-,75	-2,05	,79	10,72	3,32	11,82
15	6,67	-,69	-2,25	,73	10,71	3,35	11,98
16	6,78	-,69	-2,41	,72	10,72	3,36	12,18
17	6,68	-,32	-2,68	,50	10,62	3,44	12,27
18	6,77	-,15	-2,66	,36	10,66	3,29	12,36
19	7,17	,23	-2,52	,33	10,68	3,26	12,44
20	7,58	,67	-2,87	,21	10,58	3,29	12,58
21	7,49	,70	-3,01	,14	10,54	3,31	12,69
22	7,47	,76	-3,09	,08	10,51	3,33	12,80
23	0,00	0,00	0,00	0,00	0,00	0,00	0,00
24	0,00	0,00	0,00	0,00	0,00	0,00	0,00

THE ASSOCIATED RELIABILITIES (CLRX OUTPUT)

1	0,00	0,00	0.00	0,00	0.00	0,00	0,00
2	0,00	0.00	0.00	0,00	0.00	0,00	0,00
3	24,87	46,10	44.39	33,26	26.15	30,70	5,19
4	36,92	58,35	74.59	70,39	35.76	45,99	6,41
5	28,98	37,08	42.52	54,50	30.48	34,66	7,60
6	39,89	43,24	64.80	123,98	43.41	49,47	9,37
7	30,56	38,64	53.05	67,45	33.18	34,80	10,04
8	40,77	58,47	90.70	52,47	34.62	33,70	11,60
9	115,33	231,91	248.20	58,16	26.75	24,92	12,46
10	52,34	64,95	65.77	30,03	18.55	17,26	11,23
11	41,06	45,19	40,68	25,84	16.63	15,28	11,03
12	83,33	114,39	90.87	42,06	19.52	16,88	12,17
13	158,05	295,59	256.58	92,93	26.07	20,78	14,48
14	62,87	98,01	105.06	109,20	28.15	21,75	16,48
15	59,27	74,85	53.20	68,24	27.50	21,74	17,74
16	177,29	110,86	85.70	122,62	42.51	28,74	23,28
17	178,68	92,76	125.90	114,11	52.40	32,69	28,27
18	166,94	128,70	220.22	155,02	61.72	39,96	33,61
19	553,50	535,03	795.18	158,41	44.45	32,07	20,60
20	175,99	180,28	162.64	44,59	20.34	16,42	11,95
21	27,00	32,28	26.03	16,19	11.25	9,93	8,09
22	14,78	16,76	14.77	9,87	7.77	7,11	6,11
23	0,00	0,00	0.00	0,00	0.00	0,00	0,00
24	0,00	0,00	0.00	0,00	0.00	0,00	0,00

Table 10

RECORD NO. 23

THE VTPR NORMALIZED RADIANCE ANOMALIES (CLRX INPUT)

SPOT NO.	CHANNEL NO. 1	2	3	4	5	6	WINDOW
1	6.37	.68	-1.95	1.68	9.88	1.73	8.23
2	6.87	.53	-2.22	2.06	11.60	3.24	10.34
3	6.63	.17	-2.48	2.14	10.69	2.67	8.62
4	4.46	-.81	-5.27	-8.52	-14.17	-25.13	-30.23
5	5.94	-.09	-2.31	2.09	9.65	1.30	7.90
6	6.14	-.50	-1.96	1.94	8.92	.81	6.52
7	5.68	-1.05	-2.14	.91	7.36	-1.08	3.68
8	5.81	-.96	-2.30	.48	5.93	-2.58	2.30
9	4.03	-1.45	-9.19	-17.19	-26.03	-36.93	-42.48
10	4.10	-1.40	-9.29	-17.41	-27.70	-38.54	-45.25
11	4.15	-1.37	-4.98	-8.19	-12.26	-22.38	-24.31
12	6.05	-.80	-2.61	.61	8.82	.62	8.62
13	6.07	-1.34	-2.63	1.15	9.29	1.41	9.61
14	6.04	-.81	-2.60	1.24	10.33	2.95	11.72
15	6.02	-.82	-2.56	.74	9.48	2.27	10.66
16	6.57	-.87	-2.47	.51	9.76	2.46	10.66
17	6.49	-.26	-2.37	.78	10.05	2.64	10.66
18	5.76	-1.00	-4.09	-3.57	-5.67	-16.10	-19.76
19	4.99	-.43	-3.93	-3.11	-6.15	-17.00	-21.80
20	5.43	-.01	-3.74	-4.14	-8.47	-19.64	-26.41
21	7.08	.49	-2.86	-1.38	4.76	-3.79	1.25
22	6.81	.95	-3.29	-.60	7.21	-.51	7.17
23	8.22	1.24	-3.03	-.67	7.86	-.06	7.90
24	7.78	2.75	-3.32	-1.81	4.90	-3.32	3.68

Table 10 (Continued)

RECORD NO. 23

THE DIAGNOSED CLEAR-COLUMN COMPONENTS (CLRX OUTPUT)

SPOT NO.	CHANNEL NO. 1	2	3	4	5	6	WINDOW
1	0.00	0.00	0.00	0.00	0.00	0.00	0.00
2	0.00	0.00	0.00	0.00	0.00	0.00	0.00
3	6.62	.16	-2.48	2.17	10.67	2.60	8.69
4	6.33	.03	-2.33	2.27	10.56	2.48	8.84
5	6.04	-.10	-2.18	2.38	10.45	2.36	8.98
6	6.15	-.47	-1.85	2.37	10.33	2.29	9.08
7	5.98	-.79	-1.75	2.27	10.25	2.24	9.22
8	6.00	-.89	-1.76	2.12	10.16	2.18	9.38
9	6.03	-.98	-1.92	1.93	10.09	2.15	9.57
10	6.05	-1.02	-2.08	1.73	10.02	2.11	9.75
11	6.08	-.98	-2.25	1.53	9.94	2.07	9.93
12	6.12	-.89	-2.43	1.33	9.87	2.03	10.11
13	6.11	-1.30	-2.58	1.28	9.75	2.01	10.26
14	6.12	-1.04	-2.60	1.06	9.68	2.10	10.38
15	6.24	-.90	-2.56	.78	9.57	2.22	10.48
16	6.55	-.86	-2.48	.54	9.68	2.32	10.49
17	6.48	-.28	-2.40	.66	9.74	2.32	10.43
18	6.59	-.15	-2.59	.48	9.66	2.29	10.52
19	6.75	.05	-2.78	.29	9.57	2.25	10.61
20	6.91	.31	-2.91	.10	9.49	2.21	10.70
21	7.05	.61	-2.98	-.08	9.41	2.18	10.79
22	7.08	.86	-3.15	-.24	9.34	2.15	10.90
23	0.00	0.00	0.00	0.00	0.00	0.00	0.00
24	0.00	0.00	0.00	0.00	0.00	0.00	0.00

THE ASSOCIATED RELIABILITIES (CLRX OUTPUT)

1	0.00	0.00	0.00	0.00	0.00	0.00	0.00
2	0.00	0.00	0.00	0.00	0.00	0.00	0.00
3	534.55	815.53	400.07	41.39	8.56	6.91	3.69
4	46.10	46.96	44.16	23.58	8.11	6.75	3.85
5	232.01	235.36	172.06	31.82	8.87	7.26	4.16
6	139.39	117.60	111.65	27.88	8.82	7.31	4.39
7	63.00	61.36	51.62	13.98	8.43	7.18	4.62
8	38.47	43.20	32.59	15.44	8.28	7.22	4.89
9	22.23	27.81	20.69	13.67	8.44	7.48	5.28
10	20.80	28.68	19.74	14.31	9.26	8.22	5.89
11	28.34	34.27	26.59	18.22	11.19	9.76	6.87
12	145.35	159.72	106.32	35.34	15.97	13.15	8.58
13	475.74	472.97	445.56	81.55	25.11	18.73	11.05
14	68.36	61.45	180.48	47.89	29.64	20.38	13.06
15	62.84	73.01	179.97	54.97	43.18	29.01	17.34
16	809.30	838.22	832.01	188.50	48.86	35.97	19.57
17	636.82	668.21	632.13	137.02	31.41	23.23	12.68
18	32.06	34.74	32.33	25.48	14.83	12.57	8.52
19	20.64	25.88	23.57	16.76	10.14	8.85	6.47
20	19.30	25.07	23.85	14.51	7.97	6.97	5.25
21	24.27	31.34	32.82	14.92	6.75	5.85	4.44
22	29.65	37.50	48.40	16.47	5.87	5.05	3.85
23	0.00	0.00	0.00	0.00	0.00	0.00	0.00
24	0.00	0.00	0.00	0.00	0.00	0.00	0.00

Table 11

RECORD NO, 24

THE VTPR NORMALIZED RADIANCE ANOMALIES (CLRX INPUT)

SPOT NO,	CHANNEL NO, 1	2	3	4	5	6	WINDOW
1	9,06	2,79	-2,01	-2,03	1,92	-7,45	-6,92
2	8,25	3,12	-3,61	-4,21	-1,86	-11,91	-11,46
3	8,58	2,06	-2,53	-1,26	5,35	-3,29	3,22
4	8,23	1,71	-3,43	-3,63	-,85	-10,48	-7,58
5	7,21	1,20	-4,30	-7,56	-12,18	-23,64	-27,86
6	6,75	,78	-3,17	-3,83	-5,57	-16,27	-21,54
7	6,28	,22	-3,33	-4,77	-9,34	-20,00	-25,76
8	5,77	,29	-2,92	-3,55	-3,98	-14,18	-16,01
9	5,84	,34	-3,02	-3,80	-3,80	-14,34	-14,95
10	5,29	-,27	-3,66	-6,69	-10,16	-20,95	-25,08
11	5,94	-,26	-3,15	-3,65	-2,67	-12,25	-12,12
12	5,34	-,24	-3,72	-6,26	-10,32	-21,05	-26,08
13	5,32	-,80	-5,01	-8,36	-14,57	-25,91	-31,68
14	5,30	-,27	-5,53	-10,34	-16,82	-28,16	-34,12
15	5,87	-,30	-3,60	-5,47	-11,49	-22,72	-30,30
16	5,80	-,35	-2,96	-3,66	-5,98	-16,85	-23,32
17	5,71	-,41	-3,39	-4,93	-9,06	-20,09	-27,53
18	5,58	-,50	-3,90	-6,10	-11,95	-23,72	-31,02
19	5,42	,05	-4,93	-8,78	-15,31	-26,87	-33,07
20	5,22	-,09	-4,18	-6,61	-11,38	-22,21	-28,92
21	6,22	,40	-3,29	-4,31	-8,16	-19,84	-26,81
22	6,54	,72	-3,05	-3,47	-6,25	-18,48	-25,03
23	6,78	,43	-3,45	-2,99	-4,09	-16,09	-20,55
24	6,29	1,24	-3,19	-4,09	-7,63	-19,80	-28,19

Table 11 (Continued)

RECORD NO. 24

THE DIAGNOSED CLEAR-COLUMN COMPONENTS (CLRX OUTPUT)

SPOT NO.	CHANNEL NO. 1	2	3	4	5	6	WINDOW
1	0,00	0,00	0.00	0.00	0,00	0,00	0,00
2	0.00	0.00	0,00	0,00	0.00	0,00	0,00
3	7,60	1,39	-3,51	-4,27	-4.20	-15,05	-14,89
4	7,47	1,30	-3,47	-4,16	-4.16	-14,88	-15,11
5	7,14	1,10	-3,34	-4,01	-4.10	-14,70	-15,35
6	6,75	,82	-3,16	-3,84	-4,05	-14,55	-15,57
7	6,27	,51	-3,06	-3,73	-4.03	-14,43	-15,78
8	5,82	,30	-2,93	-3,64	-4.02	-14,32	-15,88
9	5,83	,31	-3,04	-3,84	-4,03	-14,35	-15,89
10	5,79	,01	-3,15	-3,84	-3,98	-14,08	-16,16
11	5,80	-,22	-3,20	-3,83	-3,93	-13,80	-16,44
12	5,69	-,26	-3,06	-3,60	-3,83	-13,54	-16,82
13	5,65	-,32	-2,92	-3,37	-3,73	-13,27	-17,21
14	5,70	-,31	-2,77	-3,13	-3,62	-13,05	-17,59
15	5,81	-,32	-2.64	-2,90	-3,52	-12,82	-17,97
16	5,84	-,34	-2,58	-2,69	-3,41	-12,64	-18,32
17	5,84	-,32	-2,59	-2,54	-3,33	-12,40	-18,64
18	5,87	-,22	-2,57	-2,39	-3,25	-12,24	-18,93
19	5,98	-,01	-2,60	-2,26	-3,18	-12,04	-19,21
20	6,18	,17	-2,63	-2,12	-3,10	-11,94	-19,47
21	6,42	,39	-2,70	-2,00	-3,02	-11,81	-19,74
22	6,58	,52	-2,74	-1,89	-2,95	-11,72	-19,97
23	0,00	0,00	0,00	0,00	0.00	0,00	0,00
24	0,00	0,00	0,00	0,00	0.00	0,00	0,00

THE ASSOCIATED RELIABILITIES (CLRX OUTPUT)

1	0,00	0.00	0.00	0,00	0,00	0,00	0,00
2	0,00	0.00	0,00	0,00	0.00	0,00	0,00
3	14,96	14.30	13.17	5,67	1.94	1.71	,74
4	24.16	24.38	23.09	7.16	2.09	1.83	,76
5	26.54	29.25	24.39	8,67	2.25	1.96	,78
6	37,36	40.92	39.06	11,37	2.43	2,11	,80
7	42,45	43,80	43.64	15,31	2.59	2,27	,82
8	224,38	433,41	331.00	30,49	2.82	2,47	,85
9	324,22	317,07	257,90	19,04	2,74	2,36	,89
10	48,20	48,32	42.19	12,44	2.58	2.21	,90
11	87,44	81,99	50,74	11,13	2.45	2,11	,91
12	38,78	39,33	23,94	8,26	2,30	2,00	,91
13	31,70	29,55	17.06	6,74	2,17	1,92	,91
14	29,74	32.19	15,58	5,90	2,08	1,85	,92
15	36,48	40,09	17,25	5,43	2.01	1,80	,92
16	54,97	61,56	22,93	5,14	1.95	1.76	,92
17	41,31	41.49	19.69	4,71	1.86	1,70	,91
18	31,78	32,13	15,78	4,32	1,78	1,65	,90
19	24.63	29,51	14,51	4,02	1.70	1,60	,88
20	21,75	28,33	15,48	3,80	1,64	1,55	,87
21	23,33	30,16	17,67	3,60	1,58	1,51	,86
22	23,67	25,06	17.09	3,34	1.51	1.45	,88
23	0,00	0,00	0,00	0,00	0,00	0,00	0,00
24	0,00	0,00	0,00	0,00	0,00	0,00	0,00

Table 12

RECORD NO. 25

THE VTPR NORMALIZED RADIANCE ANOMALIES (CLRX INPUT)

SPOT NO.	CHANNEL NO. 1	2	3	4	5	6	WINDOW
1	9,98	3,33	-2,12	-,59	7,01	-1,20	1,31
2	9,18	2,46	-2,39	,07	7,57	-,29	2,70
3	8,89	1,51	-2,09	-,35	7,84	-,26	4,80
4	8,54	1,71	-2,33	-,63	6.47	-2,10	,98
5	8,14	,66	-2,54	-,20	5,69	-2,99	1,64
6	7,70	,78	-3,28	-3,43	-,69	-10,29	-9,95
7	7,84	,88	-2,90	-2,31	2,12	-6,79	-3,63
8	7,43	,29	-4,23	-5,32	-5.45	-15,45	-15,94
9	6,26	,34	-4,33	-7,63	-11.82	-22,89	-27,20
10	6,33	-,27	-5,08	-8,94	-14,90	-26,07	-32,47
11	5,73	-,26	-5,11	-9,01	-14,02	-24,56	-28,59
12	6,38	-,79	-6,34	-11,14	-18,83	-30,31	-36,36
13	5,74	-,25	-4,47	-7,97	-12,68	-23,46	-28,26
14	6,34	-,27	-4,44	-8,38	-15,44	-26,46	-32,80
15	6,29	-,30	-4,37	-7,23	-10,54	-21,01	-25,48
16	5,59	-,35	-4,27	-6,99	-9,35	-20,12	-23,65
17	6,12	-,41	-4,16	-7,19	-13,30	-24,49	-31,09
18	6,62	-,50	-4,01	-5,70	-10,56	-21,18	-26,87
19	5,83	-,61	-3,83	-6,30	-11.98	-23,19	-29,31
20	6,25	-,09	-3,63	-4,61	-7.95	-19,35	-24,04
21	6,64	,40	-2,74	-1,80	-1,78	-12,65	-17,00
22	5,72	,17	-3,82	-6,42	-12.15	-24,50	-32,14
23	5,96	,43	-7,89	-16,41	-27,50	-40,38	-49,00
24	6,60	,70	-4,53	-6,99	-12,67	-26,01	-35,30

Table 12 (Continued)

RECORD NO. 25

THE DIAGNOSED CLEAR-COLUMN COMPONENTS (CLRX OUTPUT)

SPOT NO.	CHANNEL NO. 1	2	3	4	5	6	WINDOW
1	0,00	0,00	0,00	0,00	0.00	0,00	0,00
2	0,00	0,00	0,00	0,00	0.00	0,00	0,00
3	8,16	1,07	-3,02	-3,66	-1,81	-11,19	-11,68
4	8,03	,97	-3,10	-3,69	-1.53	-10,85	-12,23
5	7,85	,83	-3,22	-3,72	-1.25	-10,49	-12,79
6	7,65	,75	-3,38	-3,77	-1.00	-10,19	-13,30
7	7,55	,66	-3,48	-3,85	-,46	-9,49	-14,29
8	7,41	,49	-3,67	-3,91	.06	-8,83	-15,25
9	7,07	,35	-3,77	-3,97	.65	-8,10	-16,28
10	6,76	,18	-3,83	-4,00	1,16	-7,48	-17,19
11	6,52	,06	-3,85	-4,05	1,69	-6,83	-18,18
12	6,38	-,05	-3,93	-4,02	2.12	-6,32	-18,91
13	6,27	-,12	-4,02	-4,01	2,58	-5,77	-19,74
14	6,25	-,19	-4.11	-3,89	2,90	-5,38	-20,38
15	6,22	-,24	-4,13	-3,81	3.27	-4,94	-21,07
16	6,18	-,27	-4,07	-3,60	3,49	-4,67	-21,60
17	6,23	-,26	-3,93	-3,40	3,76	-4,35	-22,19
18	6,30	-,21	-3,71	-3,08	3,90	-4,17	-22,62
19	6,33	-,10	-3,40	-2,79	4,08	-3,95	-23,11
20	6,40	,05	-3,04	-2,41	4,15	-3,86	-23,47
21	6,49	,20	-2,65	-2,09	4,27	-3,70	-23,89
22	6,32	,15	-2,59	-2,06	4.56	-3,36	-24,44
23	0,00	0,00	0,00	0,00	0,00	0,00	0,00
24	0,00	0,00	0,00	0,00	0.00	0,00	0,00

THE ASSOCIATED RELIABILITIES (CLRX OUTPUT)

1	0,00	0,00	0,00	0,00	0.00	0,00	0,00
2	0,00	0,00	0,00	0,00	0.00	0,00	0,00
3	13,91	12,25	12.46	3,46	1.02	,81	,43
4	21,35	17.55	18.07	3,95	1.05	,83	,43
5	33,77	29,71	25,28	4,55	1.10	,86	,44
6	121,65	144,85	52,68	5,34	1.14	,89	,45
7	42,95	49,80	30,27	4,84	1.11	,87	,45
8	32,20	39,56	26,50	4,44	1.08	,86	,45
9	23,12	28,78	20,36	3,96	1,06	,84	,45
10	21,53	24,69	15,99	3,60	1,03	,83	,44
11	19,74	23,93	14,17	3,35	1,01	,82	,44
12	20,14	22,58	14,21	3,15	,99	,81	,44
13	20,80	26,49	16,84	3,01	,98	,80	,44
14	23,59	30,41	23,62	2,90	,98	,79	,44
15	23,43	32,09	29.04	2,83	,95	,78	,44
16	21,33	31,20	30,95	2,75	,94	,77	,44
17	22,30	29,80	29,69	2,69	,93	,77	,44
18	21,42	27,31	27,36	2,65	,92	,76	,44
19	23,06	26,47	24,16	2,63	,91	,75	,44
20	30,48	31,27	21,08	2,61	,90	,75	,44
21	42,19	45,98	19,21	2,58	,90	,74	,44
22	18,76	23,73	11,24	2,35	,87	,72	,43
23	0,00	0,00	0,00	0,00	0.00	0,00	0,00
24	0,00	0,00	0,00	0,00	0.00	0,00	0,00

Table 13

RECORD NO. 26

THE VTPR NORMALIZED RADIANCE ANOMALIES (CLRX INPUT)

SPOT NO.	CHANNEL NO. 1	2	3	4	5	6	WINDOW
1	10,60	3,88	-1,35	,02	8,17	,56	2,17
2	9,13	3,01	-1,62	,04	9,25	1.06	6,38
3	8,90	2,61	-1,87	,73	8,53	1,02	3,95
4	8,55	2,26	-1,45	1,06	9,53	2,34	9,15
5	8,77	1,10	-1,67	-,21	7,78	,23	5,66
6	7,70	,67	-3,72	-7.11	-6,28	-15,83	-16,93
7	7,22	,77	-4,54	-8,62	-10,56	-19,92	-20,82
8	6,81	,18	-4,02	-7,88	-9,95	-19,77	-20,82
9	7,41	,23	-3,46	-3,42	1,20	-6,99	-4,75
10	7,48	,28	-1,70	,05	7,57	-,33	3,22
11	8,13	-,26	-2,38	-,62	5,59	-2,69	-,27
12	5,76	-,24	-4,93	-8,02	-10.58	-20,53	-23,25
13	5,74	-,25	-4,90	-10,02	-15,26	-25,76	-29,84
14	7,49	-,27	-3,02	-3,69	-,03	-8,73	-6,85
15	7,43	,25	-2,29	-,87	5,85	-2,15	1,18
16	7,36	,20	-2,85	-1,10	4,74	-4,28	-2,31
17	7,26	.14	-1,42	1,28	9,84	2,05	6,05
18	7,76	,05	-1,26	1,72	10,33	2,74	6,71
19	7,59	,60	-2,40	-2,01	3,69	-4,88	-3,08
20	7,39	,46	-1,53	1,30	10,19	1,75	4,61
21	8,39	,83	-1,30	1,54	11,09	3,87	10,53
22	8,70	1,26	-1,71	1,82	11,75	4,20	12,64
23	8,30	,96	-1,45	1,86	12,15	4,86	14,75
24	8,42	1,77	-1,18	1,96	11,86	4,96	14,75

Table 13 (Continued)

RECORD NO. 26

THE DIAGNOSED CLEAR-COLUMN COMPONENTS (CLRX OUTPUT)

SPOT NO.	CHANNEL NO. 1	2	3	4	5	6	WINDOW
1	0,00	0.00	0.00	0,00	0.00	0,00	0,00
2	0,00	0.00	0,00	0,00	0,00	0.00	0,00
3	8,71	2.16	-1.73	,65	8,64	1,28	6,37
4	8,57	1,94	-1,61	,50	8,64	1,27	6,46
5	8,76	1,24	-1,54	,37	8,72	1,32	6,46
6	8,45	,97	-1,56	,45	8,84	1,39	6,40
7	8,18	,74	-1,58	,54	8,95	1,46	6,33
8	7,96	,51	-1,59	,63	9.06	1,54	6,28
9	7,81	,34	-1,59	,72	9,18	1,61	6,22
10	7,75	,25	-1,54	,82	9,29	1,69	6,19
11	7,94	,07	-1,64	,91	9,39	1,77	6,17
12	7,85	,04	-1,65	,97	9,50	1,85	6,18
13	7,78	,05	-1,66	1,04	9,60	1,93	6,19
14	7,69	,09	-1,67	1,10	9,70	2,01	6,21
15	7,56	,18	-1,67	1,18	9,81	2,10	6,23
16	7,41	,17	-1,54	1,29	9,91	2,18	6,25
17	7,30	,13	-1,38	1,38	10,01	2,26	6,27
18	7,72	,08	-1,33	1,53	10,11	2,36	6,27
19	7,65	,32	-1,39	1,54	10,34	2,43	6,28
20	7,58	,49	-1,44	1,56	10,57	2,49	6,27
21	7,91	,65	-1,45	1,51	10,67	2,54	6,35
22	7,98	,71	-1,55	1,61	10,81	2,60	6,36
23	0,00	0,00	0,00	0,00	0,00	0,00	0,00
24	0,00	0,00	0,00	0,00	0,00	0,00	0,00

THE ASSOCIATED RELIABILITIES (CLRX OUTPUT)

1	0,00	0.00	0,00	0,00	0.00	0,00	0,00
2	0.00	0.00	0.00	0,00	0.00	0.00	0.00
3	65,25	29.99	126,56	24,22	11.42	8,25	2,79
4	134,73	82,27	132,20	27,49	10.47	7,91	3,11
5	201,05	156.64	150,91	26,76	9.45	7,39	3,29
6	32,12	37,19	27,75	15,49	7.64	6,31	3,21
7	23,51	30.87	19.40	12,33	6.72	5,69	3,16
8	23,25	30,13	18.71	11,49	6.25	5,35	3,16
9	31,99	40,01	23,99	12,12	6.10	5,20	3,19
10	63.46	82,81	50.82	14,44	6.18	5,21	3,26
11	33,45	41,77	31,05	12,31	5,90	5,02	3,25
12	20,89	26,20	19,62	10,66	5,72	4,90	3,27
13	19,28	24,73	17,68	10,32	5.77	4,93	3,33
14	24,02	28,63	20,47	11,04	6,05	5,10	3,44
15	41,14	44,73	30,33	13,09	6,62	5,44	3,60
16	51,35	52,55	33,83	16,68	7.58	5,98	3,83
17	499,91	647,91	140,92	30,89	9.42	6,91	4,15
18	402,41	448,20	170,39	30,18	9,65	7,03	4,05
19	54,66	52,50	44,55	21,73	9,18	6,46	3,60
20	106,71	144,33	154,12	29,88	10,14	6,45	3,30
21	46,35	67,67	70,00	31,54	10.31	5,63	2,94
22	22,12	26,28	33,42	23,60	8,71	4,79	2,62
23	0,00	0,00	0,00	0,00	0,00	0,00	0,00
24	0,00	0,00	0,00	0,00	0.00	0,00	0,00

Table 14

RECORD NO. 27

THE VTPR NORMALIZED RADIANCE ANOMALIES (CLRX INPUT)

SPOT NO.	CHANNEL NO. 1	2	3	4	5	6	WINDOW
1	9.68	4.21	-1.35	-.10	9.07	2.02	9.41
2	8.88	3.89	-1.06	.45	9.61	2.59	9.08
3	9.21	2.94	-1.87	.13	8.88	1.40	6.65
4	9.48	1.93	-1.56	.36	9.89	2.27	9.08
5	8.46	2.08	-1.78	.29	9.62	1.73	8.75
6	8.01	1.55	-1.97	-.87	6.53	-1.39	4.14
7	8.16	1.65	-2.68	-3.99	.29	-7.84	-4.61
8	6.50	1.17	-4.67	-8.47	-9.52	-19.17	-19.63
9	6.57	.56	-5.43	-10.37	-12.61	-22.37	-22.79
10	6.02	.61	-5.52	-11.09	-14.73	-25.18	-27.73
11	6.67	.62	-4.89	-8.04	-8.69	-18.33	-20.03
12	6.70	.64	-3.73	-7.05	-6.88	-16.08	-16.47
13	6.05	.63	-6.76	-13.83	-19.13	-29.39	-32.60
14	6.66	.61	-3.02	-3.21	.31	-8.44	-6.66
15	6.60	.58	-2.95	-3.02	1.02	-7.57	-5.27
16	6.52	.53	-2.30	-2.77	2.24	-6.58	-4.61
17	5.81	.47	-4.59	-7.77	-7.92	-17.47	-18.97
18	6.92	1.04	-2.58	-3.12	.60	-8.76	-8.43
19	5.52	.93	-4.26	-7.37	-10.30	-20.71	-24.57
20	7.18	1.33	-2.19	-1.99	3.78	-4.87	-1.78
21	7.45	1.81	-1.96	-.16	6.58	-1.57	4.14
22	7.15	1.58	-1.71	1.22	9.17	.68	6.65
23	8.00	1.94	-1.45	1.76	11.97	5.17	16.46
24	7.50	2.09	-1.18	1.87	12.71	5.68	16.79

Table 14 (Continued)

RECORD NO. 27

THE DIAGNOSED CLEAR-COLUMN COMPONENTS (CLRX OUTPUT)

SPOT NO.	CHANNEL NO. 1	2	3	4	5	6	WINDOW
1	0.00	0.00	0.00	0.00	0.00	0.00	0.00
2	0.00	0.00	0.00	0.00	0.00	0.00	0.00
3	8.97	2.07	-1.98	.03	8.52	.32	6.46
4	8.71	1.96	-1.84	-.08	8.33	.75	6.39
5	8.39	1.90	-1.88	-.19	8.13	.60	6.30
6	8.17	1.64	-1.79	-.22	7.91	.49	6.15
7	8.03	1.51	-1.75	-.27	7.66	.42	6.00
8	7.77	1.29	-1.75	-.30	7.45	.34	5.84
9	7.49	1.05	-1.76	-.32	7.23	.27	5.69
10	7.25	.88	-1.75	-.32	7.07	.16	5.53
11	7.09	.77	-1.75	-.33	6.90	.07	5.38
12	6.94	.70	-1.73	-.32	6.79	-.06	5.22
13	6.86	.67	-1.75	-.31	6.67	-.18	5.07
14	6.82	.65	-1.75	-.29	6.62	-.34	4.91
15	6.84	.66	-1.76	-.29	6.55	-.49	4.77
16	6.93	.71	-1.69	-.29	6.54	-.66	4.62
17	7.08	.86	-1.72	-.30	6.50	-.82	4.50
18	7.23	1.08	-1.73	-.29	6.51	-1.01	4.37
19	7.32	1.28	-1.79	-.28	6.50	-1.18	4.25
20	7.41	1.51	-1.84	-.25	6.52	-1.38	4.12
21	7.44	1.79	-1.96	-.18	6.52	-1.57	4.01
22	7.19	1.60	-1.89	-.09	6.49	-1.67	3.86
23	0.00	0.00	0.00	0.00	0.00	0.00	0.00
24	0.00	0.00	0.00	0.00	0.00	0.00	0.00

THE ASSOCIATED RELIABILITIES (CLRX OUTPUT)

1	0.00	0.00	0.00	0.00	0.00	0.00	0.00
2	0.00	0.00	0.00	0.00	0.00	0.00	0.00
3	26.87	15.30	29.40	80.30	12.81	7.96	3.32
4	32.23	26.97	58.03	38.80	10.46	7.42	3.41
5	52.00	70.31	124.24	30.10	9.05	6.93	3.40
6	79.50	115.07	90.84	22.03	7.74	6.17	3.23
7	28.91	36.30	25.99	13.35	6.33	5.26	2.95
8	19.64	26.10	16.04	9.96	5.45	4.65	2.75
9	18.25	24.64	12.61	8.32	4.88	4.23	2.58
10	18.21	26.71	11.16	7.44	4.50	3.94	2.44
11	21.45	30.27	10.87	6.99	4.25	3.73	2.33
12	23.69	32.15	11.34	6.63	4.09	3.60	2.23
13	23.36	32.09	12.47	6.87	3.99	3.51	2.16
14	31.15	38.26	15.61	7.20	3.97	3.47	2.10
15	34.55	40.66	18.52	7.57	3.97	3.45	2.04
16	29.19	36.70	18.13	7.93	4.00	3.45	1.99
17	21.05	27.14	16.28	8.24	4.05	3.47	1.94
18	21.58	27.10	17.88	9.12	4.17	3.53	1.90
19	23.73	28.56	21.16	10.73	4.37	3.64	1.87
20	44.94	52.73	40.54	14.59	4.70	3.83	1.85
21	375.30	733.98	253.54	24.57	5.18	4.07	1.83
22	47.56	60.70	60.07	13.83	4.42	3.56	1.70
23	0.00	0.00	0.00	0.00	0.00	0.00	0.00
24	0.00	0.00	0.00	0.00	0.00	0.00	0.00

4. Retrieval Demonstration

The present section is included in order to illustrate that we have developed the major technical components for an operational capability to exploit satellite-observed sounding data for resolution of atmospheric thermal-structure variabilities. We include a demonstration of thermal-structure retrieval using clear-column radiances, diagnosed by CLRX, as input to the general structure-blending retrieval capability developed under Phase One.*

This demonstration required modification of the structure-blending retrieval scheme from the 13-level, 11-layer atmospheric-structure model used in Phase One, to the 18-level, 16-layer model used in Phase Two.

Two examples are selected: one spot from Record No. 19 and one spot from Record No. 27--both nearest to zero nadir angle for the scan. The CLRX-produced radiances and weights must be transformed, as shown in Tables 15 and 16, for input to the retrieval scheme. The input first-guess estimates and weights for the atmospheric thermal-structure parameters and sea-surface temperatures are based on information independently provided to us.

The standard output for these two retrieval examples are given in Tables 17 and 18, respectively. In both examples channels 722.0 and 746.5 are rejected as gross errors in the reevaluations. These values do not check out on the basis of all information (i.e., weighted estimates) and the relationships. The implication is that channels are not reading as advertized by their specified transmission functions. This is a plausible conclusion. Expectations based on Figs. 2 through 9 are not borne out by, e.g., Figs. 10 and 11.

---

*Detailed and documented in the Task Three Report referenced on page 5.

Table 15

Spot 13 of Record No. 19. Columns (2) and (5) are th[illegible] CLRX products. Columns (4) and (8) express the inp[illegible] radiance information to the structure-blending retrieval s[illegible] [illegible]o.

(1) ν	(2) π^*_ν	(3) f_ν	(4) $\epsilon^*_\nu \equiv E$	(5) A^*_ν	(6)	(7)	(8) $\equiv W$
668.4	6.14	0.958	5.88	27.39	29.84	25	3.53
677.0	-0.02	0.908	-0.02	795.87	965.32	36	2.77
695.0	-1.76	0.916	-1.61	600.56	715.76	49	2.04
707.5	0.13	1.026	0.13	58.47	55.54	64	1.52
722.0	9.26	1.163	10.77	67.62	49.99	81	1.20
746.5	2.50	1.350	3.38	47.87	26.27	00	0.96
834.0	11.59	1.518	17.59	40.91	17.75	00	0.25

Legend to the columns:

(1) Channel identification

(2) CLRX-diagnosed clear-column normalized radiance anomal[illegible] [illegible]xtracted from Table 6

(3) The normalizing factor extracted from Table 4

(4) The radiance anomaly adjusted according to Eq. (34)

(5) CLRX-diagnosed reliability associated with column (2), ex[illegible]ted from Table 6

(6) The reliability adjusted according to Eq. (35)

(7) Example of estimated variances, σ^2, contributing to Eq. ([illegible]) [illegible]s explained in Section 3.5

(8) The reliability, adjusted according to Eq. (36), for associ[illegible] with column (4), as input to the retrieval scheme

Table 16

Spot 13 of Record No. 27. Columns (2) and (5) are the CLRX products. Columns (4) and (8) express the input radiance information to the structure-blending retrieval scheme.

(1)	(2)	(3)	(4)	(5)	(6)	(7)	(8)
ν	$\mathfrak{I}^*_\nu$	f_ν	$\epsilon^*_\nu = E$	A^*_ν			$\equiv W$
668.4	6.86	0.958	6.57	23.35	25.44	0.25	3.46
677.0	0.67	0.908	0.61	32.09	38.92	0.36	2.59
695.0	-1.75	0.916	-1.60	12.48	14.87	0.49	1.79
707.5	-0.31	1.026	-0.32	6.91	6.56	0.64	1.26
722.0	6.69	1.163	7.78	4.08	3.02	0.81	0.88
746.5	-0.17	1.350	-0.23	3.61	1.98	1.00	0.66
834.0	5.06	1.518	7.68	2.15	0.93	4.00	0.20

Legend to the columns:

(1) Channel identification

(2) CLRX-diagnosed clear-column normalized radiance anomalies extracted from Table

(3) The normalizing factor extracted from Table 4

(4) The radiance anomaly adjusted according to Eq. (34)

(5) CLRX-diagnosed reliability associated with column (2), extracted from Table 14

(6) The reliability adjusted according to Eq. (35)

(7) Example of estimated variances, σ^2, contributing to Eq. (1) as explained in Section 3.5

(8) The reliability, adjusted according to Eq. (36), for association with column (4), as input to the retrieval scheme

TABLE 17. SPOT 13 OF RECORD NO.19

	INPUT INFORMATION			INTERFACE TEMPERATURES		CYCLE NUMBER ONE							
LL	PARAMETER	ESTIMATE	WEIGHT			E*	T*	W*	E(A)	T(A)	E*A	T*A	W(R)
1	T GROUND	14.3000	.3000	1000:	297.05	9.37	291.3	1.075	7.46	251.2	9.31	291.5	.234
2	300-1000	388.00	100$	775:	285.79	237.	280.7	962$	219.	278.4	244.	280.9	100$
3	SIGMA 1	-2.7300	.3000	600:	273.16	-2.49	268.8	.302	38.45	273.8	-2.45	269.1	.300
4	SIGMA 2	.0200	.3000	450:	259.08	.49	255.4	.317	8.72	262.2	.59	255.7	.300
5	SIGMA 3	.4900	.3000	350:	245.50	.82	242.1	.344	3.08	248.9	.85	242.1	.300
6	SIGMA 4	-1.1200	.3000	275:	232.39	-1.06	229.1	.337	-.55	234.2	-1.36	229.0	.300
7	SIGMA 5	-3.2800	.3000	225:	224.65	-3.43	221.4	.331	-4.91	224.2	-3.65	221.1	.300
8	SIGMA 6	-4.4800	.3000	175:	211.36	-4.64	208.2	.316	-7.73	207.6	-4.86	208.0	.300
9	SIGMA 7	-10.8800	.3000	125:	208.36	-11.10	204.5	.318	-14.76	200.0	-11.03	202.4	.300
10	SIGMA 8	.5400	.1000	95:	205.26	-.36	199.9	.125	-3.88	192.2	-2.01	199.0	.100
11	SIGMA 9	-2.1400	.0600	60:	218.15	-3.61	212.3	.090	-6.55	201.5	-2.90	212.4	.060
12	SIGMA 10	4.8900	.0600	40:	222.96	7.39	217.3	.077	4.74	205.0	8.85	218.1	.060
13	SIGMA 11	1.8800	.1000	25:	227.89	1.57	222.9	.115	-.51	211.6	2.03	224.0	.100
14	SIGMA 12	1.8900	.1000	15:	232.54	1.85	228.4	.113	1.50	220.9	2.17	229.8	.100
15	SIGMA 13	.4200	.1000	8.5:	236.97	.55	233.8	.110	1.92	231.2	.77	235.3	.100
16	SIGMA 14	1.4600	.1000	5.5:	239.91	1.65	237.3	.109	3.73	238.4	1.84	238.9	.100
17	SIGMA 15	5.1000	.1000	0:	262.13	5.21	273.5	.104	7.58	277.5	5.41	266.2	.100
18	SIGMA 16	1.0100	.1000			1.94		.381	2.27		1.35		.100
19	CH 668.4	5.8800	3.53			5.87		3.63	5.37		5.85		3.53
20	CH 677.0	-.0200	2.77			.21		3.41	1.18		.35		2.77
21	CH 695.0	-1.6100	2.04			-1.71		4.26	-1.80		-1.87		2.04
22	CH 707.5	.1300	1.52			1.61		3.54	2.72		1.54		1.52
23	CH 722.0	10.7700	1.20			5.34		3.09	1.89		5.41		0.00
24	CH 746.5	3.3800	.96			9.72		2.19	14.69		9.79		0.00
25	CH 834.0	17.5900	.25			14.23		.47	10.34		14.14		.25

LL	CYCLE NUMBER TWO E*	T*	W*	E(A)	T(A)	E*^	T*^	W(R)	CYCLE NUMBER THREE E*	T*	W*	E(A)	T(A)	E*^	T*^
1	12.35	292.1	.810	11.56	365.6	12.35	291.8	.242	12.43	291.6	.771	11.57	349.3	12.43	291.5
2	222.	281.1	.382$	163.	289.2	220.	280.9	42$	217.	280.6	222$	178.	284.1	217.	280.6
3	-2.88	268.5	.301	-73.10	257.7	-2.75	268.5	.300	-2.79	268.2	.300	-61.38	258.9	-2.74	268.3
4	-.32	254.4	.305	-21.70	236.8	-.12	254.4	.300	-.11	254.4	.303	-14.83	242.1	-.06	254.4
5	.09	240.9	.315	-7.79	221.0	.11	240.9	.300	.36	241.1	.310	-3.52	228.3	.33	241.1
6	-1.41	227.8	.320	-5.68	206.3	-1.42	227.9	.300	-1.20	228.2	.315	-2.74	215.1	-1.21	228.2
7	-3.57	220.2	.324	-7.22	197.3	-3.58	220.2	.300	-3.37	220.7	.318	-4.84	207.1	-3.37	220.7
8	-4.65	207.1	.314	-8.44	183.4	-4.67	207.1	.300	-4.55	207.6	.311	-6.29	193.3	-4.55	207.6
9	-11.03	204.0	.316	-13.80	180.1	-11.02	203.9	.300	-10.97	204.4	.314	-12.81	189.2	-10.97	204.4
10	.04	200.1	.125	-2.02	176.5	.00	200.1	.100	.08	200.4	.123	-1.97	184.0	.08	200.4
11	-3.05	212.7	.090	-4.89	188.1	-3.06	212.7	.060	-3.19	212.7	.089	-5.35	194.0	-3.19	212.7
12	8.15	217.6	.076	5.46	192.2	8.16	217.6	.060	7.98	217.4	.076	4.65	196.3	7.98	217.4
13	1.49	222.8	.115	-1.15	197.8	1.50	222.8	.100	1.39	222.6	.114	-2.00	200.2	1.39	222.6
14	1.66	228.1	.112	-.19	206.2	1.66	228.1	.100	1.58	227.8	.112	-.97	207.3	1.58	227.8
15	.40	233.5	.109	.23	218.3	.41	233.5	.100	.35	233.2	.109	-.36	218.7	.35	233.2
16	1.63	237.2	.109	3.48	230.2	1.63	237.2	.100	1.61	236.9	.109	3.23	230.6	1.61	236.9
17	5.30	273.7	.104	9.86	277.8	5.30	273.7	.100	5.30	274.8	.104	9.84	279.3	5.30	274.8
18	1.96		.380	2.29		1.96		.100	2.05		.380	2.42		2.05	
19	5.83		3.63	3.96		5.83		3.53	5.83		3.63	3.89		5.83	
20	.17		3.39	.99		.16		2.77	.17		3.34	1.07		.17	
21	-2.12		4.22	-2.60		-2.12		2.01	-1.97		3.56	-2.43		-1.97	
22	.98		2.18	2.92		.98		.66	1.10		1.12	2.49		1.11	
23	5.45		.98	5.45		5.42		0.00	5.42		.55	5.42		5.42	
24	11.42		.06	11.42		11.38		0.00	11.37		.45	11.37		11.37	
25	18.76		.35	21.64		18.76		.23	18.88		.33	21.68		18.88	

$ NOTE--THE $ ON W(2) DENOTES: TIMES 10 TO THE MINUS 6

1 2 3 4

TABLE 17. CONTINUED

SUPPLEMENTAL LEGEND

1 THE COLUMN OF WEIGHTS UPON SECOND REEVALUATION

2 THE RESULTANT WEIGHTS

3 THE RESULTANT ESTIMATES (CONSTRAINED BLENDING REQUIRED)

4 THE CORRESPONDING INTERFACE TEMPERATURES

TABLE 18. SPOT 13 OF RECORD NO.27

LL	PARAMETER	ESTIMATE	WEIGHT	INTERFACE TEMPERATURES		E*	T*	W*	E(A)	T(A)	E*A	T*A	W(R)
	INPUT INFORMATION					CYCLE NUMBER ONE							
1	I GROUND	11.3000	.3000	1000:	297.33	4.97	288.8	.913	1.87	259.7			.11
2	300-1000	438.000	100$	775:	285.39	202.	277.6	796$	168.	273.5			75$
3	SIGMA 1	-3.5000	.3000	600:	273.03	-3.36	266.1	.302	23.48	268.4			.300
4	SIGMA 2	.3100	.3000	450:	263.12	.66	257.1	.315	7.76	261.9			.300
5	SIGMA 3	4.8100	.3000	350:	248.50	5.17	243.0	.339	7.98	249.0			.300
6	SIGMA 4	-2.0200	.3000	275:	232.93	-1.83	227.8	.334	-.15	233.1			.300
7	SIGMA 5	-6.0600	.3000	225:	224.51	-6.08	219.7	.329	-6.33	224.5			.300
8	SIGMA 6	-5.4400	.3000	175:	210.90	-5.45	206.4	.315	-5.68	211.3			.300
9	SIGMA 7	-11.2700	.3000	125:	206.73	-11.25	202.8	.317	-10.87	207.7			.300
10	SIGMA 8	-.5500	.1000	85:	202.41	-.44	199.1	.125	.01	204.0			.100
11	SIGMA 9	-3.2300	.0600	60:	215.23	-3.03	212.5	.090	-2.64	217.7			.060
12	SIGMA 10	8.5900	.0600	40:	220.75	8.77	218.5	.076	9.45	224.5			.060
13	SIGMA 11	2.1600	.1000	25:	226.42	2.33	224.7	.115	3.36	232.3			.100
14	SIGMA 12	2.1900	.1000	15:	231.77	2.37	230.6	.112	3.86	240.0			.100
15	SIGMA 13	.7200	.1000	8.5:	236.86	.89	236.1	.110	2.64	246.3			.100
16	SIGMA 14	1.7600	.1000	5.5:	240.24	1.87	239.6	.109	3.11	249.5			.100
17	SIGMA 15	5.4000	.1000	0:	265.78	5.43	268.5	.104	6.01	269.5			.100
18	SIGMA 16	1.3100	.1000			1.53		.377	1.61				.100
19	CH 668.4	6.5700	3.46			6.57		3.56	6.67				3.46
20	CH 677.0	.6100	2.59			.75		3.20	1.35				2.59
21	CH 695.0	-1.6000	1.79			-1.94		3.84	-2.23				1.79
22	CH 707.5	-.3200	1.26			1.04		2.97	2.04				1.23
23	CH 722.0	7.7800	.88			3.62		2.42	1.25				0.00
24	CH 746.5	-.2300	.66			5.89		1.69	9.81				0.00
25	CH 834.0	7.6800	.20			7.54		.40	7.41				.20

	CYCLE NUMBER TWO								CYCLE NUMBER THREE						
LL	E*	T*	W*	F(A)	T(A)	F*^	T*^	W(R)	E*	T*	W*	E(A)	T(A)	E*^	T*^
1	6.20	290.3	.567	5.03	382.1	6.20	289.9	0.000	5.04	288.2	.218	5.04	36.2		
2	210.	278.7	326$	142.	287.3	207.	278.5	0$	173.	276.9	140$	173.	270.3		
3	-3.65	266.5	.301	-93.37	252.2	-3.52	266.5	.300	-3.49	265.2	.300	262.38	296.2		
4	-.03	256.8	.304	-25.92	235.5	.19	256.8	.300	.37	256.1	.300	43.60	298.5		
5	4.44	242.4	.313	-4.00	219.5	4.44	242.4	.299	5.00	242.2	.303	19.34	289.9		
6	-2.24	227.1	.318	-5.91	203.6	-2.25	227.2	.300	-1.76	227.3	.308	8.06	278.5		
7	-6.25	219.0	.321	-8.87	195.8	-6.14	219.0	.300	-5.78	219.3	.310	2.45	273.8		
8	-5.50	205.7	.312	-6.86	184.6	-5.52	205.8	.300	-5.22	206.3	.307	3.81	262.3		
9	-11.25	202.3	.315	-10.77	184.4	-11.29	202.3	.300	-11.05	203.2	.311	-4.79	257.2		
10	-.28	199.1	.124	.84	184.3	-.33	199.1	.100	.02	199.8	.120	2.85	249.3		
11	-2.73	212.6	.070	-1.73	200.6	-2.73	212.6	.060	-2.80	212.9	.089	-1.88	257.9		
12	8.91	218.6	.076	10.08	209.3	8.91	218.6	.060	8.62	218.6	.076	8.74	257.9		
13	2.33	224.7	.114	3.35	218.1	2.33	224.7	.100	2.11	224.4	.114	1.58	257.7		
14	2.31	230.5	.112	3.30	226.7	2.31	230.5	.100	2.11	230.0	.112	1.41	258.3		
15	.83	236.0	.109	2.03	235.1	.83	236.0	.100	.70	235.4	.109	.42	260.5		
16	1.87	239.6	.109	3.13	241.4	1.88	239.6	.100	1.81	239.1	.109	2.35	263.5		
17	5.48	268.4	.104	7.33	269.3	5.48	268.4	.100	5.47	270.2	.104	7.09	271.9		
18	1.52		.376	1.60		1.52		.100	1.68		.376	1.81			
19	6.55		3.56	5.94		6.55		3.46	6.55		3.56	5.67			
20	.71		3.17	1.14		.70		2.59	.76		3.08	1.53			
21	-2.14		3.77	-2.72		-2.18		1.66	-2.04		2.82	-2.68			
22	.82		1.77	3.36		.82		.41	.58		.67	1.95			
23	3.93		.82	3.93		3.90		0.00	3.08		.33	3.08			
24	6.92		.53	6.92		6.87		0.00	5.46		.23	5.46			
25	9.42		.25	16.98		9.42		.09	7.66		.09	-397.16			

$ NOTE--THE $ ON W(2) DENOTES: TIMES 10 TO THE MINUS 6

1 3 4 2

TABLE 18. CONTINUED

SUPPLEMENTAL LEGEND

1 THE COLUMN OF WEIGHTS UPON SECOND REEVALUATION

2 THE RESULTANT WEIGHTS

3 THE RESULTANT ESTIMATES (CONSTRAINED BLENDING NOT REQUIRED)

4 THE CORRESPONDING INTERFACE TEMPERATURES

5. Design of the Basic Comprehensive Capability

Supplemental developments and refinements are necessary in order to establish the basic capability for processing satellite VTPR sounding data for atmospheric thermal-structure resolution. The required components and interfaces are shown schematically in Fig. 17. Commentary follows. Components are identified by number in the figure.

Component 1:

The major requirement is for independent thermal-structure estimates, to be used in diagnosing the radiances and for purging the diagnosed correction vectors in CLRX, and for blending with the radiances in the Structure Blending operation (7). A complete set of thermal-structure parameters is required for every spot of a scan. The time of the scan determines the timeliness of the charts required. The position of successive spots are transformed into I,J locations.

New subroutines developed by MII for FNWC will be used for interpolation to I,J locations. These are identified as INTRP and INTRPS. Both are based on zero-order and first-order spatial continuity, INTRPS is for application to ocean parameters--in the present context, sea-surface temperature--and involves a spatial-covariance-dissociation (SCD) field demarcating oceanic continuity. The interpolation will also be designed to establish that the scan is in an oceanic region.

Transforms will be required to transform the available set of FNWC thermal-structure parameters, into the set selected for the exploitation of the VTPR system.

Component 2:

The first-guess thermal-structure scan sets must be transformed into first-guess values of normalized clear-column radiance anomalies. The necessary transforms for a VTPR system of specified transmission functions, can be produced by the capability described under Section 2.1

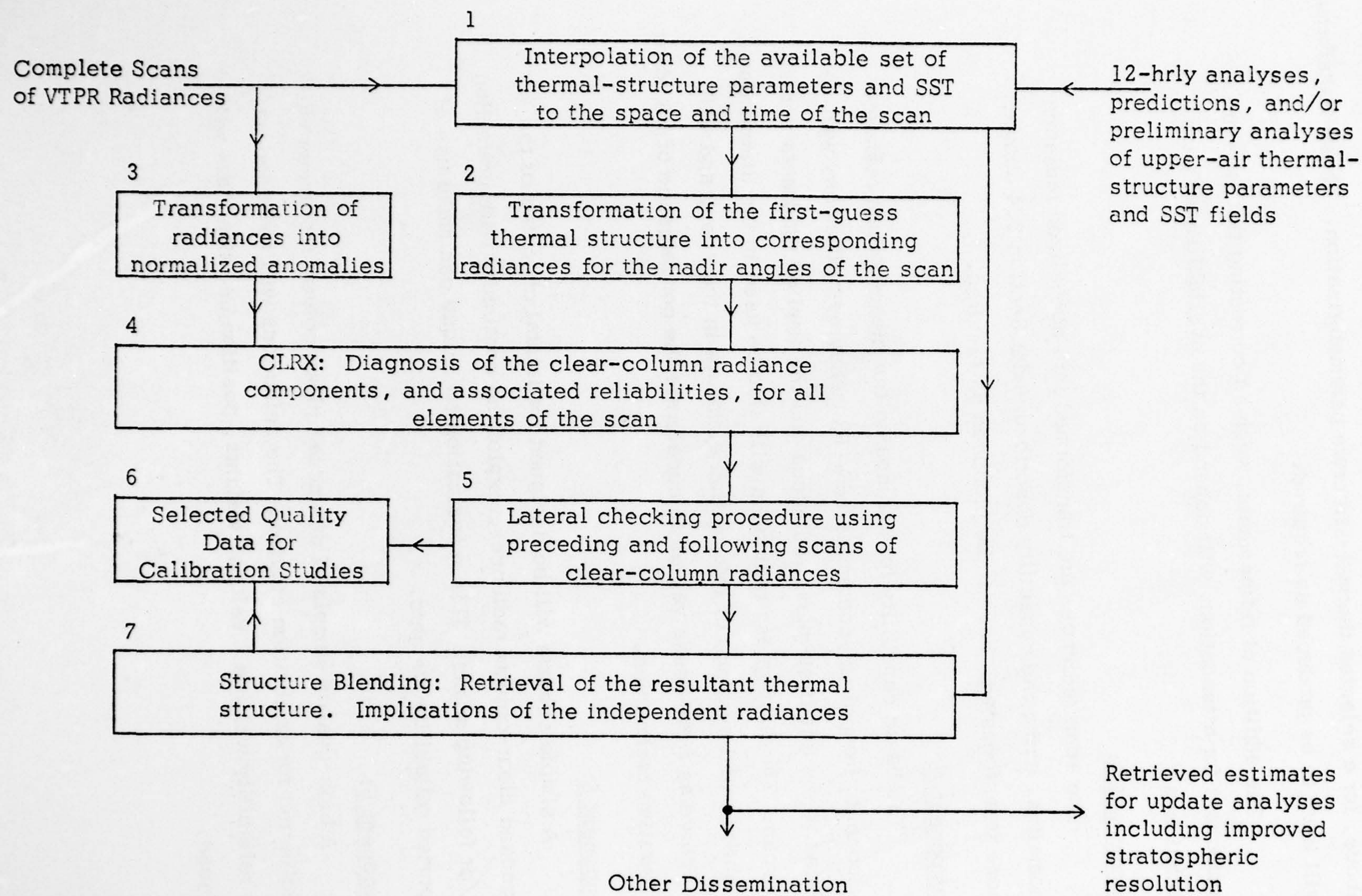

Fig. 17 Schematic Block Diagram

above, for a selected thermal-structure parameterization. These transforms will have to be produced as required.

The addition of refinements, such as correcting the sea-surface component for attenuation, will depend on the availability of such techniques.

Component 3:

The scan radiances are transformed into normalized radiance anomalies, using the capability described under Section 2.4 above. These transforms will have to be produced as required.

Component 4:

The basic capability for diagnosing the clear-column radiance components from cloud-contaminated VTPR measured radiances, will be refined to exploit first-guess radiances and the implied gradients across the scan. The first-guess radiances will also be used in the diagnosis, weighting, and purging, of information elements in the scan, and will also serve as first-guess values to accelerate the convergence of blending by iterative techniques.

Component 5:

A simple scheme will be designed for lateral checking of the diagnosed clear-column radiances, exploiting continuity with preceding and/or following scans. This reevaluation technique can make use of purported reliability weights.

Component 6:

A high-quality sample of diagnosed clear-column radiances will be collected for calibration studies. The selections will be based on high reliability weights. Values, weights, position and time data will be saved.

AD-A074 776 METEOROLOGY INTERNATIONAL INC MONTEREY CALIF F/G 4/2
TECHNIQUES FOR PROCESSING VTPR SIDE-SCAN RADIANCES INCLUDING DI--ETC(U)
FEB 75 M M HOLL N66314-74-C-1281
UNCLASSIFIED MII-M-205 EPRF-TR-4-75-MII NL

2 OF 2
AD
A074776

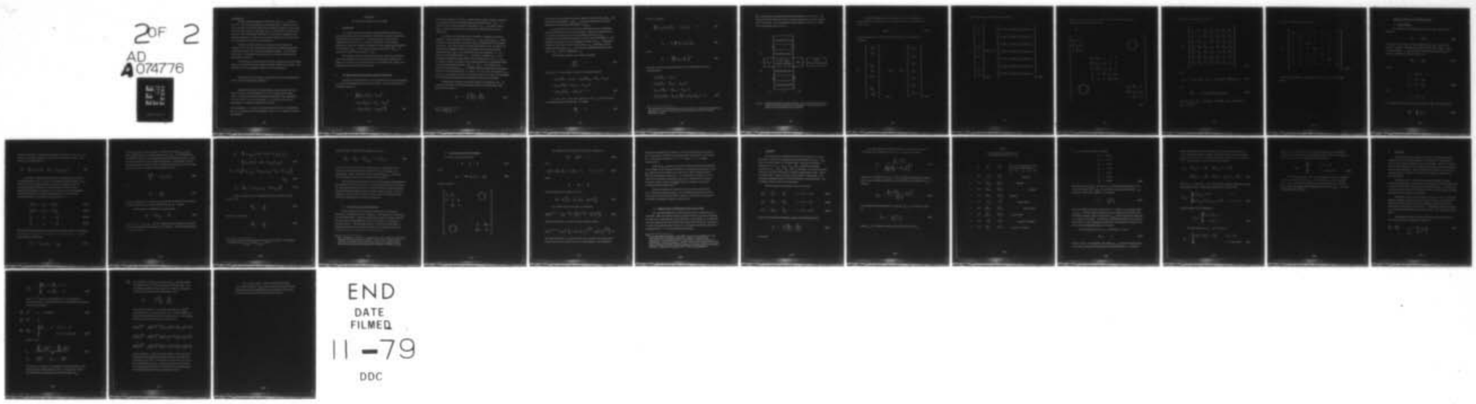

END
DATE
FILMED
11 -79
DDC

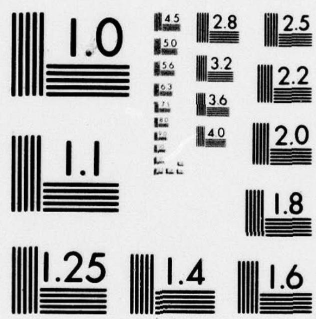

MICROCOPY RESOLUTION TEST CHART
NATIONAL BUREAU OF STANDARDS-1963-A

Component 7:

Structure Blending applies to individual spots (i.e., columns) of the scan. The retrieval technique is one dimensional. Blending retrieval can be limited to only those spots having highest reliability in any portion of a scan, and relative to adjoining scans, or every spot of a scan may be retrieved. The combination coefficients, which relate a radiance to the thermal-parameter set, differs for each spot dependent on the nadir angle. This dependency will have to be incorporated.

The clear-column radiances are diagnosed and weighted by component (4). The first-guess thermal-structure estimates produced by component (1) must have associated reliability weights. Class weights may be used. Refinements may be added for estimating associated and contributing variances.

The combined resultant thermal-structure parameters and sea-surface temperature estimates and associated reliability weights are produced. The implication of the independent radiances are also expressed.

The development of the basic capability will involve evaluations at various stages of component operations.

Instead of listing all the improvements and extensions that have come to mind for these developments--in this already overly lengthy report--we will make do with one sweeping statement: The improvement of applications of the FIB methodology, is, by the very nature of the methodology, a continuous constructive process.

Acknowledgment. -- A sense of appreciation behooves me to acknowledge Mrs. B. A. Hawkins for all programming, and Dr. W. F. Weigle for writing the Appendix.

APPENDIX A

The Component Operations of FIB-CLRX

1. Introduction

The general Fields by Information Blending (FIB) methodology has been developed by MII and successfully used for the analysis of horizontal distributions of both scalar (e.g., sea-level pressure, sea-surface temperature) and vector (e.g., surface wind) fields. For the current application it has been designed to analyze the two-dimensional distribution of corrections, $\varphi^*_{\nu,n}$, to the measured radiance anomalies, $\mathfrak{I}^P_{\nu,n}$, to produce the clear-column anomalies, $\mathfrak{I}^*_{\nu,n}$.

The following sections will discuss the form of the error functional used in this application, the resultant blending system of equations, the methods of solution of the blending system, the assembly and, finally, the reevaluation and recycling of the analysis.

2. The Error Functional and Blending System of Equations

The basis of the FIB analysis is the minimization of an error functional, E, over the two-dimensional array of grid points. This error functional for FIB-CLRX is given as

$$E \equiv \sum_{\nu,n} \Big\{ A_{\nu,n}\left(\varphi^*_{\nu,n} - \varphi_{\nu,n}\right)^2 + B_{\nu,n}\left(\varphi^*_{\nu,n+1} - \varphi^*_{\nu,n} - \mu_{\nu,n}\right)^2 + C_n W_{\nu,n}\left(\varphi^*_{\nu,n} - L_n N_{\nu,n}\right)^2 \Big\} \quad . \tag{A1}$$

In the error functional, the $\varphi^*_{\nu,n}$ represent the blended resultant corrections to be added to the measured normalized radiance anomalies, $\mathfrak{J}^P_{\nu,n}$, to obtain the clear-column radiance components, $\mathfrak{J}^*_{\nu,n}$. The entire array of $\varphi^*_{\nu,n}$ is what we wish to arrive at by blending all available sources of information.

The sources of information are combined or assembled to produce estimates of the individual corrections $\varphi_{\nu,n}$, $\mu_{\nu,n}$ and $L_n N_{\nu,n}$. Hence, estimates of the individual corrections $\varphi_{\nu,n}$ are formed from the available information. The more valid the estimates are deemed to be, the higher the square of the disparity between the assembled values and the blended resultant values, $\varphi^*_{\nu,n}$, are weighted in the error functional; i.e., the higher the associated weights $A_{\nu,n}$. Similarly, estimates $\mu_{\nu,n}$ of the difference between the corrections for two adjacent spots, $\varphi_{\nu,n+1} - \varphi_{\nu,n}$, are formed. Again, the square of the disparity between the assembled values and the blended resultant values, $\varphi^*_{\nu,n+1} - \varphi^*_{\nu,n}$, are weighted as to reliability by the weight $B_{\nu,n}$. Note that since we cannot spread information across the lateral boundaries (i.e., spots $n=1$ and $n=N$), the weights $B_{\nu,0}$ and $B_{\nu,N}$ are always set equal to zero where they occur in the error functional, and in the blending equations to be derived from the error functional.

Independent estimates of the entire vector of corrections, $\underset{\sim}{\varphi}_n$, for a spot may be made. This vector may be written in the normalized, sign-adjusted form given by

$$\underset{\sim}{N}_n = \frac{\underset{\sim}{I} \cdot \underset{\sim}{\varphi}_n}{|\underset{\sim}{I} \cdot \underset{\sim}{\varphi}_n|} \frac{\underset{\sim}{\varphi}_n}{|\underset{\sim}{\varphi}_n|} \quad . \qquad \text{(A2)*}$$

*Note that $\sum_{\nu} N^2_{\nu,n} = 1$.

The square of the disparity between the blended resultant value, $\varphi^*_{\nu,n}$, and the individual component, $L_n N_{\nu,n}$, of the total adjustment vector are weighted as to reliability by the weight $C_n W_{\nu,n}$.

It is important to note the kind of information that is assimilated into each of the terms in the error functional. Information pertaining only to a single correction goes into the assembled estimate of $\varphi_{\nu,n}$. Information on the horizontal gradients or spot-to-spot differences in φ for a given channel goes into the assembled estimates of $\mu_{\nu,n}$. Information pertaining to the whole vector of corrections, $\underset{\sim}{\varphi}_n$, rather than just the individual corrections, $\varphi_{\nu,n}$, goes into the assembled estimates of the vector, $\underset{\sim}{N}_n$, and of the magnitude, L_n.

The blending equations are obtained by setting

$$\frac{\partial E}{\partial \varphi^*_{\nu,n}} = 0 \tag{A3}$$

for all (ν,n). This procedure produces the general equation

$$A_{\nu,n}\left(\varphi^*_{\nu,n} - \varphi_{\nu,n}\right) - B_{\nu,n}\left(\varphi^*_{\nu,n+1} - \varphi^*_{\nu,n} - \mu_{\nu,n}\right)$$

$$+ \; B_{\nu,n-1}\left(\varphi^*_{\nu,n} - \varphi^*_{\nu,n-1} - \mu_{\nu,n-1}\right)$$

$$+ \; C_n W_{\nu,n}\left(\varphi^*_{\nu,n} - L_n N_{\nu,n}\right) = 0 \; . \tag{A4}$$

We also wish to make that adjustment to the L_n parameters which will minimize the error functional. By setting

$$\frac{\partial E}{\partial L_n} = 0 \tag{A5}$$

for all n we obtain

$$\sum_{\nu} N_{\nu,n} W_{\nu,n} \left(\varphi^*_{\nu,n} - L_n N_{\nu,n} \right) = 0 \quad , \tag{A6}$$

or

$$L_n = H_n \sum_{\nu} N_{\nu,n} W_{\nu,n} \varphi^*_{\nu,n} \tag{A7}$$

where

$$H_n = \left\{ \sum_{\nu} W_{\nu,n} N^2_{\nu,n} \right\}^{-1} \quad . \tag{A8}$$

Therefore, we may write the blending system of equations (A4) in the equivalent form

$$\begin{aligned} & A_{\nu,n} \left(\varphi^*_{\nu,n} - \varphi_{\nu,n} \right) \\ + \; & B_{\nu,n} \left(\varphi^*_{\nu,n} - \varphi^*_{\nu,n+1} + \mu_{\nu,n-1} \right) \\ + \; & B_{\nu,n-1} \left(\varphi^*_{\nu,n} - \varphi^*_{\nu,n-1} - \mu_{\nu,n-1} \right) \\ + \; & C_n W_{\nu,n} \left(\varphi^*_{\nu,n} - N_{\nu,n} H_n \sum_{\omega} N_{\omega,n} W_{\omega,n} \varphi^*_{\omega,n} \right) = 0 \quad . \end{aligned} \qquad \text{(A9)*}$$

---

*The same form for the blending system of equations is obtained by substituting the form for L_n given by Eq. (A7) into the error functional Eq. (A1) and applying Eq. (A3).

This system may be expressed in the stencil format given in Fig. A1. The stencil on the left-hand side of Fig. A1 shows the coefficients that multiply the φ^* elements. The corresponding forcing function elements are shown on the right-hand side of Fig. A1.

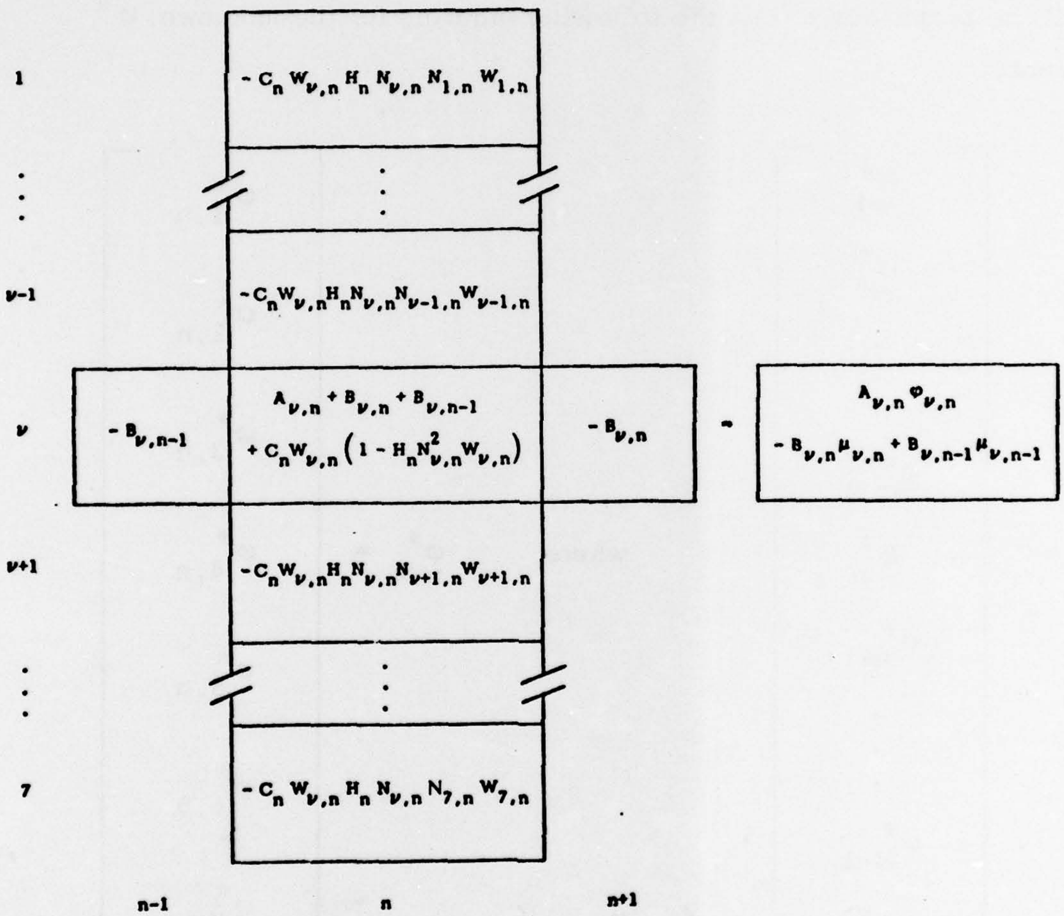

Fig. A1 Blending equations in stencil format. The left-hand-side shows the coefficients that multiply the φ^* elements. The right-hand-side shows the corresponding forcing function.

Since the blending system of equations is a set of simultaneous equations which are linear in the φ^* elements, they may be expressed in matrix form as

$$\underset{\approx}{M}\,\underset{\sim}{\varphi}^* = \underset{\sim}{F} \quad . \tag{A10}$$

It will be propitious to use the following ordering for the unknown φ^* elements:

$$\underset{\sim}{\varphi}^* = \begin{bmatrix} \underset{\sim}{\varphi}^*_1 \\ \underset{\sim}{\varphi}^*_2 \\ \cdot \\ \cdot \\ \cdot \\ \underset{\sim}{\varphi}^*_{n-1} \\ \underset{\sim}{\varphi}^*_n \\ \underset{\sim}{\varphi}^*_{n+1} \\ \cdot \\ \cdot \\ \cdot \\ \underset{\sim}{\varphi}^*_{N-1} \\ \underset{\sim}{\varphi}^*_N \end{bmatrix} \tag{A11}$$

where

$$\underset{\sim}{\varphi}^*_n = \begin{bmatrix} \varphi^*_{1,n} \\ \varphi^*_{2,n} \\ \varphi^*_{3,n} \\ \varphi^*_{4,n} \\ \varphi^*_{5,n} \\ \varphi^*_{6,n} \\ \varphi^*_{7,n} \end{bmatrix} . \tag{A12}$$

The forcing function vector then takes the form

$$
\underset{\sim}{F} = \begin{bmatrix} \underset{\sim}{F}_1 \\ \underset{\sim}{F}_2 \\ \cdot \\ \cdot \\ \cdot \\ \underset{\sim}{F}_{n-1} \\ \underset{\sim}{F}_n \\ \underset{\sim}{F}_{n+1} \\ \cdot \\ \cdot \\ \cdot \\ \underset{\sim}{F}_{N-1} \\ \underset{\sim}{F}_N \end{bmatrix} \quad \text{(A13)} \quad \text{where } \underset{\sim}{F}_n = \begin{bmatrix} A_{1,n}\varphi_{1,n} - B_{1,n}\mu_{1,n} + B_{1,n-1}\mu_{1,n-1} \\ A_{2,n}\varphi_{2,n} - B_{2,n}\mu_{2,n} + B_{2,n-1}\mu_{2,n-1} \\ A_{3,n}\varphi_{3,n} - B_{3,n}\mu_{3,n} + B_{3,n-1}\mu_{3,n-1} \\ A_{4,n}\varphi_{4,n} - B_{4,n}\mu_{4,n} + B_{4,n-1}\mu_{4,n-1} \\ A_{5,n}\varphi_{5,n} - B_{5,n}\mu_{5,n} + B_{5,n-1}\mu_{5,n-1} \\ A_{6,n}\varphi_{6,n} - B_{6,n}\mu_{6,n} + B_{6,n-1}\mu_{6,n-1} \\ A_{7,n}\varphi_{7,n} - B_{7,n}\mu_{7,n} + B_{7,n-1}\mu_{7,n-1} \end{bmatrix} . \quad \text{(A14)}
$$

All $B_{\nu,0} = B_{\nu,N} = 0$, as noted earlier. The coefficient matrix $\underset{\approx}{M}$ may then be written in partitioned form as

$$\underset{\approx}{M} =$$

$$\begin{bmatrix}
\begin{matrix} \underset{\approx}{A}_1 & \underset{\approx}{B}_1 & \underset{\approx}{0} \\ \underset{\approx}{B}_1^T & \underset{\approx}{A}_2 & \underset{\approx}{B}_2 \\ \underset{\approx}{0} & \underset{\approx}{B}_2^T & \underset{\approx}{A}_3 \end{matrix} & & & & \bigcirc \\
 & \ddots & & & \\
 & & \begin{matrix} \underset{\approx}{A}_{n-2} & \underset{\approx}{B}_{n-2} & \underset{\approx}{0} & \underset{\approx}{0} & \underset{\approx}{0} \\ \underset{\approx}{B}_{n-2}^T & \underset{\approx}{A}_{n-1} & \underset{\approx}{B}_{n-1} & \underset{\approx}{0} & \underset{\approx}{0} \\ \underset{\approx}{0} & \underset{\approx}{B}_{n-1}^T & \underset{\approx}{A}_n & \underset{\approx}{B}_n & \underset{\approx}{0} \\ \underset{\approx}{0} & \underset{\approx}{0} & \underset{\approx}{B}_n^T & \underset{\approx}{A}_{n+1} & \underset{\approx}{B}_{n+1} \\ \underset{\approx}{0} & \underset{\approx}{0} & \underset{\approx}{0} & \underset{\approx}{B}_{n+1}^T & \underset{\approx}{A}_{n+2} \end{matrix} & & \\
 & & & \ddots & \\
\bigcirc & & & & \begin{matrix} \underset{\approx}{A}_{N-2} & \underset{\approx}{B}_{N-2} & \underset{\approx}{0} \\ \underset{\approx}{B}_{N-2}^T & \underset{\approx}{A}_{N-1} & \underset{\approx}{B}_{N-1} \\ \underset{\approx}{0} & \underset{\approx}{B}_{N-1}^T & \underset{\approx}{A}_N \end{matrix}
\end{bmatrix} . \tag{A15}$$

The general submatrix $\underset{\approx}{A}_n$ is given by

$$\underset{\approx}{A}_n = \begin{bmatrix} S_{1,n} & R^2_{1,n} & R^3_{1,n} & R^4_{1,n} & R^5_{1,n} & R^6_{1,n} & R^7_{1,n} \\ R^1_{2,n} & S_{2,n} & R^3_{2,n} & R^4_{2,n} & R^5_{2,n} & R^6_{2,n} & R^7_{2,n} \\ R^1_{3,n} & R^2_{3,n} & S_{3,n} & R^4_{3,n} & R^5_{3,n} & R^6_{3,n} & R^7_{3,n} \\ R^1_{4,n} & R^2_{4,n} & R^3_{4,n} & S_{4,n} & R^5_{4,n} & R^6_{4,n} & R^7_{4,n} \\ R^1_{5,n} & R^2_{5,n} & R^3_{5,n} & R^4_{5,n} & S_{5,n} & R^6_{5,n} & R^7_{5,n} \\ R^1_{6,n} & R^2_{6,n} & R^3_{6,n} & R^4_{6,n} & R^5_{6,n} & S_{6,n} & R^7_{6,n} \\ R^1_{7,n} & R^2_{7,n} & R^3_{7,n} & R^4_{7,n} & R^5_{7,n} & R^6_{7,n} & S_{7,n} \end{bmatrix} \tag{A16}$$

where

$$S_{\nu,n} \equiv A_{\nu,n} + B_{\nu,n} + B_{\nu,n-1} + C_n W_{\nu,n}\left(1 - H_n N^2_{\nu,n} W_{\nu,n}\right) \tag{A17}$$

and

$$R^{\omega}_{\nu,n} = - C_n W_{\nu,n} H_n N_{\nu,n} N_{\omega,n} W_{\omega,n} \quad . \tag{A18}$$

Note that $R^{\omega}_{\nu,n} = R^{\nu}_{\omega,n}$ so that $\underset{\approx}{A}_n$ is symmetric. Also, here again all $B_{\nu,0} = B_{\nu,N} = 0$.

The general submatrix $\underset{\approx}{B}_n$ is given by

$$\underset{\approx}{B}_n = \begin{bmatrix} -B_{1,n} & 0 & 0 & 0 & 0 & 0 & 0 \\ 0 & -B_{2,n} & 0 & 0 & 0 & 0 & 0 \\ 0 & 0 & -B_{3,n} & 0 & 0 & 0 & 0 \\ 0 & 0 & 0 & -B_{4,n} & 0 & 0 & 0 \\ 0 & 0 & 0 & 0 & -B_{5,n} & 0 & 0 \\ 0 & 0 & 0 & 0 & 0 & -B_{6,n} & 0 \\ 0 & 0 & 0 & 0 & 0 & 0 & -B_{7,n} \end{bmatrix} \quad \text{(A19)}$$

The matrix $\underset{\approx}{M}$ of (A10) may therefore be described as a symmetric band matrix.

3. Methods of Solution of the Blending System

3.1 Exact Solution

The solution to the blending system of equations, (A10), may be written as

$$\underset{\sim}{\varphi}^{*} = \underset{\approx}{M}^{-1} \underset{\sim}{F} \qquad \text{(A20)}$$

where $\underset{\approx}{M}^{-1}$ is the inverse of the coefficient matrix, $\underset{\approx}{M}$, and is a full matrix, in general. The elements of $\underset{\approx}{M}^{-1}$ will be given by $\underset{\approx}{M}^{-1} = [m_{i,j}]$. A linear subscript, p, may be used to indicate the ordering of the $\underset{\sim}{\varphi}^{*}$ elements specified by (A11) and (A12); i.e.,

$$\varphi^{*}_{p} = \varphi^{*}_{\nu,n} \qquad \text{(A21)}$$

where

$$\begin{aligned} p &= (n-1)\,\nu_m + \nu \quad , \\ p &= 1,2,\ldots,p_m \quad , \\ \nu &= 1,2,\ldots,\nu_m \quad , \end{aligned} \qquad \text{(A22)}$$

and

$$n = 1,2,\ldots,N \quad .$$

From (A20) the solution for the arbitrary element, φ^{*}_{p}, may be written as

$$\varphi^{*}_{p} = \sum_{j} m_{p,j}\, F_j \quad , \qquad \text{(A23)}$$

where the subscript j ranges over all values of p from 1 to p_n; i.e., all elements of the forcing function contribute to all elements of $\underset{\sim}{\varphi}^*$. From (A14) we may rewrite (A23) as

$$\varphi^*_p = \sum_j m_{p,j} \left(A_j \varphi_j - B_j \mu_j + B_{j-\nu_m} \mu_{j-\nu_m} \right) \quad . \tag{A24}$$

The object of the blending procedure is to determine not only the resultant elements of $\underset{\sim}{\varphi}^*$ but also the associated resultant weights, $A^*_{\nu,n}$. A basic tenet of the implicit method of structure blending is that the resultant blended information at a given location is the sum of the independent information assembled at that location plus the independent ambient information or information propagated into the location from surrounding points by the higher-order parameters; i.e.,

$$A^*_p \varphi^*_p = A_p \varphi_p + A^a_p \varphi^a_p \quad , \tag{A25a}$$

$$B^*_p \mu^*_p = B_p \mu_p + B^a_p \mu^a_p \quad , \tag{A25b}$$

$$A^*_p = A_p + A^a_p \quad , \tag{A26a}$$

$$B^*_p = B_p + B^a_p \quad . \tag{A26b}$$

The first term on the right-hand side of (A25) and (A26) represents assembled information and the second term represents ambient information. Eq. (A24) may be rewritten in the form

$$\varphi^*_p = m_{p,p} A_p \varphi_p + X_{\varphi^*_p} \tag{A27}$$

where $X_{\varphi_p^*}$ refers to the summation in (A24) less the term $m_{p,p} A_p \varphi_p$. Since $X_{\varphi_p^*}$ contains no explicit reference to $A_p \varphi_p$, then by comparison with (A25a) it refers to the independent ambient information at point p while the first term refers to the assembled information. Consequently, we may divide both sides of (A25a) by A_p^* and equate the first term on the right-hand side of the resulting equation to that of (A27) to obtain

$$\frac{A_p \varphi_p}{A_p^*} = m_{p,p} A_p \varphi_p \tag{A28}$$

or

$$A_p^* = \frac{1}{m_{p,p}} \quad . \tag{A29}$$

Hence, the blended A^* elements are given by the reciprocal of the diagonal elements of the inverse of the coefficient matrix, $\underset{\approx}{M}$, of (A10).

The blended first differences may be written as

$$\mu_p^* = \varphi^*_{p+\nu_m} - \varphi_p^* \tag{A30}$$

for $p = 1,2,\ldots, p_m - \nu_m$. The B^* elements may be obtained by employing the same procedure used to obtain the A^* elements. The following sequence of equations results:

$$\mu^*_p = \sum_j m_{p+\nu_m, j} \left(A_j \varphi_j - B_j \mu_j + B_{j-\nu_m} \mu_{j-\nu_m} \right)$$

$$- \sum_j m_{p,j} \left(A_j \varphi_j - B_j \mu_j + B_{j-\nu_m} \mu_{j-\nu_m} \right) \quad \text{(A31)}$$

$$\mu^*_p = B_p \mu_p \left[-m_{p+\nu_m, p} + m_{p+\nu_m, p+\nu_m} + m_{p,p} - m_{p,p+\nu_m} \right]$$

$$+ X_{\mu^*_p} \quad \text{(A32)}$$

$$B^*_p = \left[m_{p,p} + m_{p+\nu_m, p+\nu_m} - 2\, m_{p+\nu_m, p} \right]^{-1} . \quad \text{(A33)*}$$

If A^*_p is interpreted as the reciprocal of the unresolved variance in φ^*_p, then

$$\sigma^2_{\varphi^*_p} = \frac{1}{A^*_p} . \quad \text{(A34)}$$

Similarly we may write

$$\sigma^2_{\mu^*_p} = \frac{1}{B^*_p} . \quad \text{(A35)}$$

---

*We have taken advantage of the fact that both $\underset{\sim}{M}$ and $\underset{\approx}{M}^{-1}$ are symmetric to combine the $m_{p,p+\nu_m}$ and $m_{p+\nu_m, p}$ terms.

Combining (A29), (A33), (A34) and (A35) we arrive at

$$\sigma^2_{\mu^*_p} = \sigma^2_{\varphi^*_p} + \sigma^2_{\varphi^*_{p+\nu_m}} - 2\, m_{p+\nu_m,\, p} \quad . \tag{A36}$$

The sum of the variances on the right-hand side of (A36) would be the variance associated with the first difference if φ^*_p and $\varphi^*_{p+\nu_m}$ were independent. Hence, the subtraction of the term $2\, m_{p+\nu_m,\, p}$ indicates the interdependent nature of the resultant $\underset{\sim}{\varphi}^*$ elements.

The solution by matrix inversion has both advantages and drawbacks. The advantages are that it is exact, it can be employed for any form of the error functional which produces a non-singular coefficient matrix $\underset{\approx}{M}$ and it yields the blended weights as well as object parameter values. The main drawback is that the matrix inversion routines may be prohibitively time-consuming compared to some iterative techniques.

3.2 Point Successive-Over-Relaxation

Point successive-over-relaxation (SOR) could be employed to iteratively solve (A10) for the φ^* elements. This technique is well-known, and well-documented. Unlike the exact matrix inversion method, however, the formulation is dependent upon the form of the error functional and resulting stencil for the blending equations. Solution by point SOR of a blending system of the form given by (A10) and a perturbation method for approximating the A^* elements are discussed in [1].

[1] Holl, Manfred M. and Bruce R. Mendenhall, 1971; "Fields by Information Blending, Sea-Level Pressure Version", Final Report, Project M-167, Contract No. N66314-70-C-5226 (Fleet Numerical Weather Central), Meteorology International Incorporated, Monterey, California, 66 pp.

3.3 Line Successive-Over-Relaxation

The matrix $\underset{\approx}{M}$ may be written as

$$\underset{\approx}{M} = \underset{\approx}{A} + \underset{\approx}{B} \tag{A37}$$

where

$$\underset{\approx}{A} = \text{diag}\ \underset{\approx}{A}_1, \underset{\approx}{A}_2, \ldots, \underset{\approx}{A}_N \tag{A38}$$

and $\underset{\approx}{B}$ is given by

$$\begin{bmatrix} \underset{\approx}{O} & \underset{\approx}{B}_1 & & & & \bigcirc \\ \underset{\approx}{B}_1^T & \underset{\approx}{O} & \underset{\approx}{B}_2 & & & \\ & \underset{\approx}{B}_2^T & \underset{\approx}{O} & & & \\ & & & \cdot & & \\ & & & & \cdot & \\ & & & & & \cdot \\ & & & & \underset{\approx}{O} & \underset{\approx}{B}_{N-1} \\ \bigcirc & & & & \underset{\approx}{B}_{N-1}^T & \underset{\approx}{O} \end{bmatrix}$$

The blending system equations may then be rewritten as

$$\left(\underset{\approx}{A} + \underset{\approx}{B}\right)\underset{\sim}{\varphi}^{*} = \underset{\sim}{F} \qquad \text{(A39)}$$

or as

$$\underset{\approx}{A}_{n}\,\underset{\sim}{\varphi}^{*}_{n} + \underset{\approx}{B}^{T}_{n-1}\,\underset{\sim}{\varphi}^{*}_{n-1} + \underset{\approx}{B}_{n}\,\underset{\sim}{\varphi}^{*}_{n+1} = \underset{\sim}{F}_{n} \qquad n = 1, 2, \ldots, N \qquad \text{(A40)}$$

where

$$\underset{\approx}{B}_{o} \equiv \underset{\approx}{B}_{N} \equiv \underset{\approx}{O} \;.$$

Equation (A40) may be solved for $\underset{\sim}{\varphi}^{*}_{n}$ as

$$\underset{\sim}{\varphi}^{*}_{n} = \underset{\approx}{A}_{n}^{-1}\left[\underset{\sim}{F}_{n} - \underset{\approx}{B}^{T}_{n-1}\,\underset{\sim}{\varphi}^{*}_{n-1} - \underset{\approx}{B}_{n}\,\underset{\sim}{\varphi}^{*}_{n+1}\right] \;. \qquad \text{(A41)}$$

The solution by line relaxation is defined by

$$\left(\underset{\sim}{\varphi}^{*}_{n}\right)^{(r+1)} = \left(\underset{\sim}{\varphi}^{*}_{n}{}^{(r)}\right) + \left[\underset{\sim}{\varphi}^{*}_{n}{}^{(r+1/2)} - \left(\underset{\sim}{\varphi}^{*}_{n}\right)^{(r)}\right]\omega \;, \qquad \text{(A42)}$$

where the superscript (r) refers to pass number and where

$$\left(\underset{\sim}{\varphi}^{*}_{n}\right)^{(r+1/2)} = \left(\underset{\approx}{A}_{n}\right)^{-1}\left[\underset{\sim}{F}_{n} - \underset{\approx}{B}^{T}_{n-1}\left(\underset{\sim}{\varphi}^{*}_{n-1}\right)^{\substack{(r)\\(r+1)}} - \underset{\approx}{B}_{n}\left(\underset{\sim}{\varphi}^{*}_{n+1}\right)^{\substack{(r)\\(r+1)}}\right] . \qquad \text{(A43)}$$

The upper superscript (r) applies to the term in brackets for the first half of each pass in which either the even or odd numbered n are solved for.

The lower superscript (r+1) applies to the term in brackets for the second half of each pass in which the remaining (either odd or even) n are solved for. The method converges for $0 < \omega < 2$ where $1 < \omega < 2$ implies overrelaxation.

When the $\underset{\approx}{A}_n$ matrices are positive-definite the inversion specified by Eq. (A43) may be obtained explicitly by a triangular decomposition of the $\underset{\approx}{A}_n$ matrices into the product of an upper and a lower triangular matrix, followed by Gaussian elimination. If a large number of passes are to be used and the weights comprising the $\underset{\approx}{A}_n$ matrix elements do not change from pass to pass, then a significant saving in computer time may be realized by this decomposition.[2]

Note that solution by line SOR will be possible as long as the form of the error functional yields a set of blending equations which may be put into the form given by (A10) in which the coefficient matrix $\underset{\approx}{M}$ may be written in symmetric, block tri-diagonal form.

3.4 Method Used in Development Version of FIB-CLRX

The line SOR technique has been employed in the current version of FIB-CLRX. After the explicit solution by matrix inversion has been performed for each line in each half pass of the iteration, a new weight C_n is computed using the relations (A7) and (A50) (to be discussed in Section 4). The new C_n is used in the next iteration for that line. Ten passes through the line SOR technique with $\omega = 1.2$ give adequate convergence.

---

[2] A more detailed discussion of line SOR is given in the Appendix to "The Sea-Level Pressure Analysis Capability, FIB/SLP: Improvements, Refinements, and Generalizations", by William F. Weigle and Bruce R. Mendenhall, Technical Summary, M-209, Contract No. N66314-74-C-1528 (Fleet Numerical Weather Central), Meteorology International Incorporated, Monterey, California, November 1974, 37 pp. plus Appendix A.

4. <u>Assembly</u>

The sole source of information for this developmental version of FIB-CLRX is the field of normalized measured radiance anomalies, $\mathfrak{I}^{P}_{\nu,n}$, from a scan of 24 spots of 7 channels each. From these anomalies, estimates of the $\varphi_{\nu,n}$, $\mu_{\nu,n}$, $N_{\nu,n}$ and L_n and the associated reliabilities $A_{\nu,n}$, $B_{\nu,n}$, $W_{\nu,n}$ and C_n are made. Two spots have been omitted on each end of the scan to simplify computational loops. Hence, for blending the n index runs from 3 to 22 and the ν index from 1 to 7, producing a blending system of 140 simultaneous, linear equations. The assembly procedure will now be described.

The following first-difference vectors are formed:

$$\underset{\sim}{\psi}^{1}_{n} = \underset{\sim}{\mathfrak{I}}^{P}_{n+1} - \underset{\sim}{\mathfrak{I}}^{P}_{n} \qquad n = 1,2,\ldots,N-1 \tag{A44a}$$

$$\underset{\sim}{\psi}^{2}_{n} = \underset{\sim}{\mathfrak{I}}^{P}_{n+1} - \underset{\sim}{\mathfrak{I}}^{P}_{n-1} \qquad n = 2,3,\ldots,N-1 \tag{A44b}$$

$$\underset{\sim}{\psi}^{3}_{n} = \underset{\sim}{\mathfrak{I}}^{P}_{n+2} - \underset{\sim}{\mathfrak{I}}^{P}_{n-1} \qquad n = 2,3,\ldots,N-2 \tag{A44c}$$

From each of these first-difference vectors the normalized vectors

$$\underset{\sim}{N}^{i}_{n} = \frac{\underset{\sim}{I} \cdot \underset{\sim}{\psi}^{i}_{n}}{|\underset{\sim}{I} \cdot \underset{\sim}{\psi}^{i}_{n}|} \; \frac{\underset{\sim}{\psi}^{i}_{n}}{|\underset{\sim}{\psi}^{i}_{n}|} \tag{A45}$$

are formed.

The $\underset{\sim}{N}{}_n^i$ vectors surrounding each point are then used to provide an estimate of the adjustment vector $\underset{\sim}{N}{}_n$ at the point as follows:

$$\underset{\sim}{N}{}_n = \frac{\sum_{i=1}^{9} W^i \hat{\underset{\sim}{N}}{}_n^i}{\left\{ \sum_{\nu} \left(\sum_{i=1}^{9} W^i \hat{N}_{\nu,n}^i \right)^2 \right\}^{1/2}} \tag{A46}$$

where $W^i = \omega^i \, | \hat{\psi}_n^i |^2$ and the ω^i, $\hat{\psi}_n^i$ and $\hat{\underset{\sim}{N}}{}_n^i$ are specified in Table A1 below. An estimate of the variance associated with the component $N_{\nu,n}$ is given by

$$\sigma_{\nu,n}^2 = \frac{\sum_i W^i \left(\hat{N}_{\nu,n}^i - N_{\nu,n} \right)^2}{\sum_i W^i} \quad . \tag{A47}$$

The reliability associated with the component $N_{\nu,n}$ for blending is given by

$$W_{\nu,n} = \frac{1}{\sigma_{\nu,n}^2 + \epsilon_\nu} \tag{A48}$$

where ϵ_ν is a minimum variance associated with the $N_{\nu,n}$.

Table A1

First Differences and Weights used to Estimate Adjustment Vector $\underset{\sim}{N}_n$

i	ω^i	$\hat{\underset{\sim}{\psi}}{}^i_n$	$\hat{\underset{\sim}{N}}{}^i_n$	Spots surrounding nth spot used to estimate difference at n: $n-2$	$n-1$	n	$n+1$	$n+2$
1	1.0	$\underset{\sim}{\psi}{}^1_n$	$\underset{\sim}{N}{}^1_n$	•	•	•	•	•
2	1.0	$\underset{\sim}{\psi}{}^1_{n-1}$	$\underset{\sim}{N}{}^1_{n-1}$	•	•	•	•	•
3	0.4	$\underset{\sim}{\psi}{}^1_{n+1}$	$\underset{\sim}{N}{}^1_{n+1}$	•	•	•	•	•
4	0.4	$\underset{\sim}{\psi}{}^1_{n-2}$	$\underset{\sim}{N}{}^1_{n-2}$	•	•	•	•	•
5	1.0	$\underset{\sim}{\psi}{}^2_n$	$\underset{\sim}{N}{}^2_n$	•	•	•	•	•
6	0.6	$\underset{\sim}{\psi}{}^2_{n+1}$	$\underset{\sim}{N}{}^2_{n+1}$	•	•	•	•	•
7	0.6	$\underset{\sim}{\psi}{}^2_{n-1}$	$\underset{\sim}{N}{}^2_{n-1}$	•	•	•	•	•
8	0.8	$\underset{\sim}{\psi}{}^3_n$	$\underset{\sim}{N}{}^3_n$	•	•	•	•	•
9	0.8	$\underset{\sim}{\psi}{}^3_{n-1}$	$\underset{\sim}{N}{}^3_{n-1}$	•	•	•	•	•

The ϵ_ν have been estimated as follows:

$$\begin{aligned}
\epsilon_1 &= 0.001 \\
\epsilon_2 &= 0.001 \\
\epsilon_3 &= 0.001 \\
\epsilon_4 &= 0.005 \\
\epsilon_5 &= 0.015 \\
\epsilon_6 &= 0.025 \\
\epsilon_7 &= 0.030
\end{aligned} \tag{A49}$$

Note that for a given $\underset{\sim}{N}_n$, the larger L_n is the larger the magnitude of the vector difference $\underset{\sim}{\varphi}^*_n - L_n \underset{\sim}{N}_n$ is and the less the associated weight, C_n, should be. Hence, the weight C_n is given by

$$C_n = \frac{1}{L_n^2 + q} \tag{A50}$$

where the minimum variance is given by $q = 1$. Hence, the combined weight, $C_n W_{\nu,n}$, will be largest where there is little disparity between the first-difference estimates used to produce the $N_{\nu,n}$ and the associated magnitude, L_n, appears to be small. Conversely, the combined weight will be smallest where there are large differences between the first-difference estimates and the associated magnitude appears to be large.

The assembled value of $\varphi_{\nu,n}$ for blending is given by

$$\varphi_{\nu,n} = 0 \tag{A51}$$

for all ν and n. Consequently, the weight $A_{\nu,n}$, should reflect how close to the clear column value the measured radiance anomaly is. A method of

weighting has been used which appears to give satisfactory results for all cases except those where a uniform, cloud layer exists over many adjacent spots. The first step is to compute at each point a measure of the disparity in $\mathfrak{T}^P$ between adjacent spots according to the formula

$$F_{\nu,n} = \left\{ |\psi^1_{\nu,n}| - 0.2 \right\}^2 + \left\{ |\psi^1_{\nu,n-1}| - 0.2 \right\}^2$$

$$+ \left\{ |\psi^2_{\nu,n}| - 0.4 \right\}^2 + \left\{ |\psi^1_{\nu,n} - \psi^1_{\nu,n-1}| - 0.2 \right\}^2 \qquad \text{(A52)}$$

for $\nu = 1,\ldots,7$ and $n = 3,\ldots,22$. The square of negative quantities in (A52) is set equal to zero. A tentative weight field is then given by

$$\hat{A}_{\nu,n} = \begin{cases} \left(0.25\, F_{\nu,n} + 0.2\right)^{-1} & \nu = 1 \\ \left(0.2\, F_{\nu,n} + 0.05\, F_{\nu-1,n} + 0.2\right)^{-1} & \nu = 2,\ldots,7 \end{cases} \qquad \text{(A53)}$$

and the weight field for blending by

$$A_{\nu,n} = \begin{cases} \hat{A}_{\nu,n} & \text{if } \hat{A}_{\nu,n} \geqq 1 \\ 0 & \text{if } \hat{A}_{\nu,n} < 1 \end{cases} \quad . \qquad \text{(A54)}$$

The first difference, $\underset{\sim}{\mu}_n$, may be written as

$$\underset{\sim}{\mu}_n = \begin{cases} -\underset{\sim}{\psi}^1_n + \left(\underset{\sim}{\mathfrak{T}}^*_{n+1} - \underset{\sim}{\mathfrak{T}}^*_n\right) & n = 3,\ldots,21 \\ 0 & n = 1,2,22,23,24 \end{cases} \quad . \qquad \text{(A55)}$$

Since $\underset{\sim}{\mathfrak{T}}^* = \underset{\sim}{\mathfrak{T}}^P + \underset{\sim}{\varphi}^*$ is what we're trying to determine by the blending operation, the second term on the right-hand-side of (A55) is initially set equal to zero. The associated weights are given by

$$B_{\nu,n} = \begin{cases} 10 & n = 3,\ldots,21 \\ 0 & n = 1,2,22,23,24 \end{cases} . \tag{A56}$$

The first-guess field of $\underset{\sim}{\varphi}^*$ for the blending operation is set equal to zero for all (ν,n) where $A_{\nu,n} \geqq 1.0$. Where $A_{\nu,n} = 0.0$, the first-guess value is the difference between the linearly interpolated value of $\mathfrak{T}^P_{\nu,n}$, using the nearest adjacent bracketing spots with $A_{\nu,n} \geqq 1.0$, and the reported value of $\mathfrak{T}^P_{\nu,n}$.

5. Recycling

After assembly and blending the $\underset{\sim}{\varphi}^*$ and $\underset{\sim}{A}^*$ elements reflect the assimilation of all available information according to the formulation of the error functional and blending system of equations. Hence, $\underset{\sim}{\varphi}^*$ and $\underset{\sim}{A}^*$ may be used to compare each individual piece of information for consistency with all other information. These comparisons will then be the basis of a reevaluation of the weights of the individual information elements used during assembly.

Recycling, then, is the iterative process involving the above-mentioned reevaluation, assembly and blending stages of the FIB methodology. It begins after the initial assembly and blending operations. Its purpose is to assess more accurately the independent worth of the individual information elements that were used during assembly.

Recycling could continue ad infinitum; however, there is a trade-off between increasing computer time and decreasing return. In previous FIB applications, three cycles (one initial assembly and blending and two reevaluation cycles) have been adequate. Consequently, we have employed three cycles in FIB-CLRX with good results to date. The details will now be given.

The following changes are made to the weights and values for the second and third cycle assembly and blending:

1. $$\hat{A}^{(j)}_{\nu,n} = \frac{2}{\dfrac{1}{\hat{A}_{\nu,n}} + \left(\varphi^{*\,(j-1)}_{\nu,n}\right)^2} \tag{A57}$$

$$A^{(j)}_{\nu,n} = \begin{cases} \hat{A}^{(j)}_{\nu,n} & \text{for } \hat{A}^{(j)}_{\nu,n} \geq 1.0 \\ 0 & \text{for } \hat{A}^{(j)}_{\nu,n} < 1.0 \end{cases} \qquad \text{(A58)}$$

where $(\ )^{(j)}$ refers to cycle number 2 or 3. Note that this formulation permits information which was rejected during a previous cycle to be reinstated.

2 $\quad \underset{\sim}{\varphi}^{(j)} = \underset{\sim}{0}$ as in cycle 1. (A59)

3 $\quad \underset{\sim}{B}^{(j)} = \underset{\sim}{25}$.

4 $$\mu^{(j)}_{\nu,n} = \begin{cases} \mu^{(1)}_{\nu,n} + f K & \text{for } n = 3,\ldots,21 \\ 0 & \text{for } n = 1,2,22,23,24 \end{cases} \qquad \text{(A60)}$$

where $f = 0.8$,

$$K_\nu = \frac{\sum_{n=13}^{22} \mathfrak{J}^{*(j-1)}_{\nu,n} - \sum_{n=3}^{12} \mathfrak{J}^{*(j-1)}_{\nu,n}}{100} \qquad \text{(A61)}$$

and $\quad \mathfrak{J}^{*(j-1)}_{\nu,n} = \mathfrak{J}^{P}_{\nu,n} + \varphi^{*(j-1)}_{\nu,n}$.

The term fK_ν in (A60) is an estimate of the term in (A55) that was set equal to zero during the first cycle. It is inclusion of this term that permits increasing the associated weights $B_{\nu,n}$.

(5) The calculation of the $\underset{\sim}{N}_n$ by (A46) and $W_{\nu,n}$ by (A47) involve the weight factors W^i and the individual estimates $\hat{\underset{\sim}{N}}{}^i_n$. The reevaluation consists of measuring the consistency between the estimates $\hat{\underset{\sim}{N}}{}^i_n$ and the blended adjustment vector

$$\underset{\sim}{N}{}^*_n = \frac{\underset{\sim}{I} \cdot \underset{\sim}{\varphi}{}^*_n}{|\underset{\sim}{I} \cdot \underset{\sim}{\varphi}{}^*_n|} \quad \frac{\underset{\sim}{\varphi}{}^*_n}{|\underset{\sim}{\varphi}{}^*_n|}$$

and using this measure to reevaluate the coefficient $|\underset{\sim}{\psi}{}^i_n|^2$ in the definition of the weight factors W^i. Equations (A46) and (A47) are then applied with the new weight factors. The following formulas are used to reevaluate the coefficients:

$$\left\{|\hat{\underset{\sim}{\psi}}{}^1_n|^2\right\}^{(j)} = \left\{|\hat{\underset{\sim}{\psi}}{}^1_n|^2\right\}^{(1)} \left\{\left(\hat{\underset{\sim}{N}}{}^1_n \cdot \underset{\sim}{N}{}^{*(j-1)}_{n+1}\right)\left(\hat{\underset{\sim}{N}}{}^1_n \cdot \underset{\sim}{N}{}^{*(j-1)}_{n}\right)\right\}$$

$$\left\{|\hat{\underset{\sim}{\psi}}{}^2_n|^2\right\}^{(j)} = \left\{|\hat{\underset{\sim}{\psi}}{}^2_n|^2\right\}^{(1)} \left\{\left(\hat{\underset{\sim}{N}}{}^2_n \cdot \underset{\sim}{N}{}^{*(j-1)}_{n}\right)\left(\hat{\underset{\sim}{N}}{}^2_n \cdot \underset{\sim}{N}{}^{*(j-1)}_{n-1}\right)\right\}$$

$$\vdots \qquad\qquad\qquad \vdots$$

$$\left\{|\hat{\underset{\sim}{\psi}}{}^9_n|^2\right\}^{(j)} = \left\{|\hat{\underset{\sim}{\psi}}{}^9_n|^2\right\}^{(1)} \left\{\left(\hat{\underset{\sim}{N}}{}^9_n \cdot \underset{\sim}{N}{}^{*(j-1)}_{n+1}\right)\left(\hat{\underset{\sim}{N}}{}^9_n \cdot \underset{\sim}{N}{}^{*(j-1)}_{n-2}\right)\right\}$$

where the symbol $\cdot$ refers to the dot product. When the initial estimates and the blended adjustment vectors are parallel, the dot products equal one. Where they are not parallel, the values range between one and zero. Negative values are set equal to zero since estimates which are more than 90° out of phase with the blended adjustment vector are deemed worthless.

The net result, then, is that in both (A46) and (A47) those initial estimates of $\underset{\sim}{N}_n$ which are more consistent with the blended analysis are reinforced during reevaluation while those which are less consistent have their effect reduced.